NASA TECHNICAL MEMORANDUM

NASA TM X-71945

COPY NO.

NASA TM X-71945

HEAT TRANSFER TO SURFACE AND GAPS OF RSI TILE ARRAYS IN TURBULENT FLOW AT MACH 10.3

David A. Throckmorton

April 1974

NATIONAL AERONAUTICS AND SPACE ADMINISTRATION

LANGLEY RESEARCH CENTER, HAMPTON, VIRGINIA 23665

HEAT TRANSFER TO SURFACE AND GAPS OF RSI TILE ARRAYS IN TURBULENT FLOW AT MACH 10.3

David A. Throckmorton

Summary

Heat transfer to gap walls and surface of a simulated reusable surface insulation (RSI) tile array are presented. The data were obtained in the thick, turbulent tunnel wall boundary layer of the Langley Continuous Flow Hypersonic Tunnel at a freestream Mach number of 10.2 and a freestream unit Reynolds number of 1×10^6/ft. Pertinent test variables were: tile array orientation (staggered and in-line), gap width, flow angularity, and tile mismatch.

INTRODUCTION

The shuttle thermal protection system (TPS) design concept calls for the vehicle surface to be covered with a brick-like array of silica reusable surface insulation (RSI) tiles. A major concern associated with this TPS design results from interference heating to the tile surface and the small thermal-expansion gaps between tiles. Presence of the gaps may result in increased boundary layer turbulence and surface heating; heating levels within the gaps may also be severe due to flow reattachment phenomena. In addition, radiation blockage within the gaps may produce extreme gap wall temperatures even at low heating levels, and the short heat paths may result in excessive bond-line temperatures.

In order to better define the heating which the tile surface and gap walls will experience, tests were conducted on a full-scale simulated tile array in the thick, turbulent, tunnel wall boundary layer of the Langley Continuous Flow Hypersonic Tunnel. Test conditions were freestream Mach number, $M_\infty = 10.3$; and freestream unit Reynolds number, $R_N = 1 \times 10^6$/ft. Geometric parameters varied during the test were gap width, tile array orientation (staggered/in-line), flow angularity, and tile mismatch.

Detailed analysis and correlation of the data obtained from this test are being conducted by McDonnell Douglas Astronautics Company under NASA Contract NAS9-13439, Data Correlation and Analysis of Arc Tunnel and Wind Tunnel Tests of RSI Joints and Gaps. This report presents the test data only; no data analysis is included.

SYMBOLS

C_p	specific heat of model material
h	heat transfer coefficient
h_{fp}	heat transfer coefficient to flat plate on tunnel side wall
M_∞	freestream Mach number
R_N	freestream unit Reynolds number
t	time
T_{aw}	adiabatic wall temperature
T_w	wall temperature
w	gap width
X	model surface coordinate
Y	model surface coordinate
λ	model wall thickness
ρ	model material density
θ	flow angle

MODEL DESCRIPTION

The simulated full-scale tile-array model utilized in these tests is illustrated schematically in Figure 1. The model consisted of a single 6- by 6-inch thin skin tile surrounded by six RSI tiles as shown. This array was set in an adapter (Figure 2) to the facility model injection mechanism in order to provide testing flush to the tunnel side wall. Photographs of the model installed on the injection mechanism, and injected flush to the tunnel side wall (both in-line and staggered orientations) are shown in Figures 3 and 4, respectively.

The tile array was constructed such that gap width between tiles could be varied. Metal shims (Figure 2) were used to aline all tiles flush with the tunnel wall, as well as to provide mismatch of the instrumented thin-skin tile relative to the surrounding tiles. For all test runs, the gaps between the adapter walls and the RSI tile side walls were eliminated by filling with a high temperature rubber sealant.

The thin-skin tile was fabricated of #304 stainless steel with a uniform thickness of 0.010 inch. The tile was instrumented with 81, 30-gage chromel-alumel thermocouples nominally located as indicated in Figure 5. Orientation of the instrumented portion of the thin skin tile relative to the surrounding RSI tiles is illustrated in Figure 6. The entire tile array could be rotated a full 360^{0} to allow measurement of the heat transfer to all tile surfaces for the full range of possible flow angularities.

TEST CONDITIONS AND VARIABLES MATRIX

Tests were conducted in the tunnel wall boundary layer of the Langley Continuous Flow Hypersonic Tunnel with freestream flow conditions of Mach number, $M_{\infty} = 10.3$, and unit Reynolds number, $R_N = 1 \times 10^6/ft$. At these conditions, the tunnel wall boundary layer is fully turbulent wi .h a displacement thickness, δ^*, of approximately 4.75 inches. Varied test parameters were: tile orientation (staggered/ in-line), gap width, flow angularity, and tile mismatch. An outline of the full test matrix is presented below:

GAP WIDTH (in.)	TILE ARRAY ORIENTATION	TILE MISMATCH (in.)	FLOW ANGULARITY (degs.)
0.05	Staggered	0, +0.10	0, 7.5, 15, 30, 45
	In-line	0, +0.10	0, 7.5, 15, 30
0.09	Staggered	0, +0.10, -0.066	0, 7.5, 15, 30, 45
	In-line	0, +0.10, -0.066	0, 7.5, 15, 30
0.18	Staggered	0, +0.10	0, 7.5, 15, 30, 45
	In-line	0, +0.10	0, 7.5, 15, 30
0.28	Staggered	0, +0.10	0, 7.5, 15, 30, 45
	In-line	0, +0.10	0, 7.5, 15, 30

TEST PROCEDURE AND DATA REDUCTION

The transient calorimeter technique was used to measure the heat transfer to the surfaces of the thin skin tile. The tests were conducted with the model initially at room temperature in an injection chamber adjacent to the tunnel test section, at a pressure equal to the test section static pressure. With hypersonic flow established in the test section, the model was rapidly injected to the test position and temperature data were recorded for each thermocouple at a rate of 20 samples/second.

For data reduction purposes, the one-half second interval of data immediately following model injection was ignored to allow steady state conditions to stabilize. A quadratic least squares curve was

fit to the following 10-second interval of data[1], for each thermocouple. Rate of change of temperature with time $(\frac{\partial T_w}{\partial t})$ was evaluated analytically from the curve fit expression at the initial point of the curve fit, and heat transfer coefficients were computed from the expression:

$$h = \frac{\rho C_p \lambda \frac{\partial T_w}{\partial t}}{T_{aw} - T_w}$$

Adiabatic wall temperature (T_{aw}) was calculated with an assumed recovery factor of 0.89.

All data were non-dimensionalized by the heat transfer coefficient measured at the centerline of a smooth flat plate on the tunnel side wall under the same nominal flow conditions as the tile array. A photograph of the flat plate model and the flat plate heating data are presented in Figures 7 and 8, respectively. The reference flat plate heat transfer coefficient was measured at a point corresponding to the forward edge of the instrumented tile,

$$h_{fp} = 0.000125 \frac{BTU}{ft^2\ sec^0R}$$

---

[1]The long interval (~10 seconds) of temperature-time data used for heat transfer rate calculation allowed measurement of the extremely low heating rates found in the gaps. These heating rates were not discernible when the normal interval (~1 second) of data was considered. Analysis of representative data from this test indicated that while the 10-second interval provided measurements of lower heating rate data than the shorter interval, the long interval had only a negligible effect (< 3 percent) on the accuracy of the surface heating rate measurements. Maximum difference of ~15 percent was observed at the thermocouple within the gap nearest the tile surface, where significant conduction effects would be expected. All heating rates were calculated using the 10-second time interval.

PRESENTATION OF RESULTS

All data presented in this report are in the form h/h_{fp} and are plotted versus surface coordinates defined in Figure 9. The two coordinate systems (for staggered/in-line orientations) each have their origin at the center of the thin skin tile and are fixed with respect to the tile array. The plot symbol code used in the presentation of results is shown in Figure 10.

The test data are presented in Figures 11-28 categorized by mismatch, gap width, and array orientation. Data for flush-mounted tiles are shown in Figures 11-18 for the four gap widths. In similar manner, data for a protruding tile are contained in Figures 19-26 and for a recessed tile in Figures 27 and 28. Test geometries and corresponding figure numbers are listed in Table I.

TABLE I - DATA FIGURE CONTENTS

Figure Number	Gap Width, w (Inches)	Mismatch, s (Inches)	Tile Orientation
11	0.05	0	Staggered
12	0.05		In-line
13	0.09		Staggered
14	0.09		In-line
15	0.18		Staggered
16	0.18		In-line
17	0.28		Staggered
18	0.28	0	In-line
19	0.05	0.100	Staggered
20	0.05		In-line
21	0.09		Staggered
22	0.09		In-line
23	0.18		Staggered
24	0.18		In-line
25	0.28		Staggered
26	0.28	0.100	In-line
27	0.09	-0.066	Staggered
28	0.09	-0.066	In-line

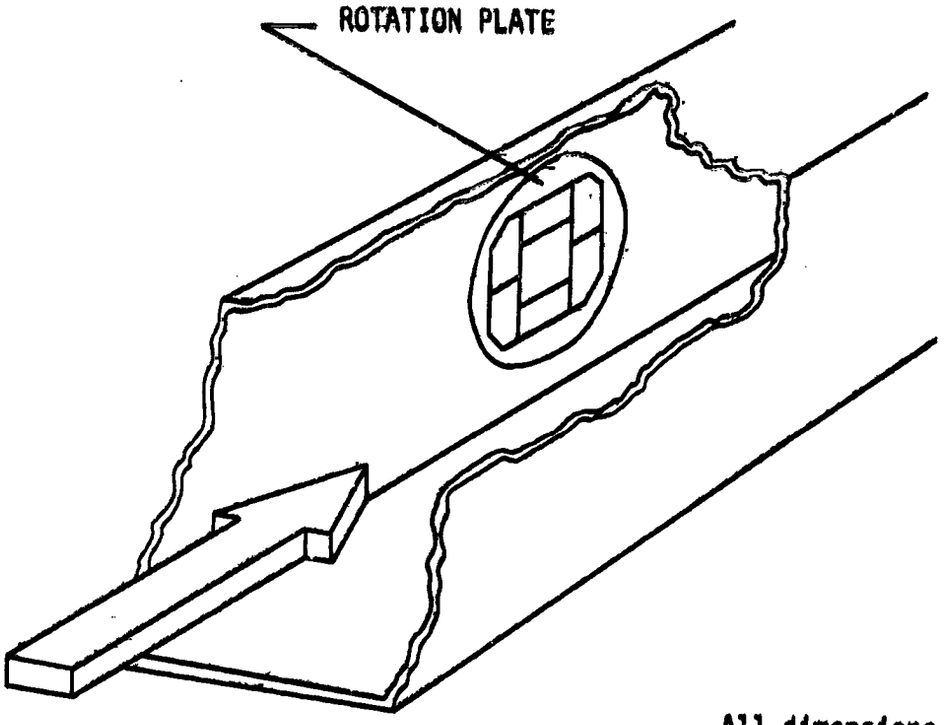

All dimensions in inches.

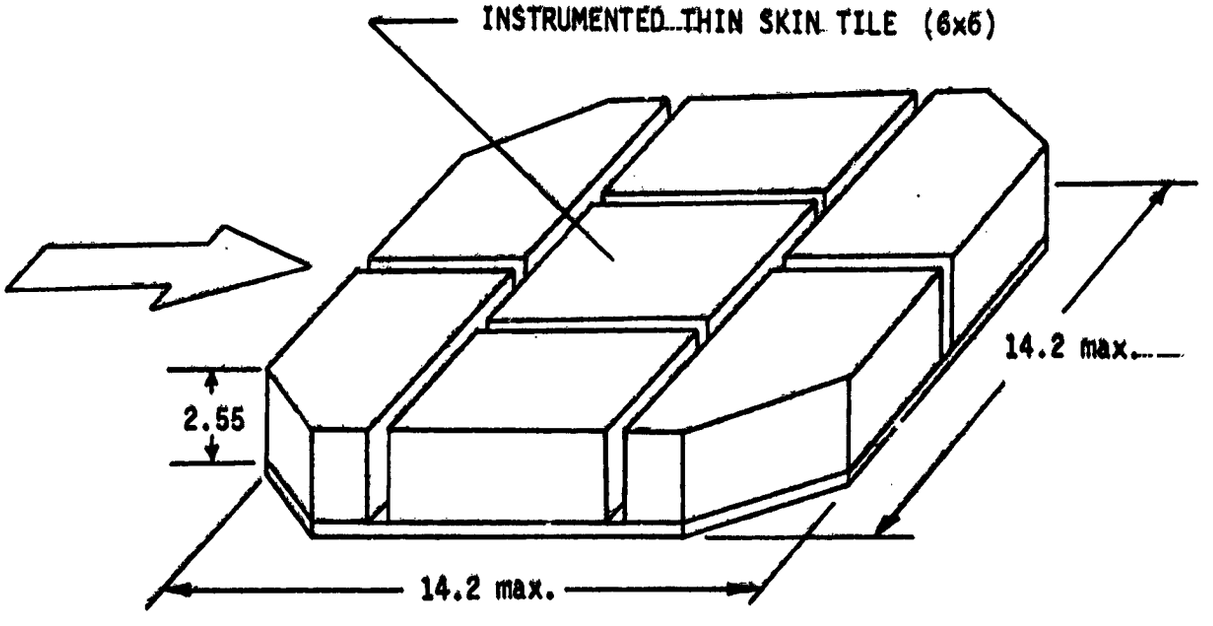

Figure 1.- Simulated Tile Array Model Schematic.

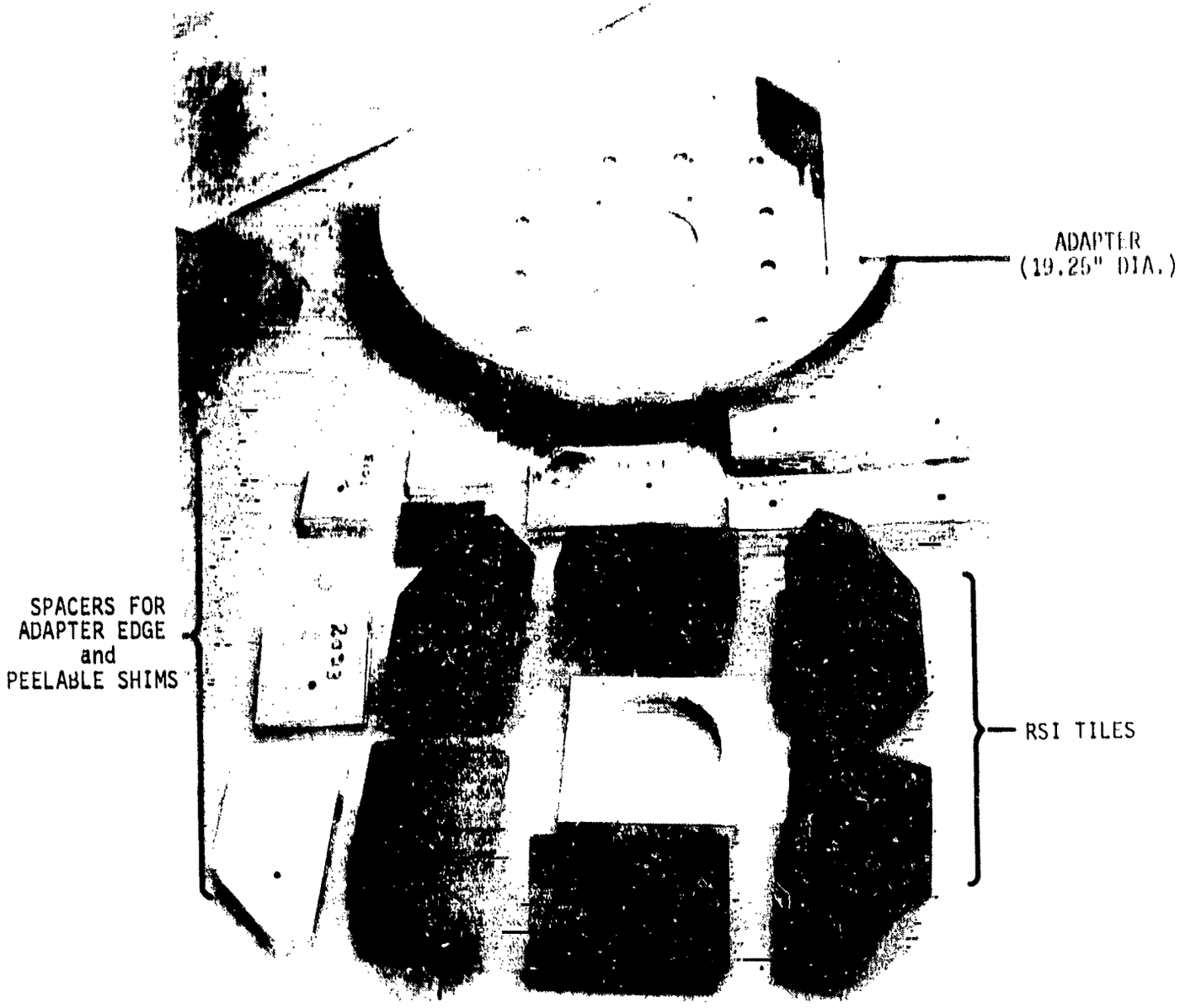

Figure 2.- Model Mo[illegible] Adapter and Associated Hardware.

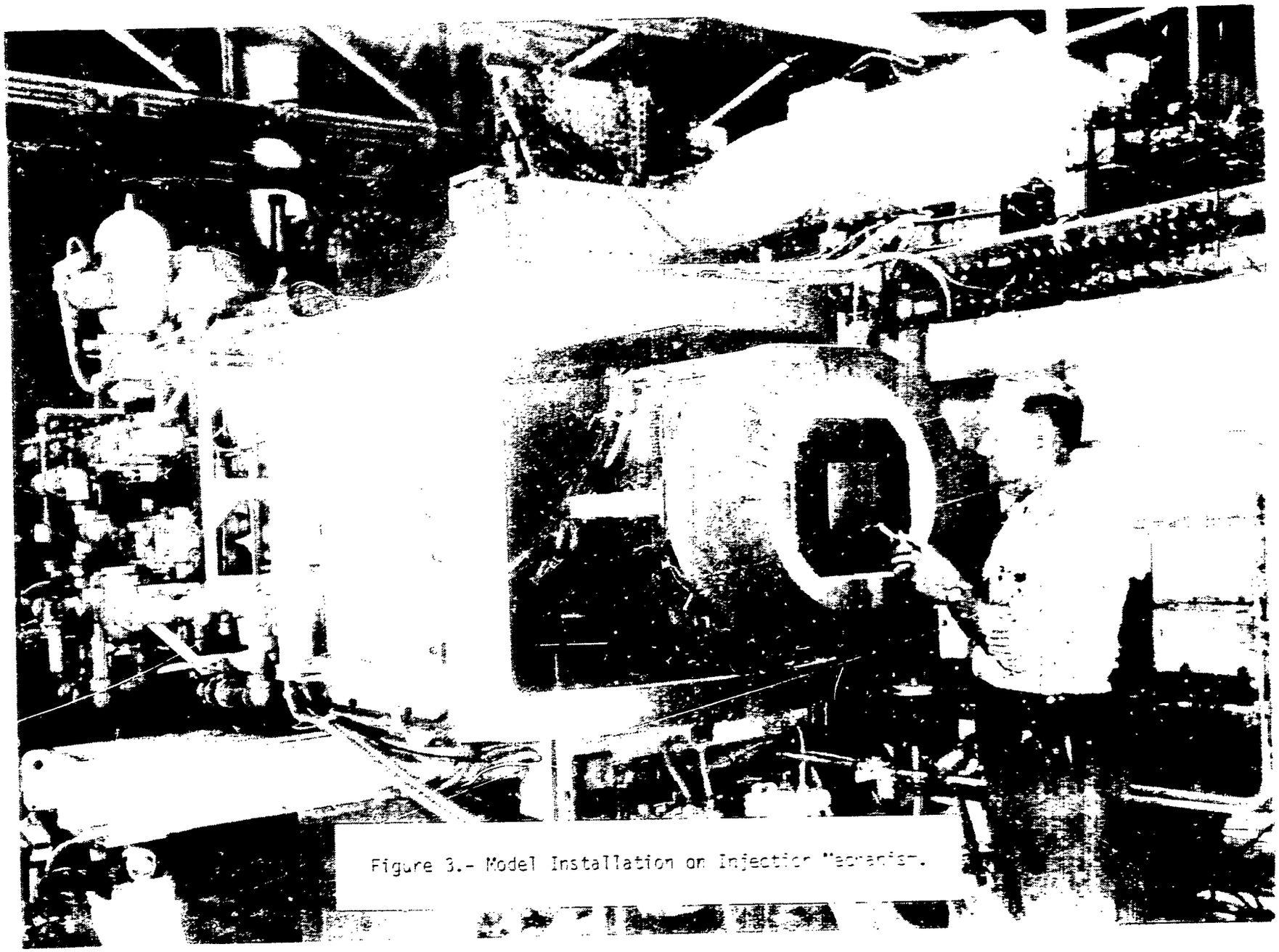

Figure 3.- Model Installation on Injection Mechanism.

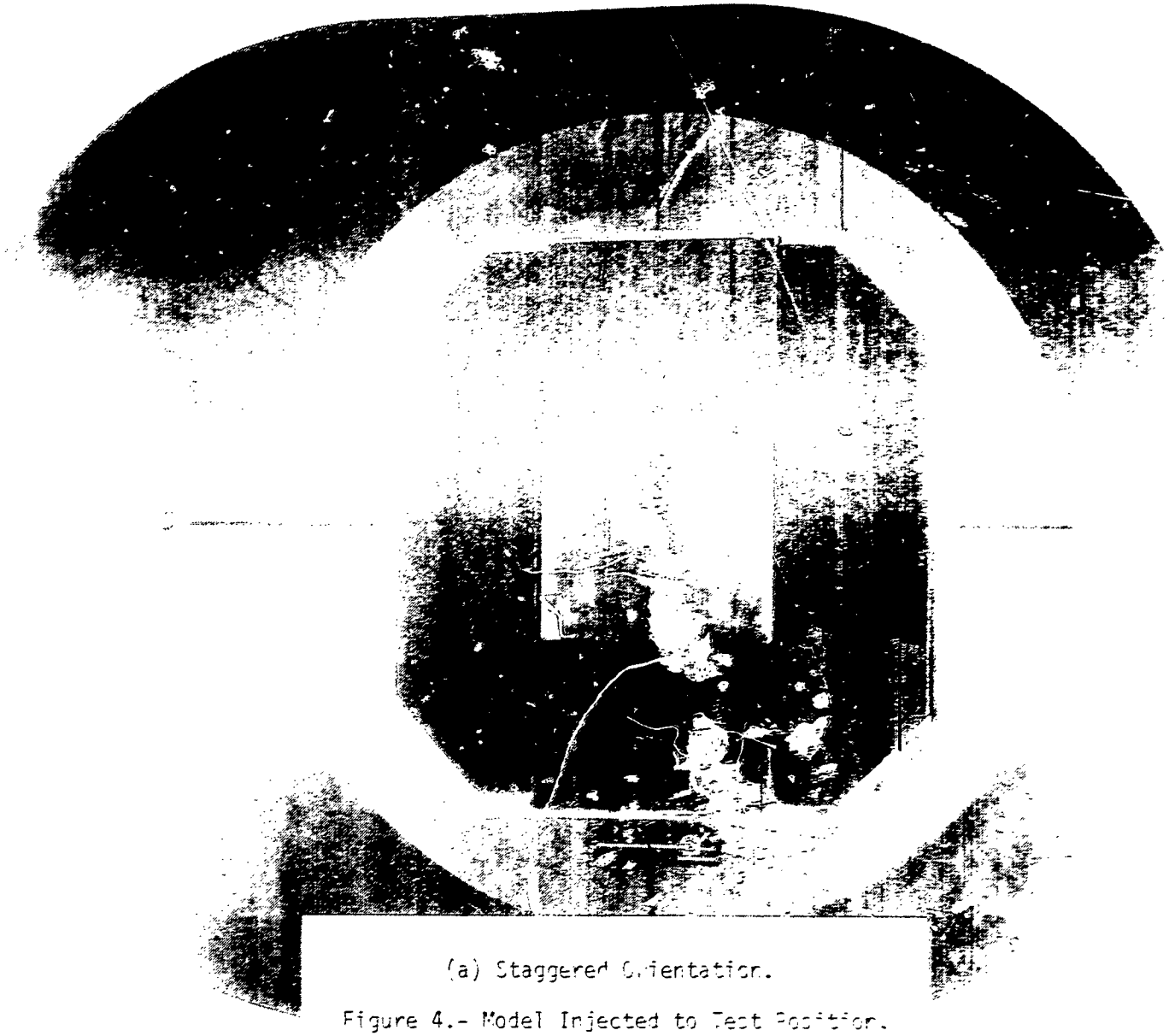

(a) Staggered Orientation.

Figure 4.- Model Injected to Test Position.

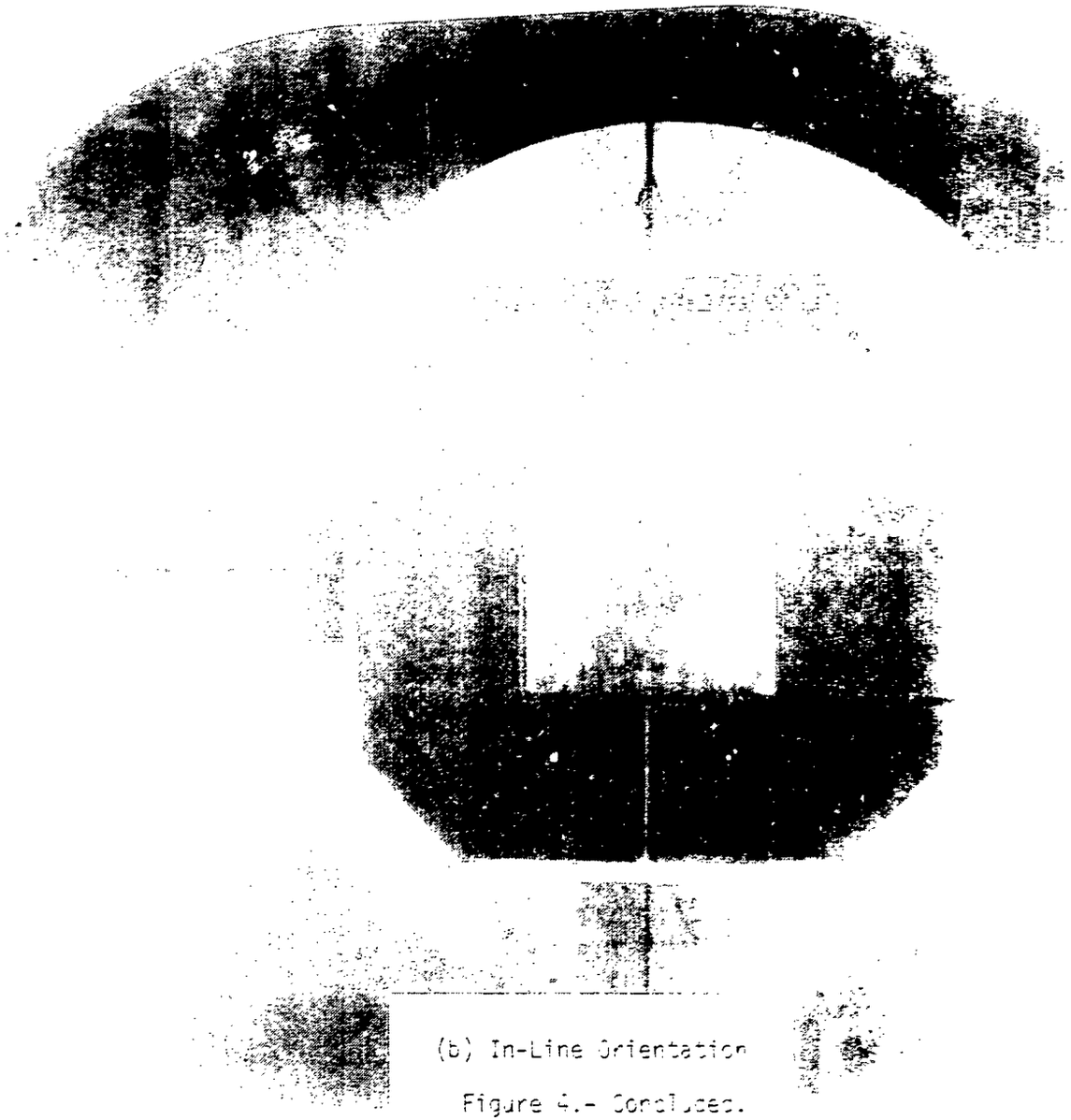

(b) In-Line Orientation

Figure 4.- Concluded.

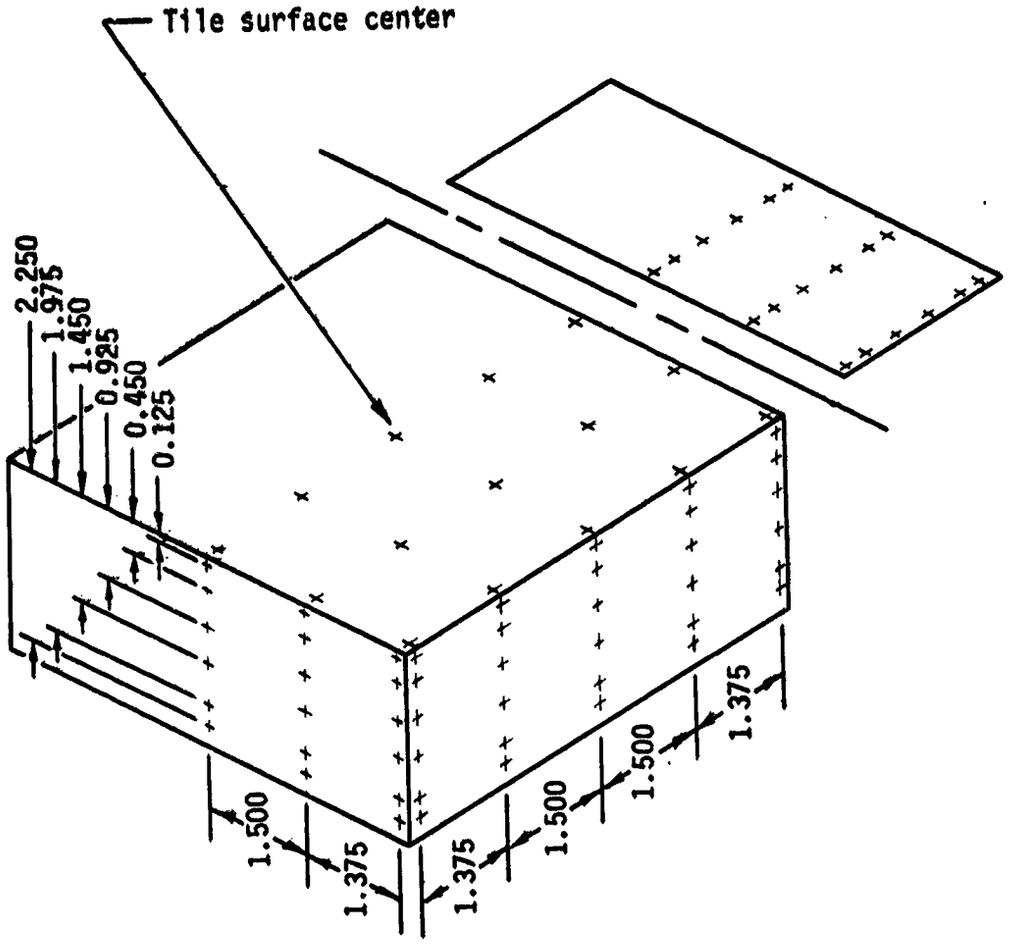

All dimensions in inches.

Figure 5.- Nominal Thermocouple Locations.

STAGGERED TILE ORIENTATION

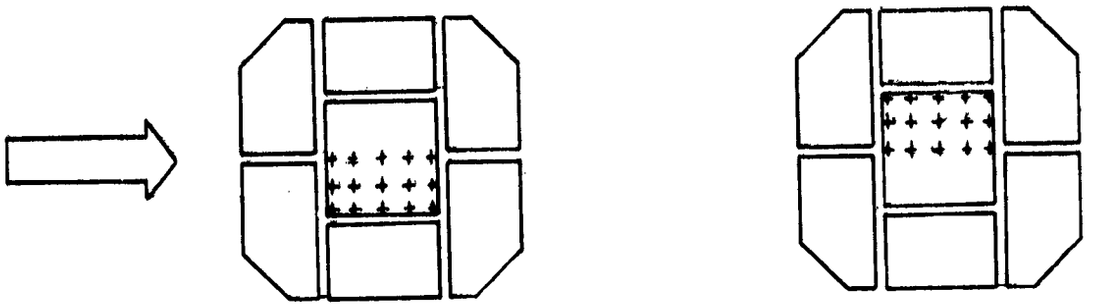

IN-LINE TILE ORIENTATION

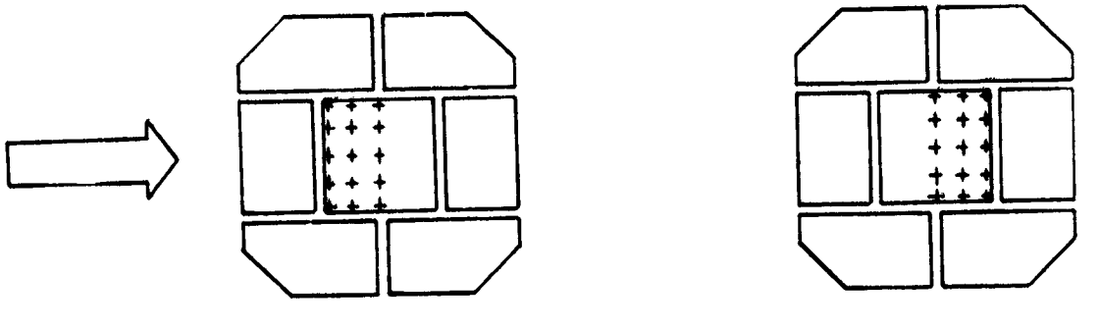

Figure 6.- Relative Location of Instrumented Portion of Thin Skin Tile.

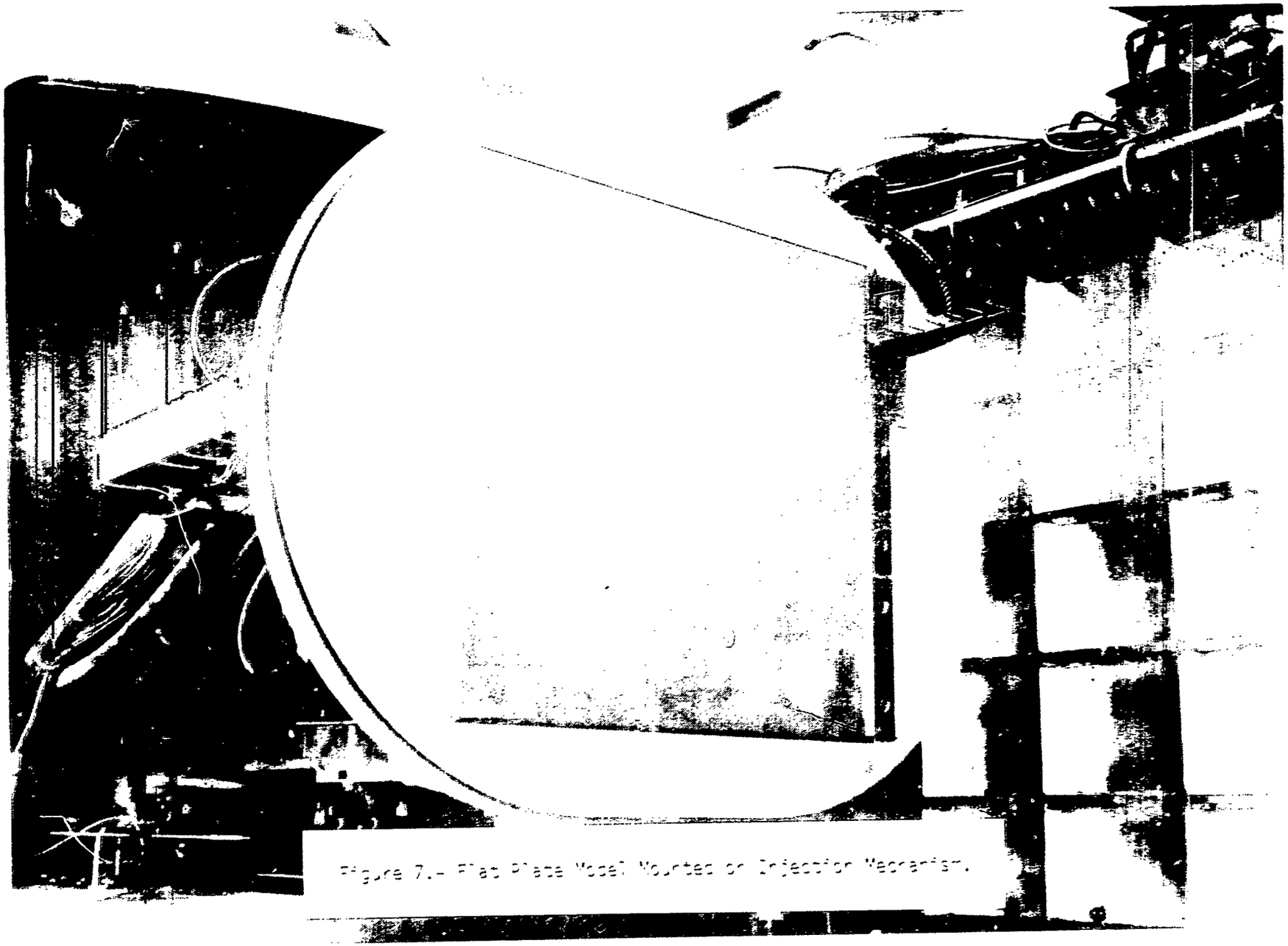

Figure 7.- Flat Plate Model Mounted on Injection Mechanism.

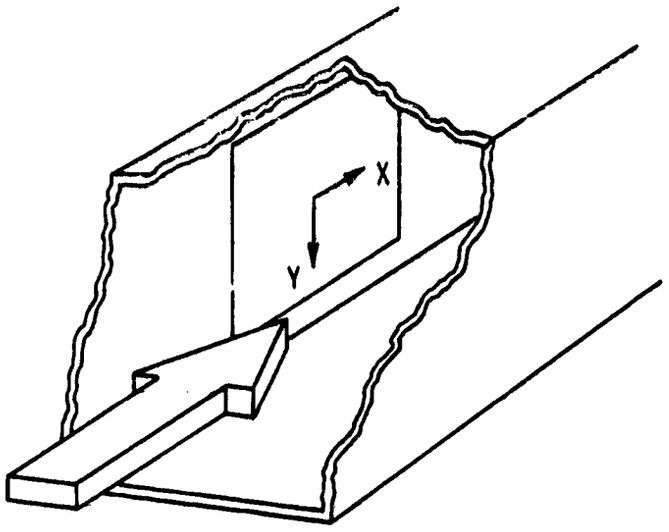

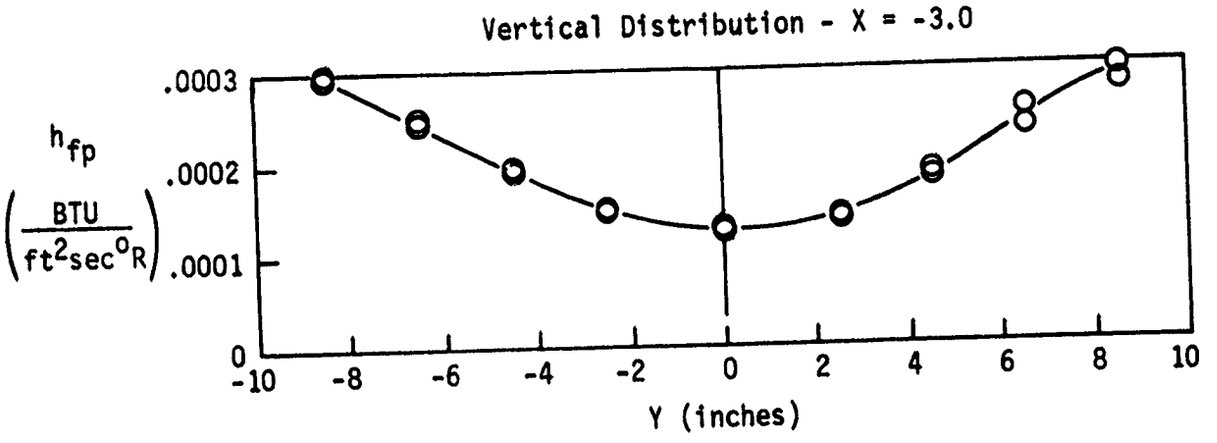

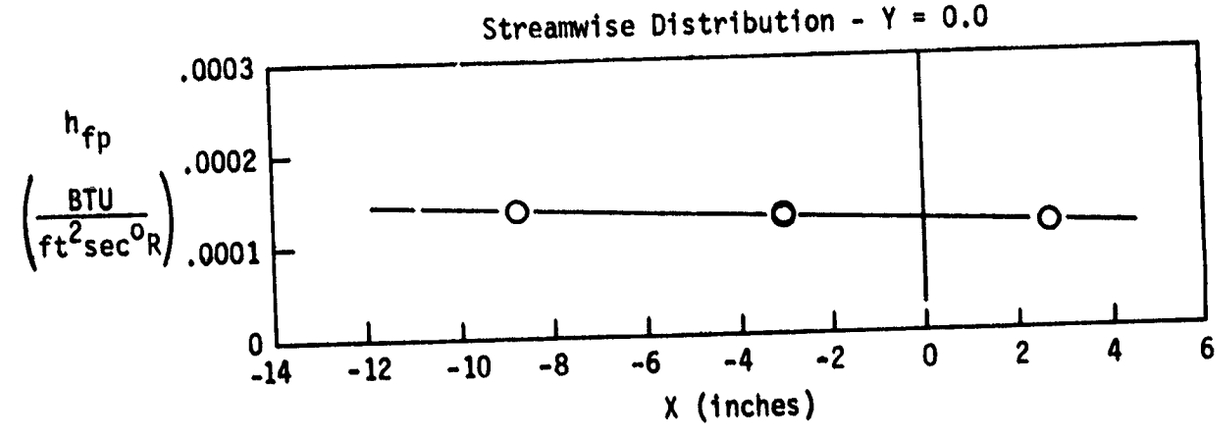

Figure 8.- Heat Transfer to Smooth Flat Plate on Tunnel Side-wall.

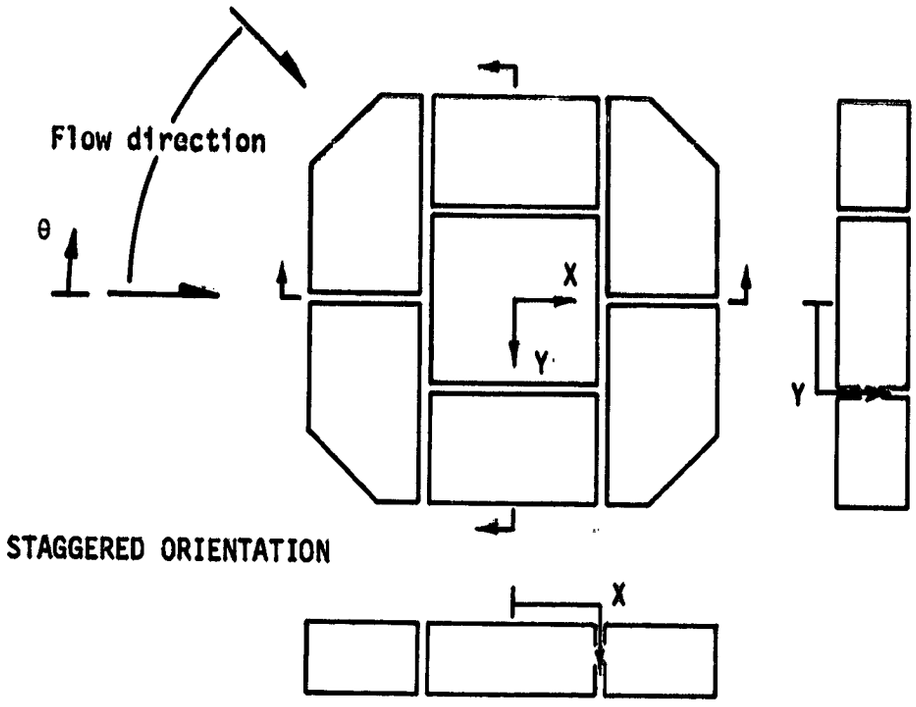

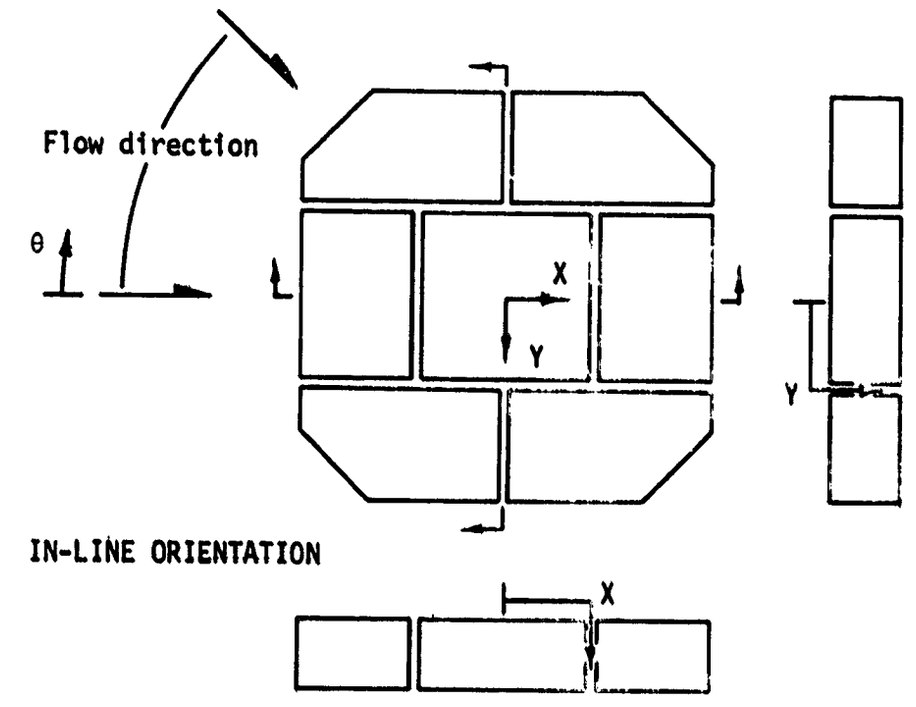

Figure 9.- Coordinate Systems Used for Data Presentation.

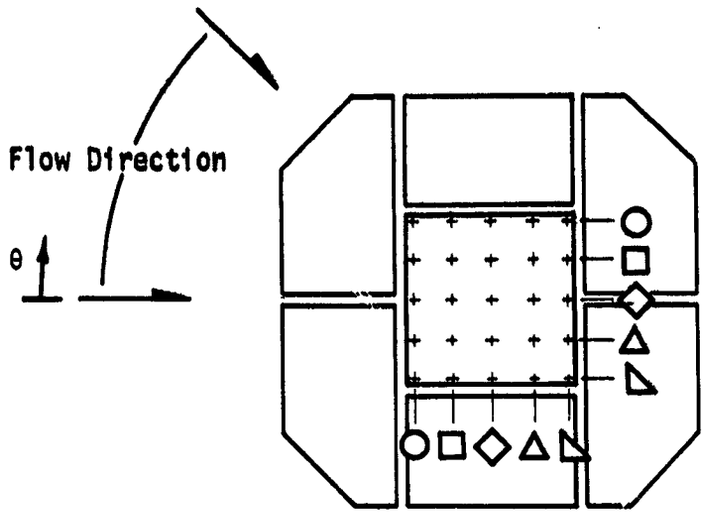

STAGGERED ORIENTATION

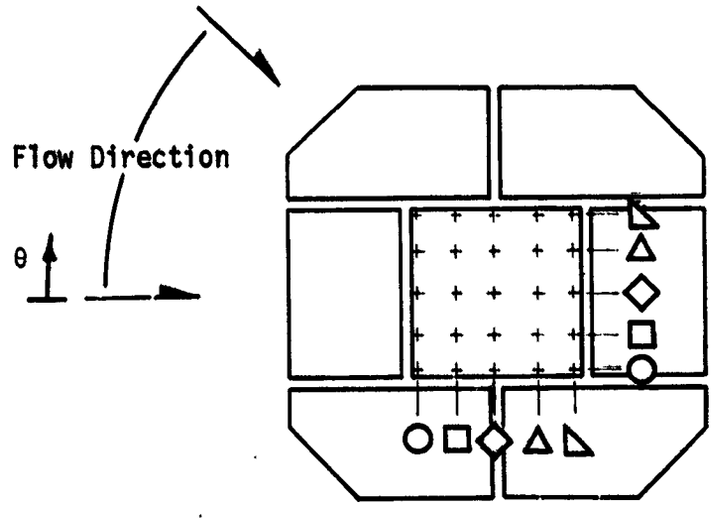

IN-LINE ORIENTATION

Figure 10.- Plot Symbols Used for Data Presentation.

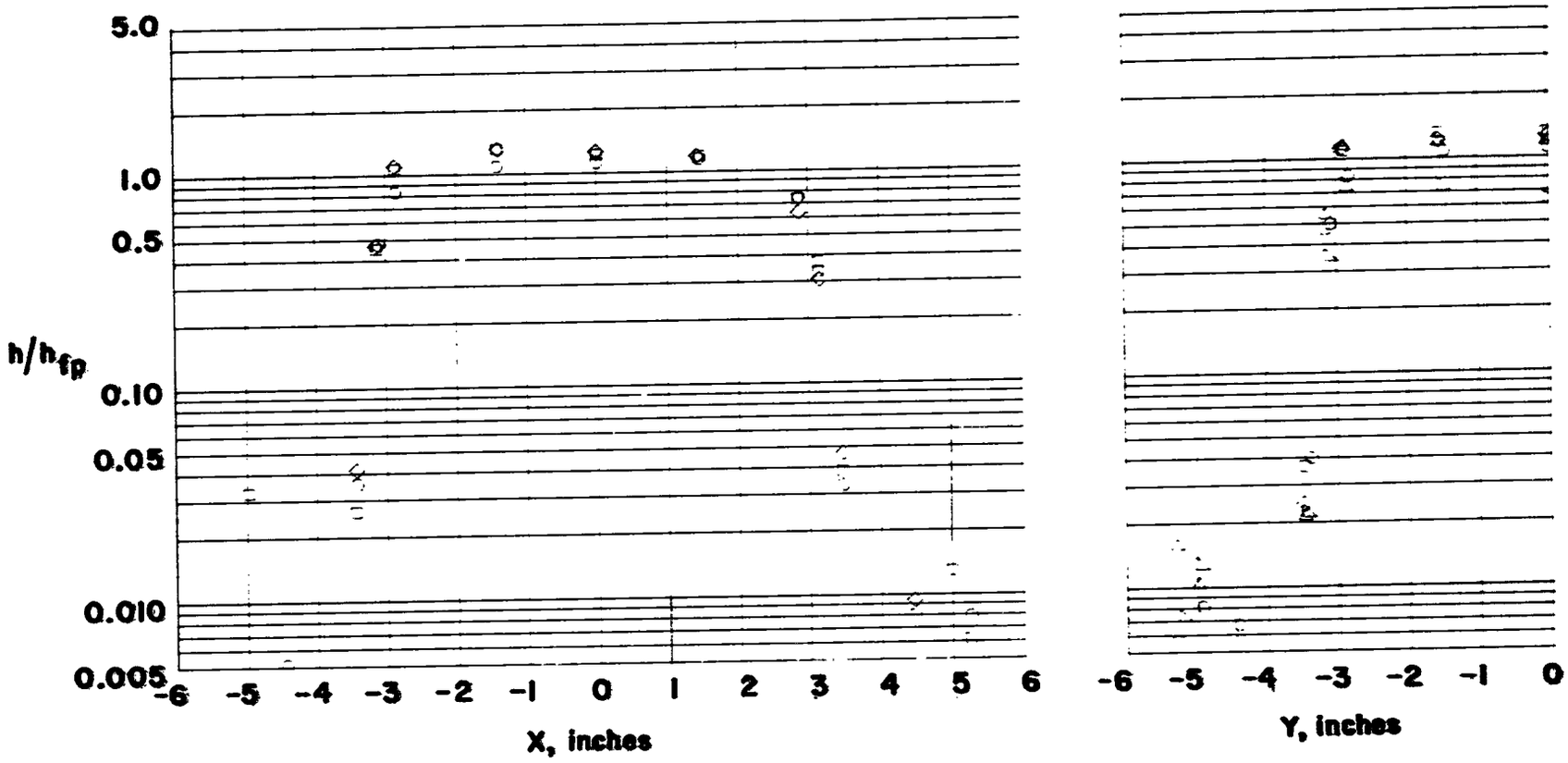

(a) θ = 0.0 degs.

Figure 11. - Heating to a flush mounted tile in a staggered array. w = 0.05 in.

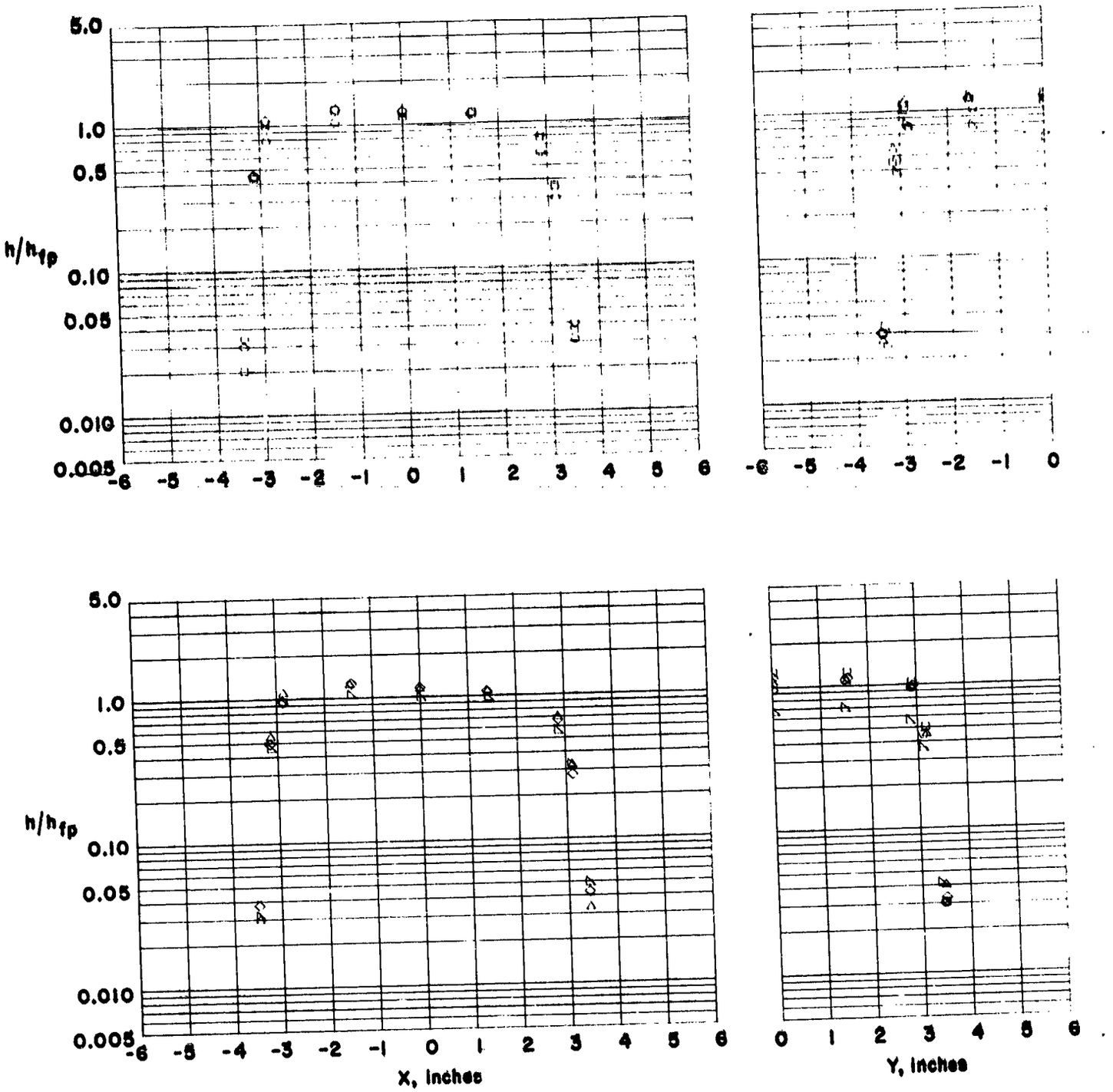

(b) θ = 7.5 degs.

Figure 11. - Continued.

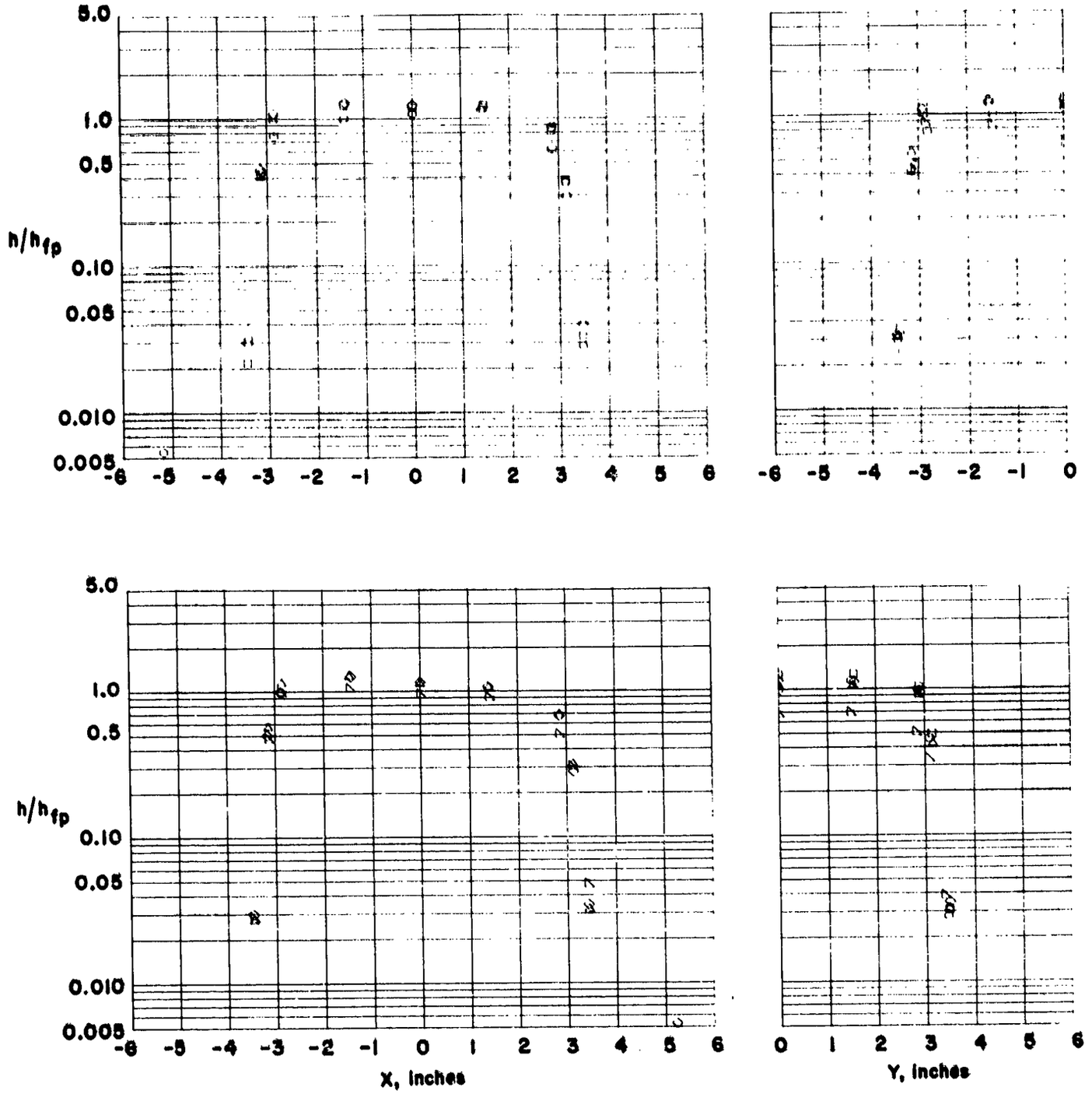

(c) θ = 15.0 degs.

Figure 11. - Continued.

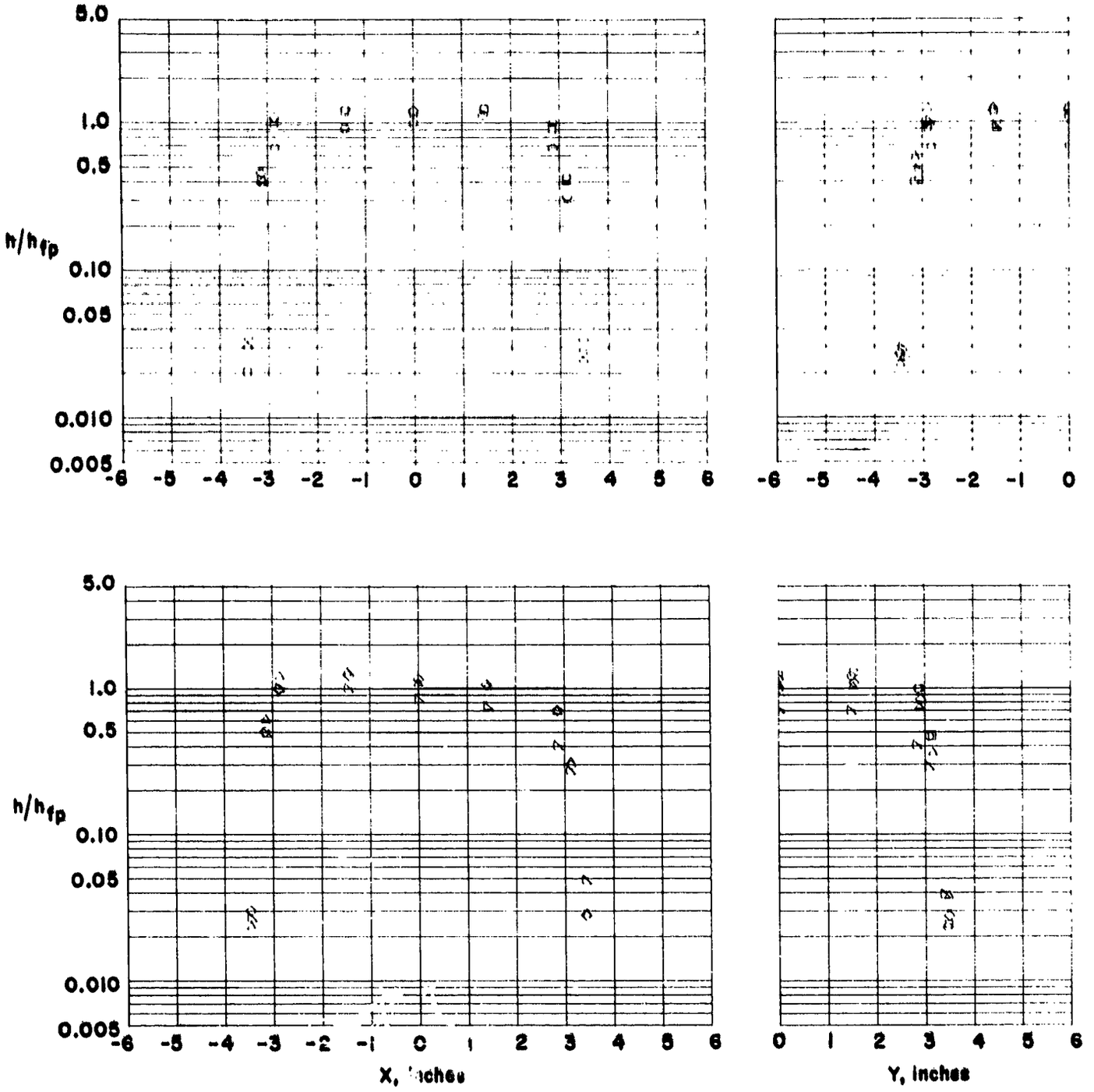

(d) θ = 30.0 degs.

Figure 11. - Continued.

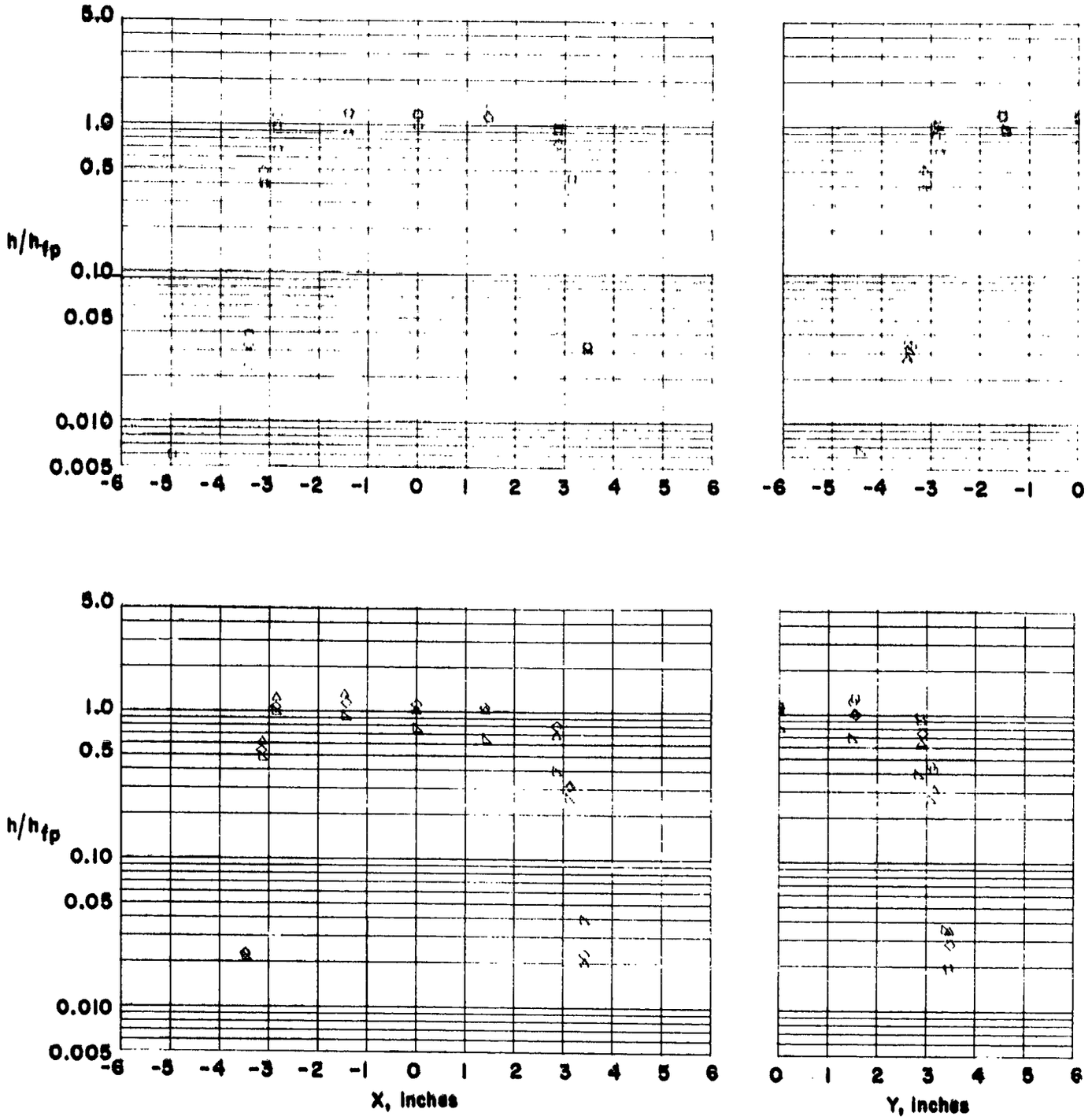

(e) θ = 45.0 degs.

Figure 11. - Concluded.

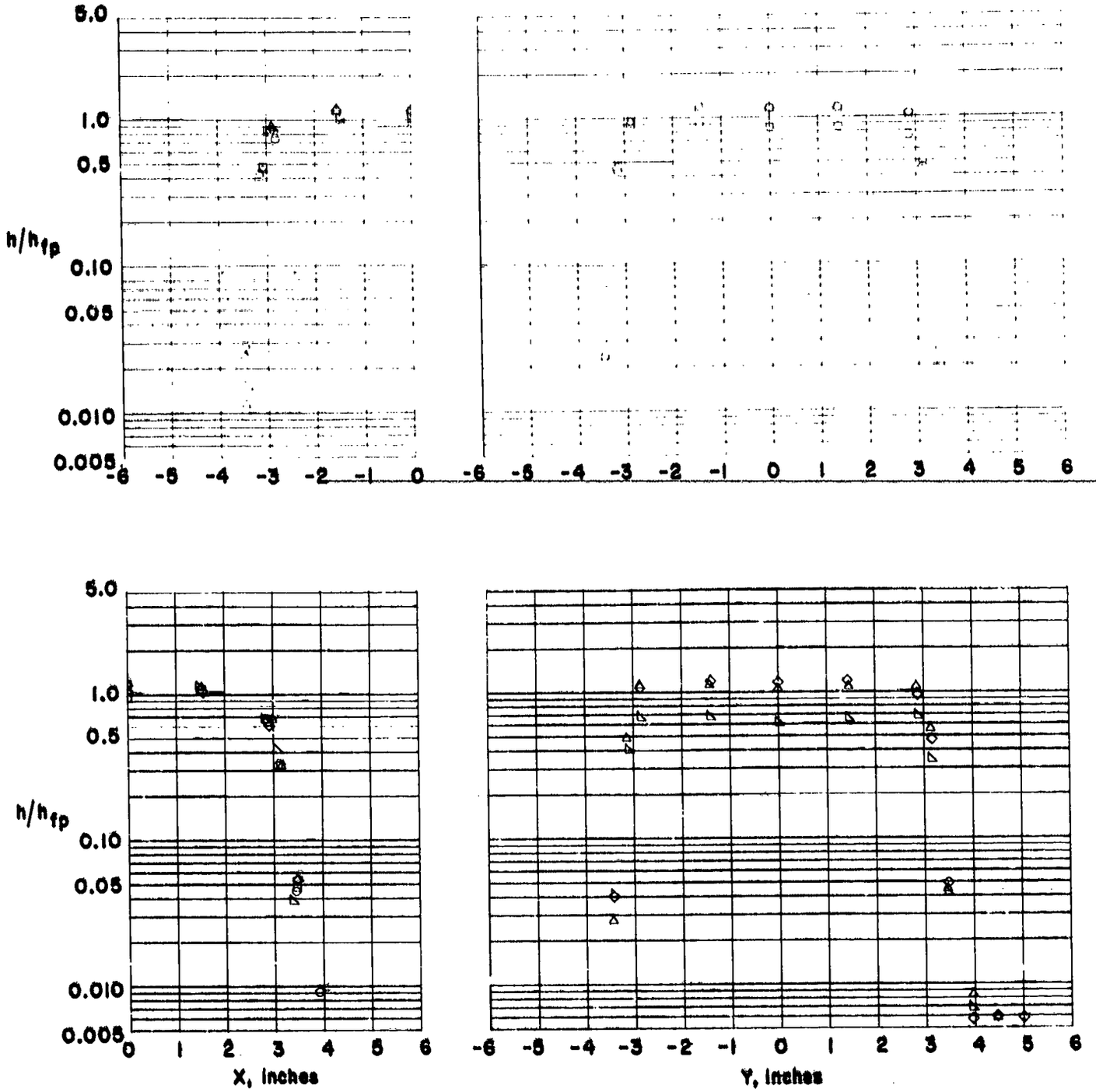

(a) θ = 0.0 degs.

Figure 12.- Heating to a flush mounted tile in an in-line array. w = 0.05 in.

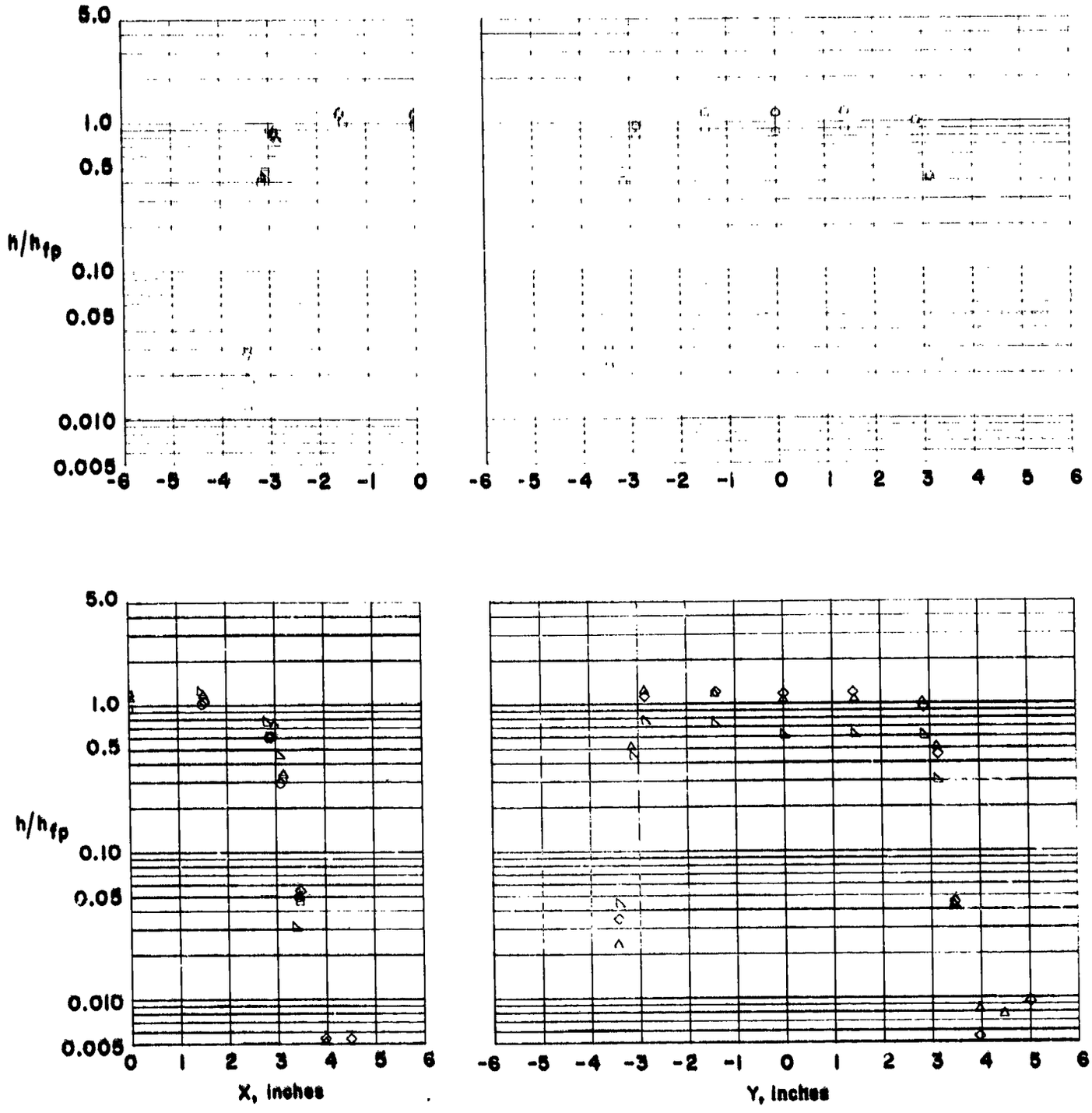

(b) θ = 7.5 degs.

Figure 12 - Continued.

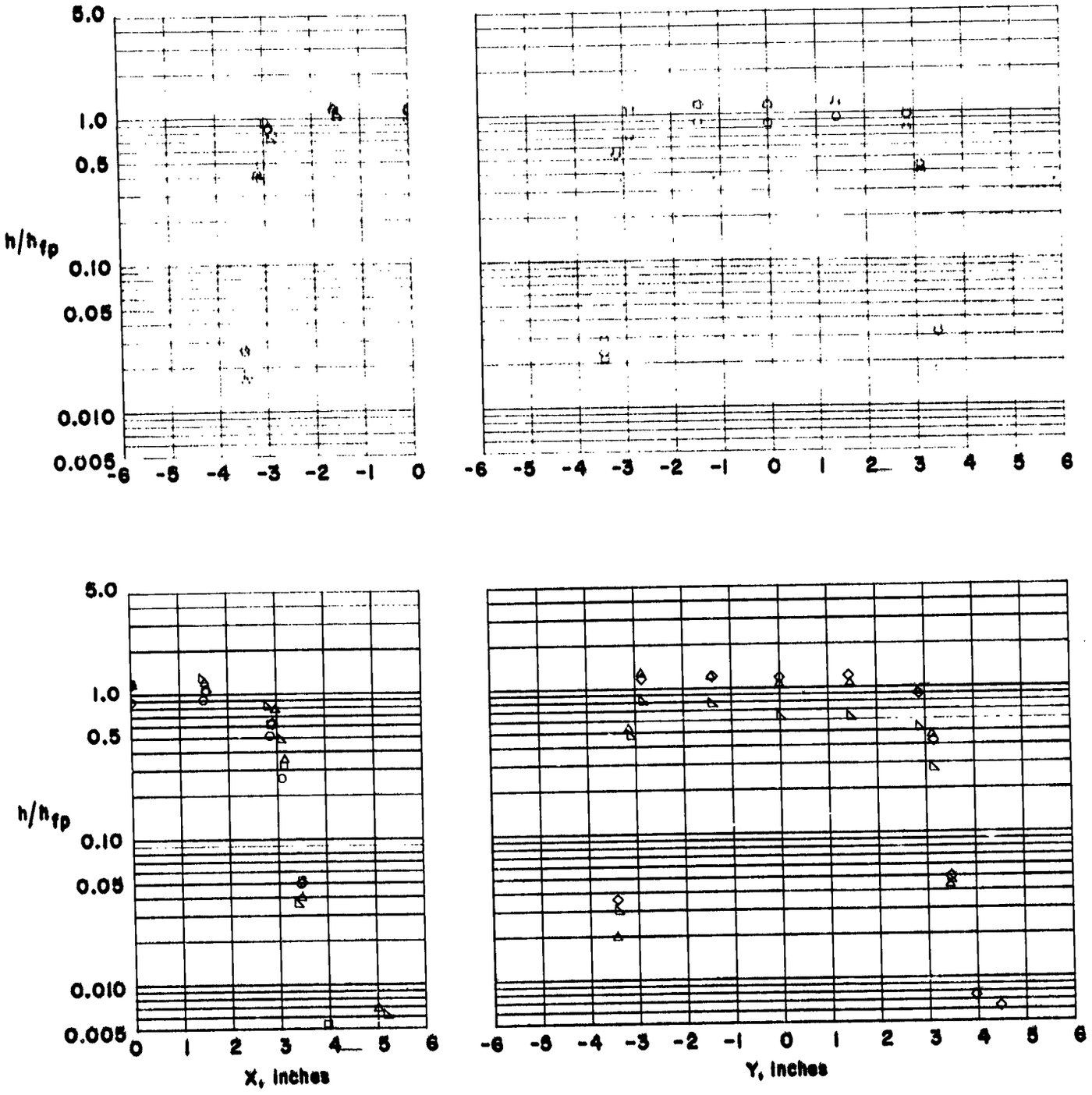

(c) θ = 15.0 degs.

Figure 12 - Continued.

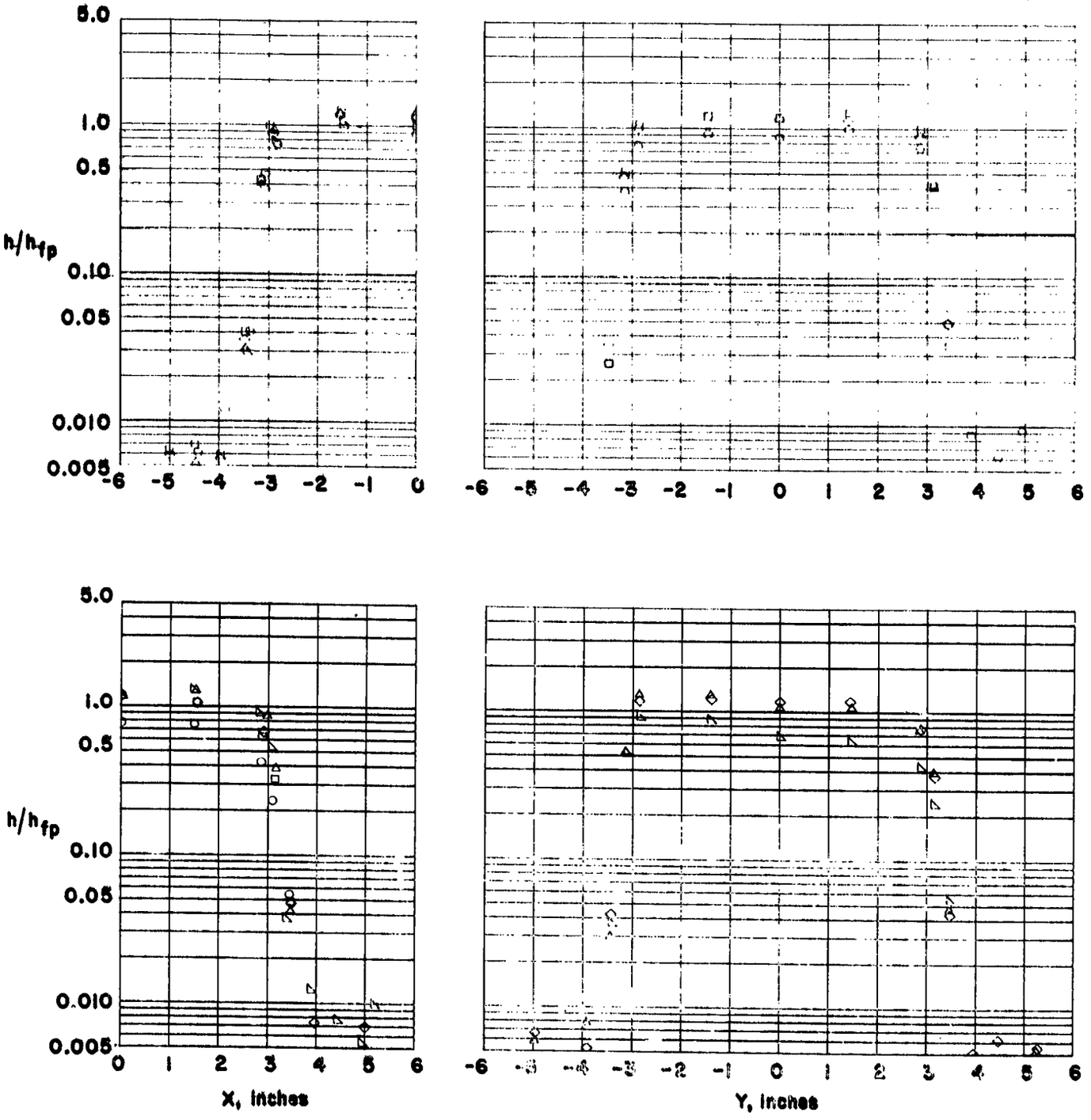

(d) θ = 30.0 degs.

Figure 12 - Concluded.

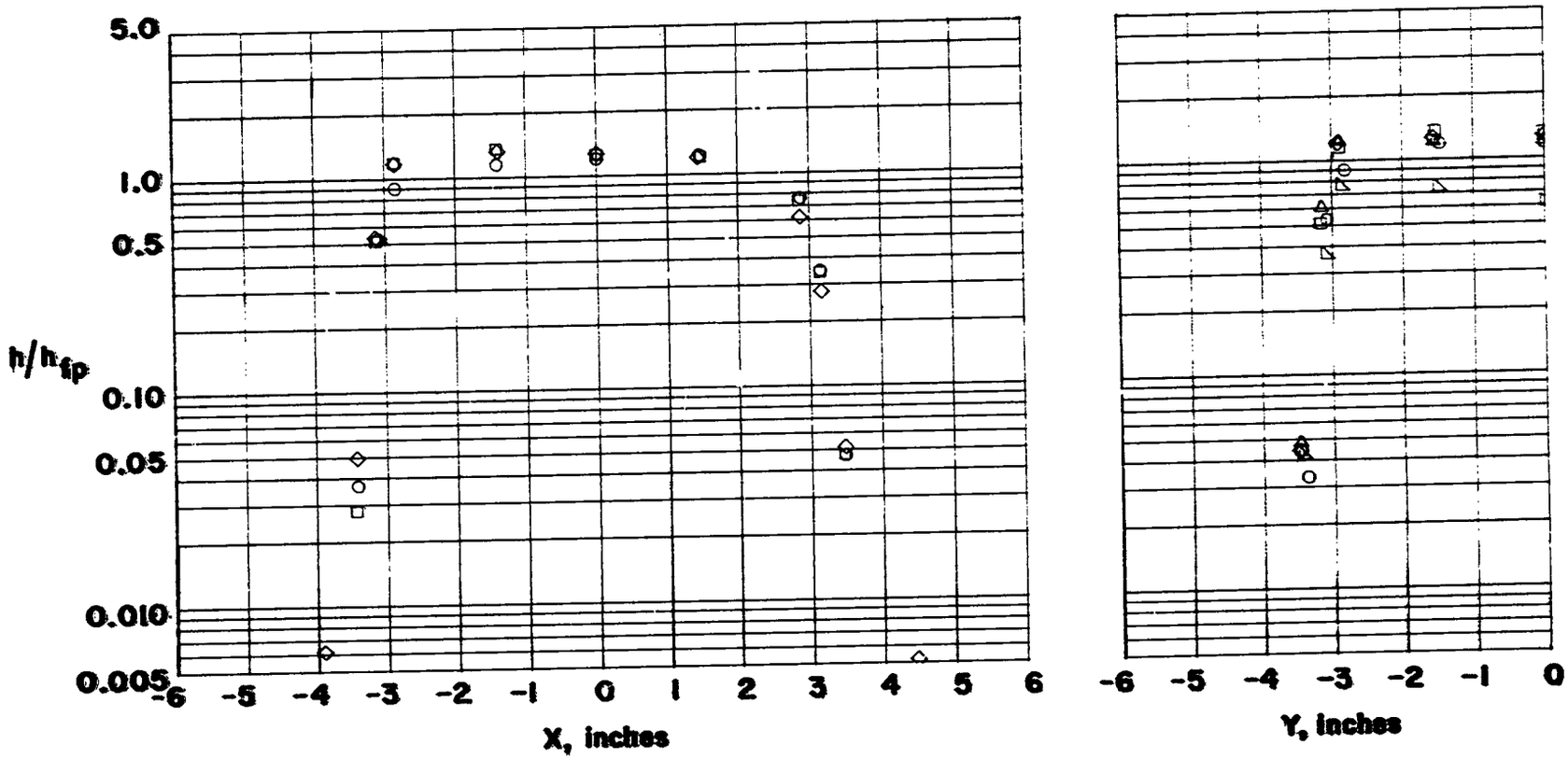

(a) θ = 0.0 degs.

Figure 13. - Heating to a flush mounted tile in a staggered array. w = 0.09 in.

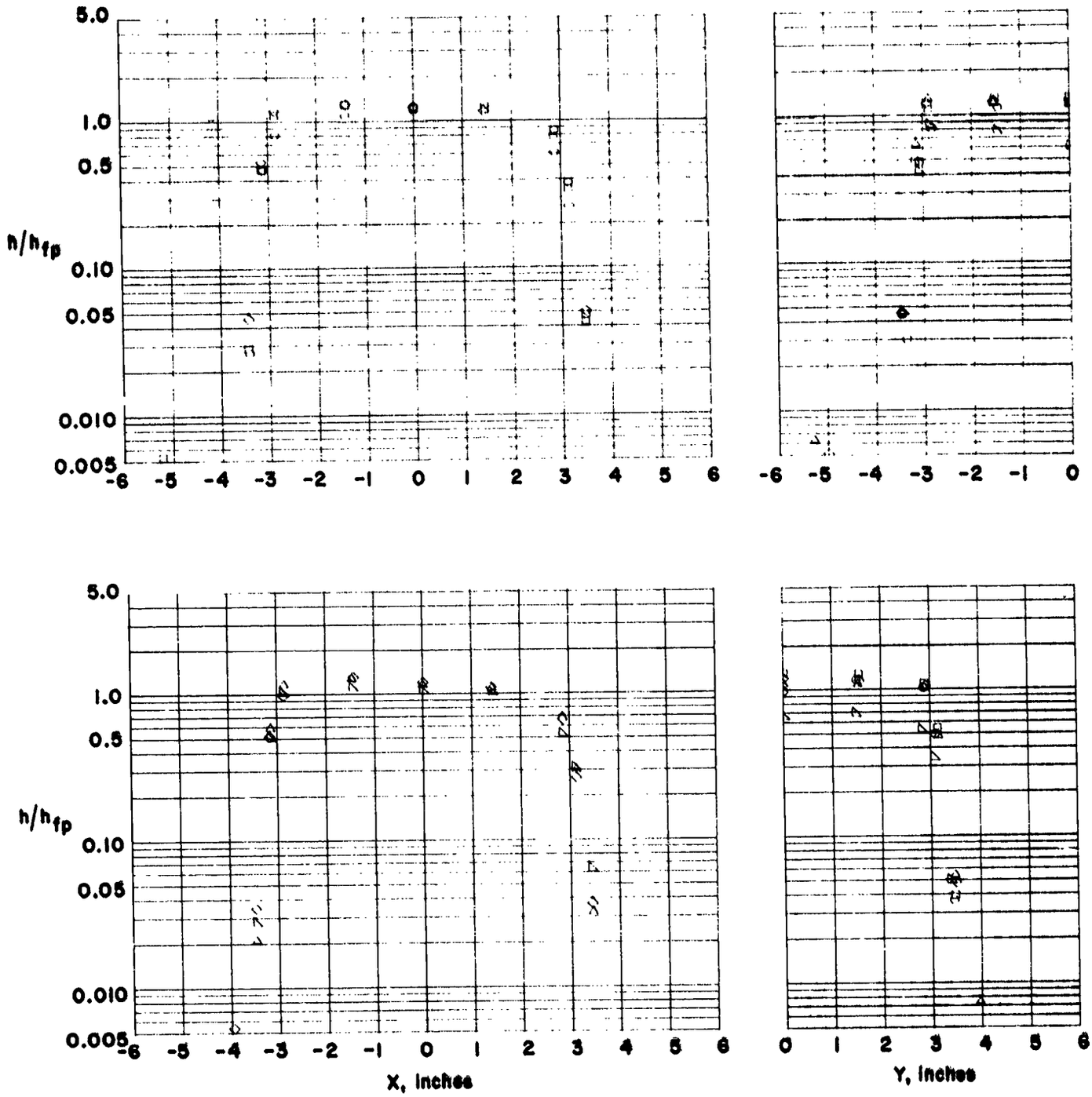

(b) θ = 7.5 degs.

Figure 13. - Continued.

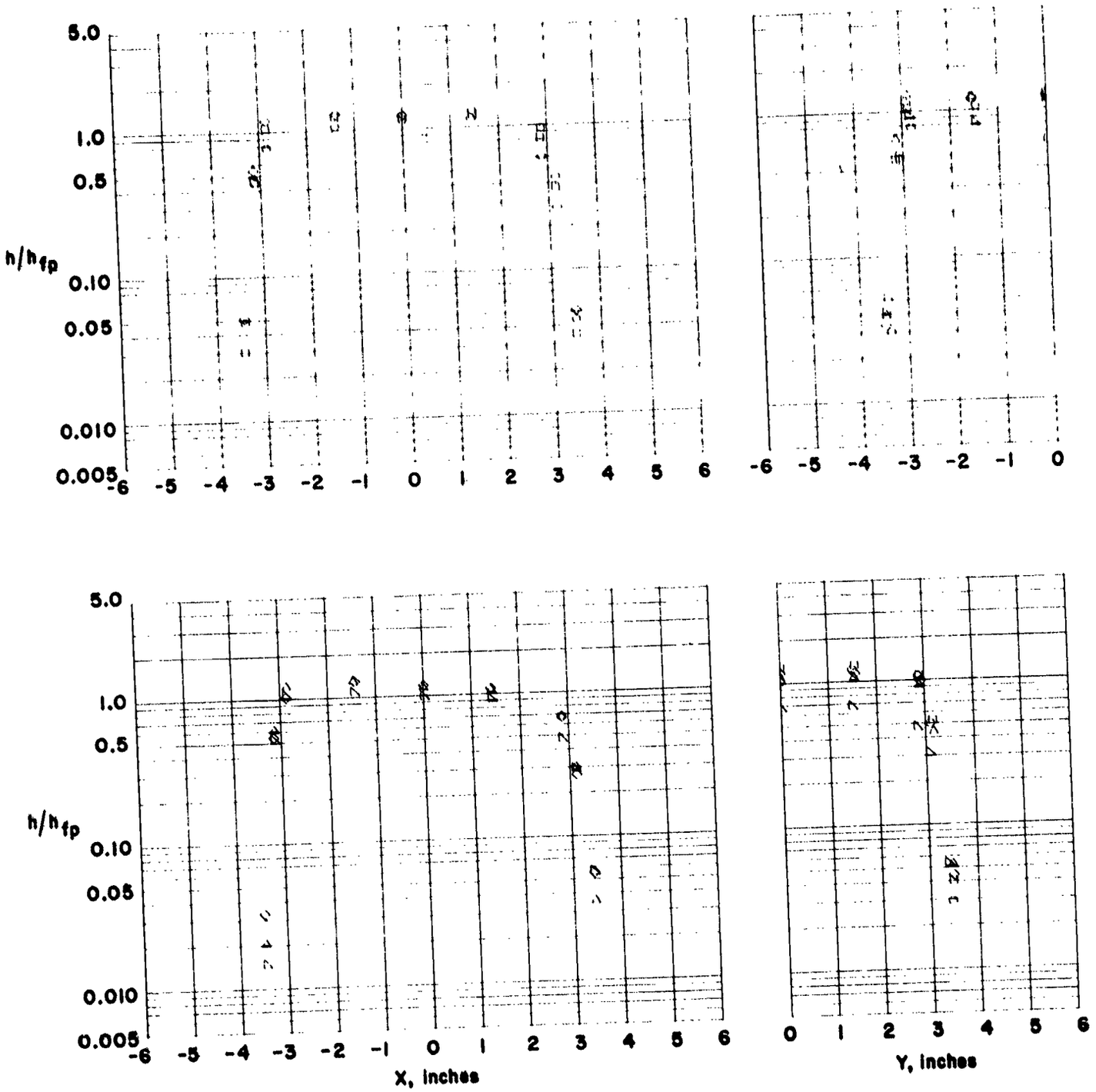

(c) θ = 15.0 degs.

Figure 13. - Continued.

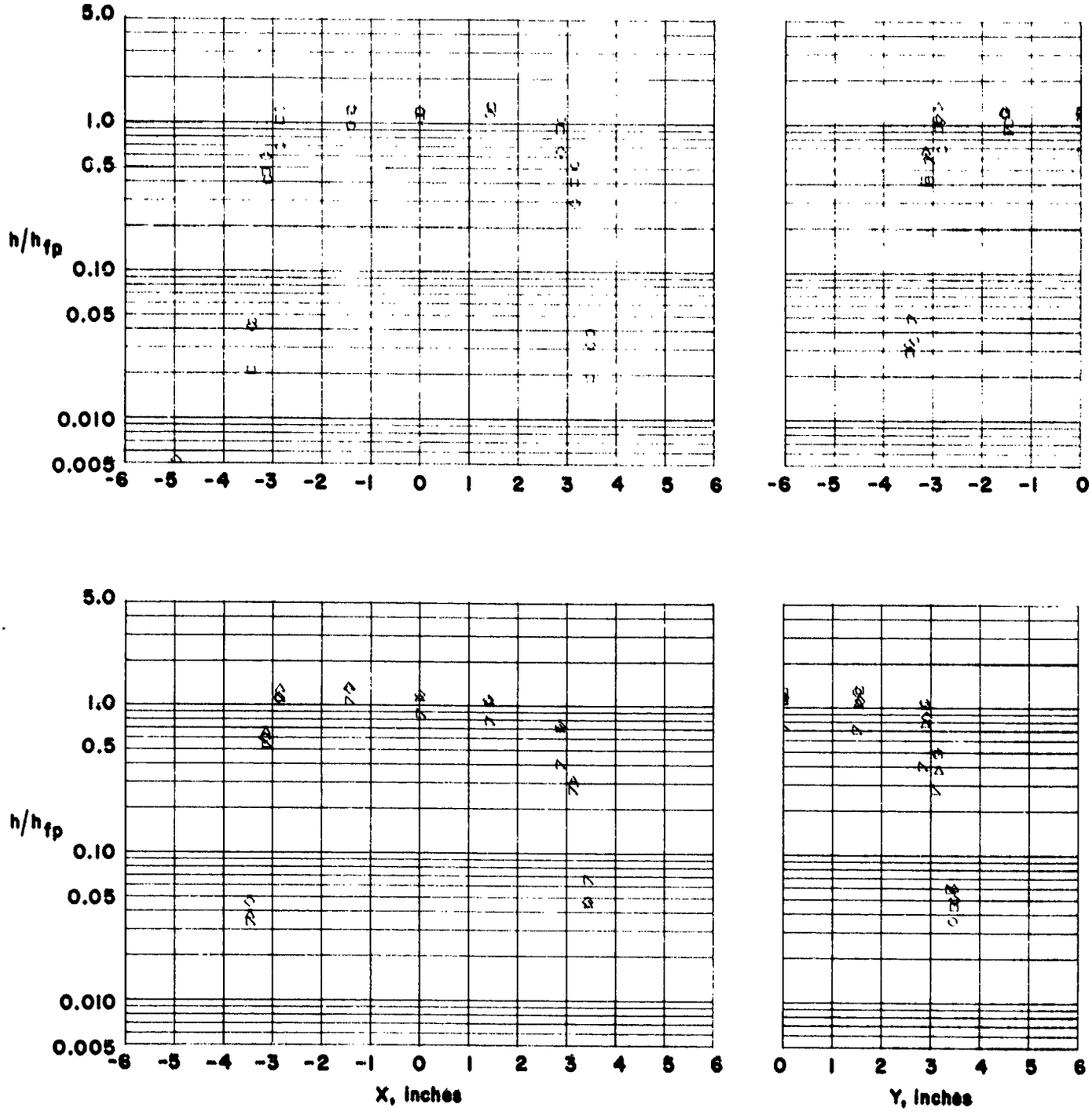

(d) θ = 30.0 degs.

Figure 13. - Continued.

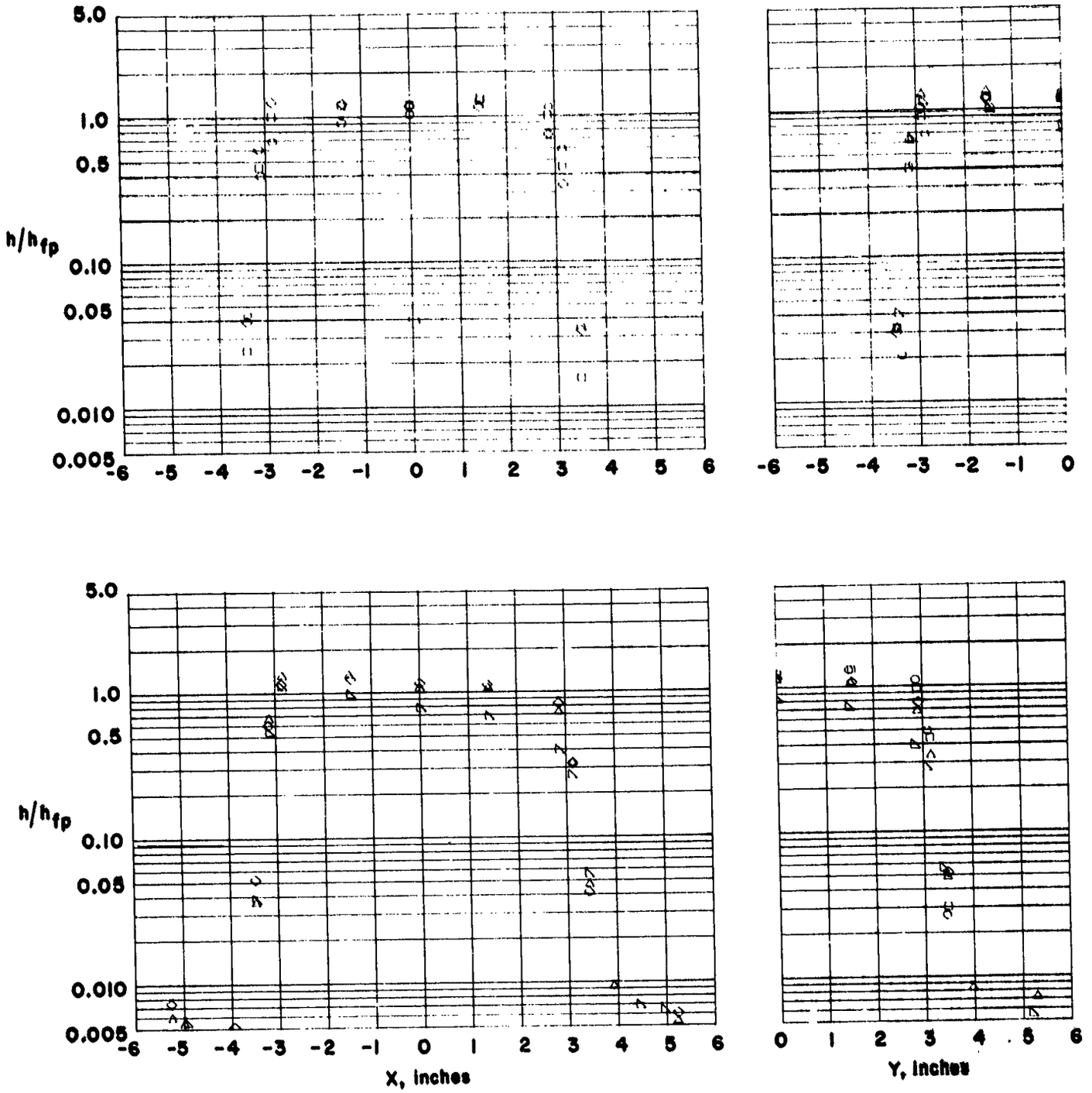

(e) θ = 45.0 degs.

Figure 13. - Concluded.

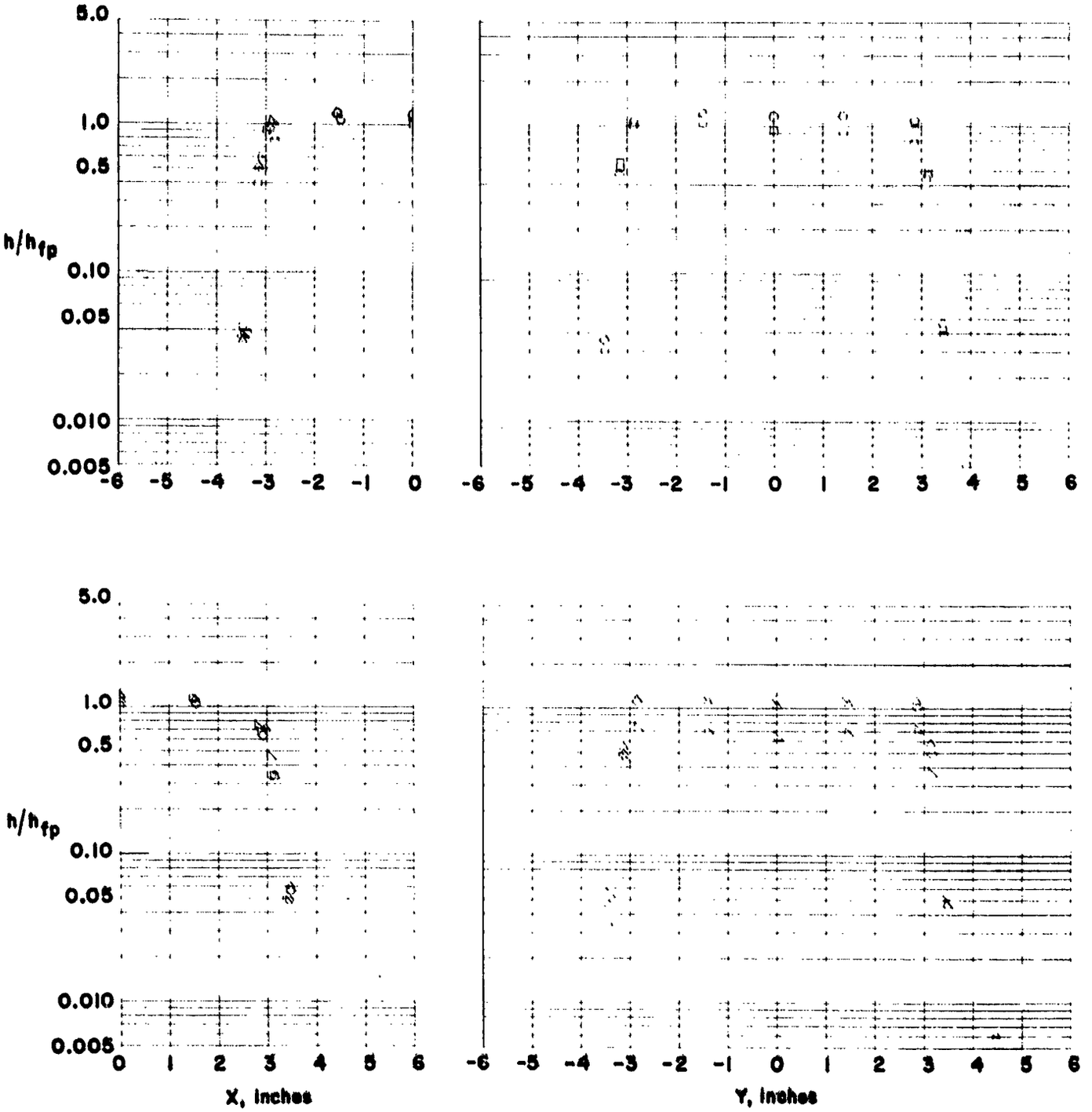

(a) θ = 0.0 degs.

Figure 14. - Heating to a flush mounted tile in an in-line array. w = 0.09 in.

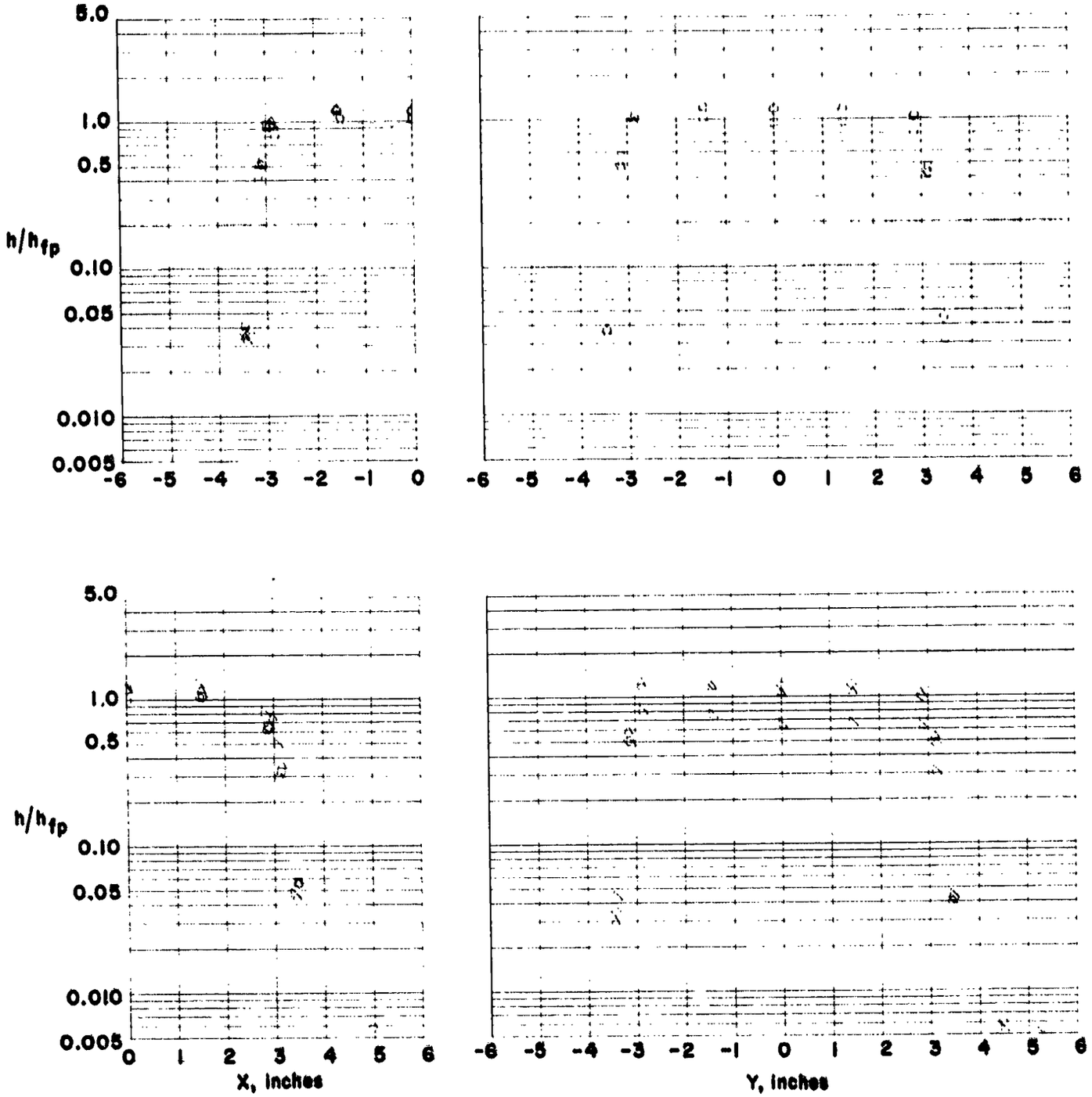

(b) θ = 7.5 degs.

Figure 14. - Continued.

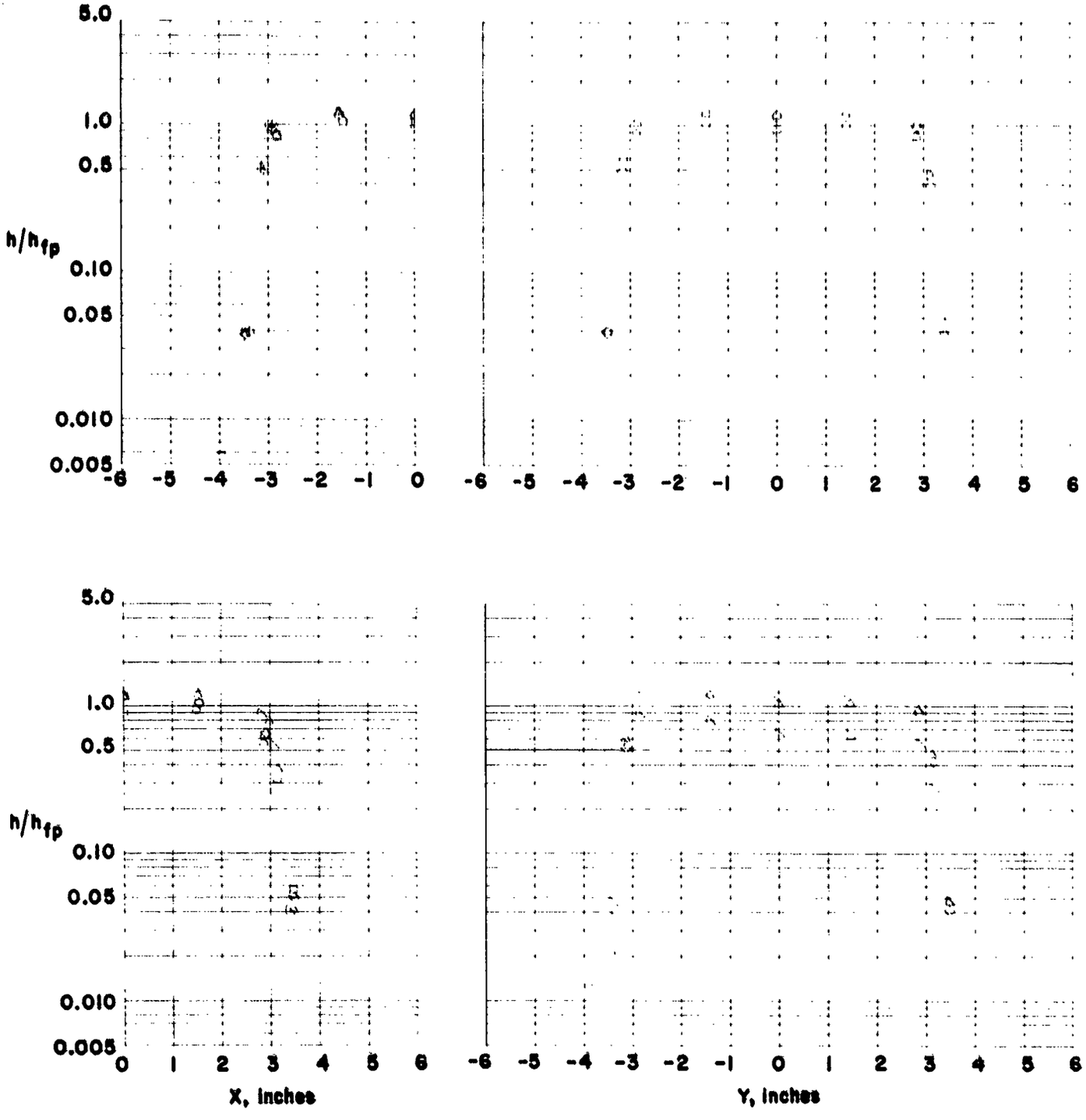

(c) θ = 15.0 degs.

Figure 14. - Continued.

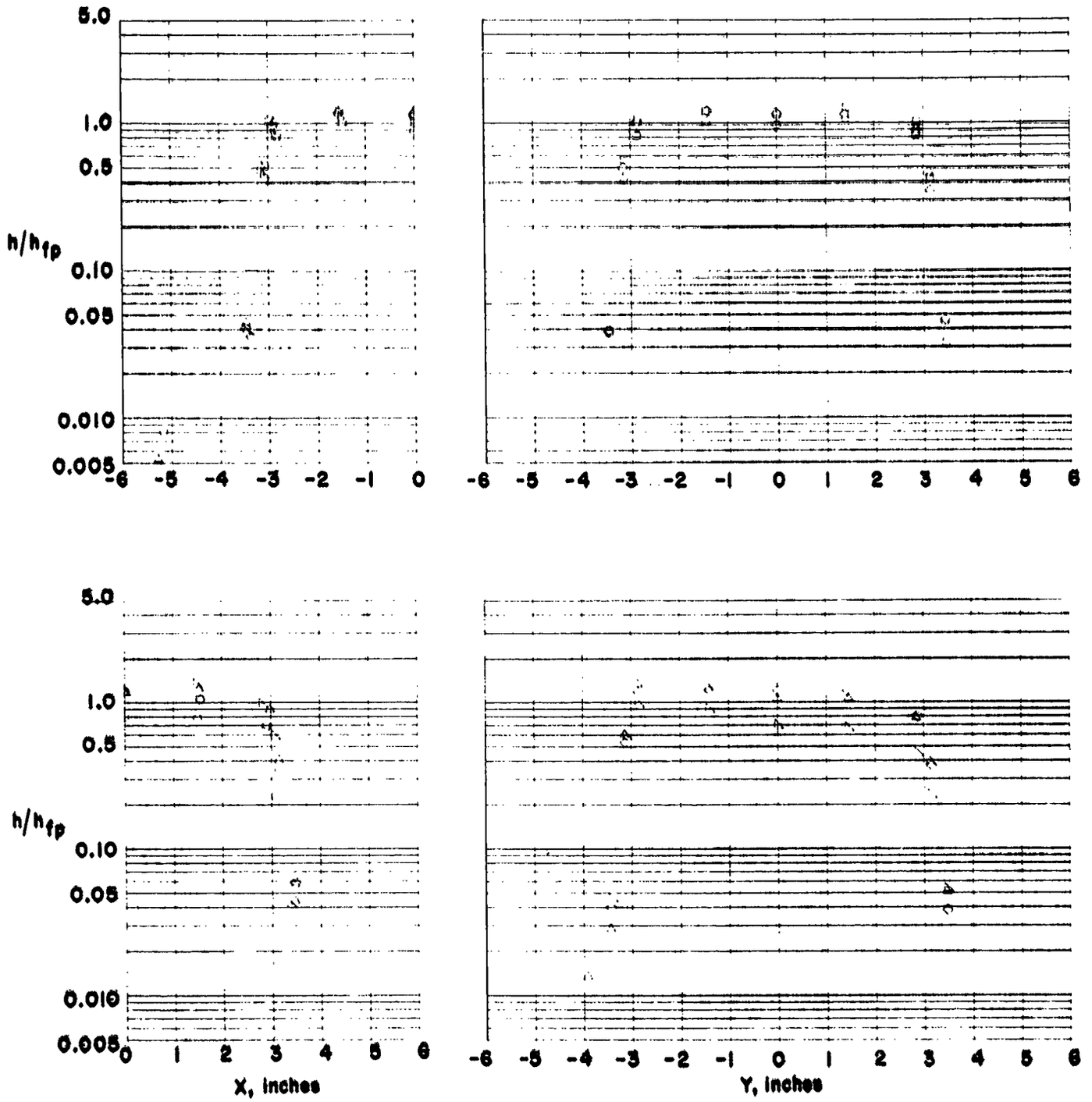

(d) θ = 30.0 degs.

Figure 14. - Concluded.

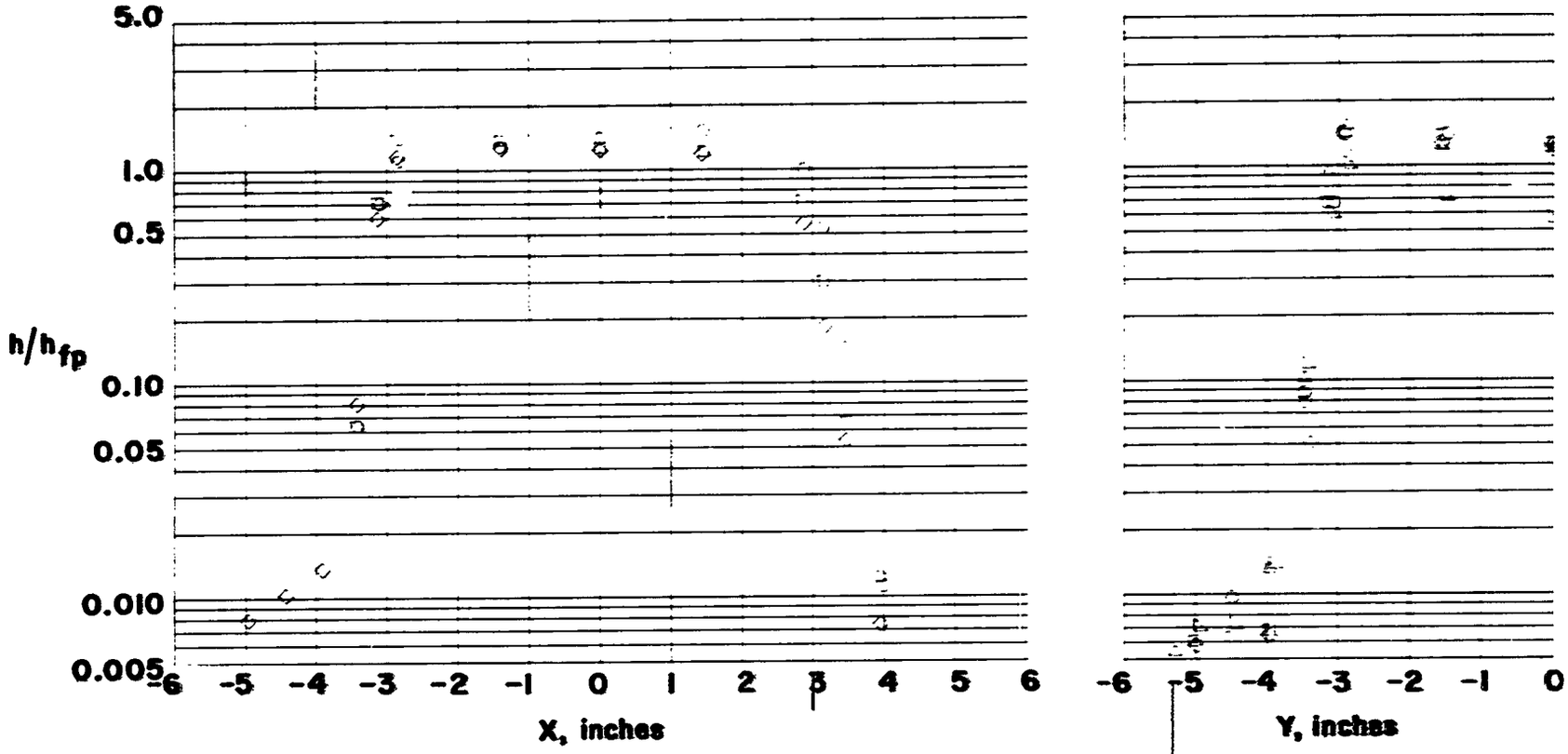

(a) θ = 0.0 degs.

Figure 15.- Heating to a flush mounted tile in a staggered array. w = 0.18 in.

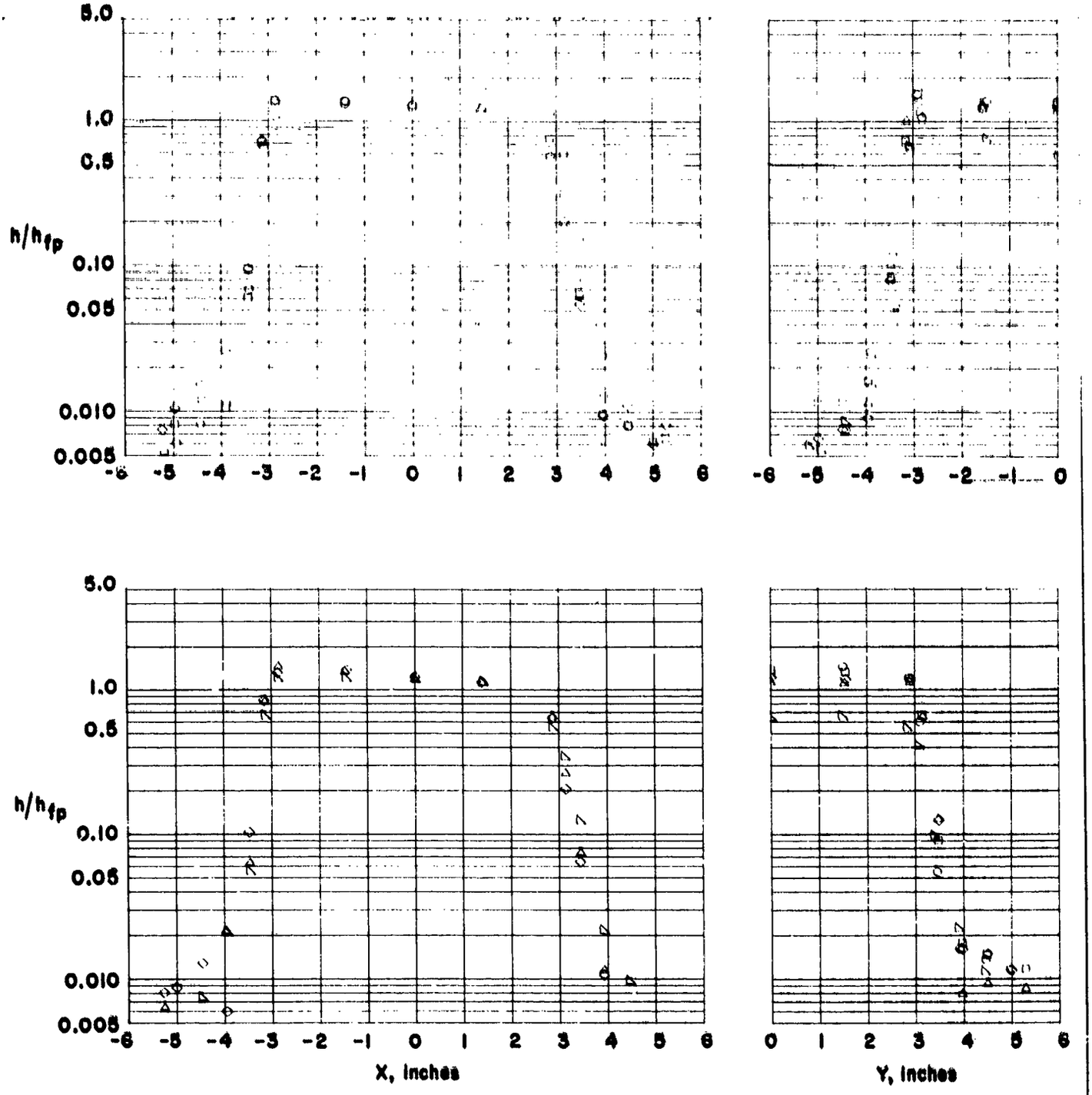

(b) θ = 7.5 degs.

Figure 15. - Continued.

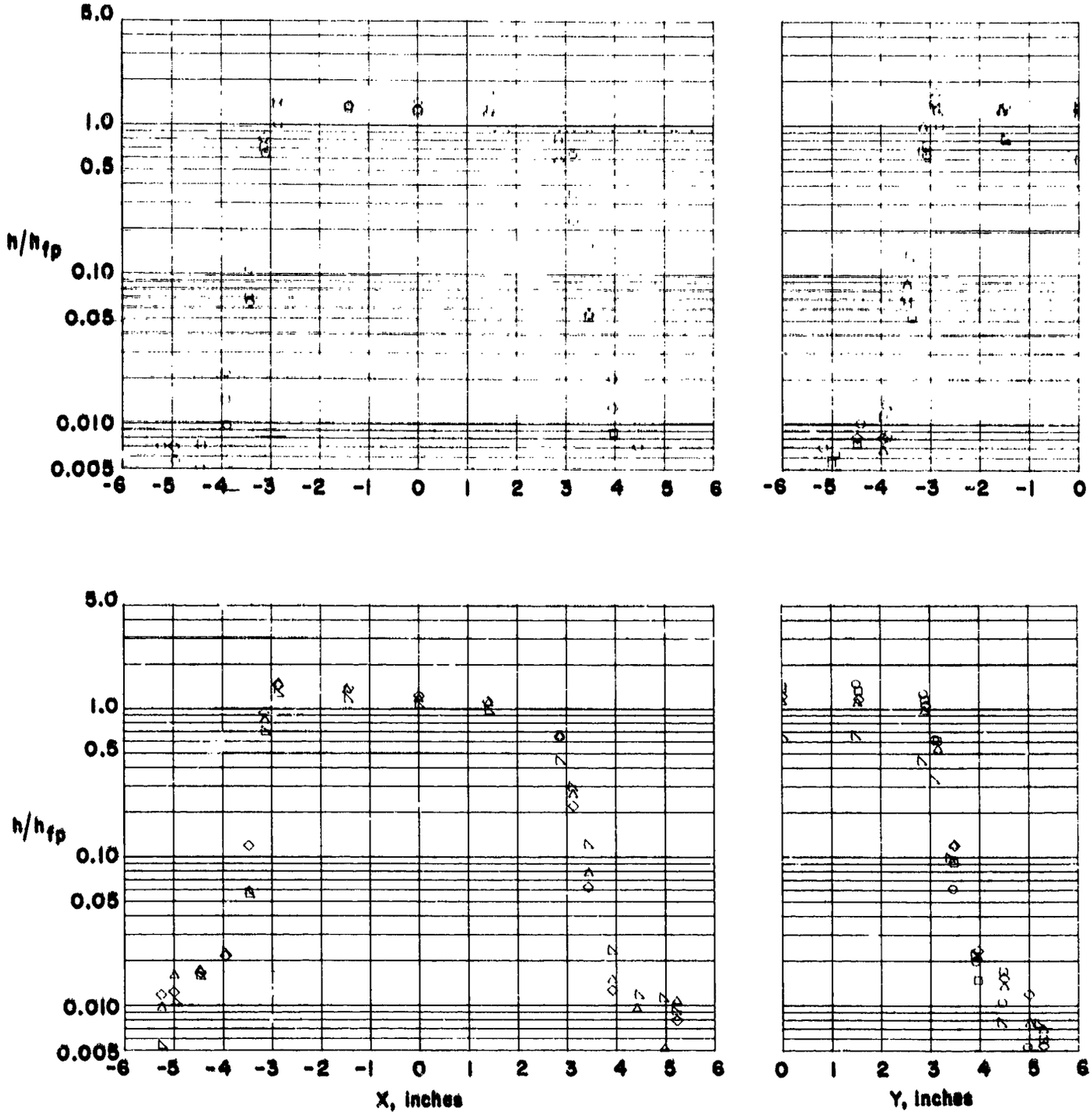

(c) θ = 15.0 degs.

Figure 15. - Continued.

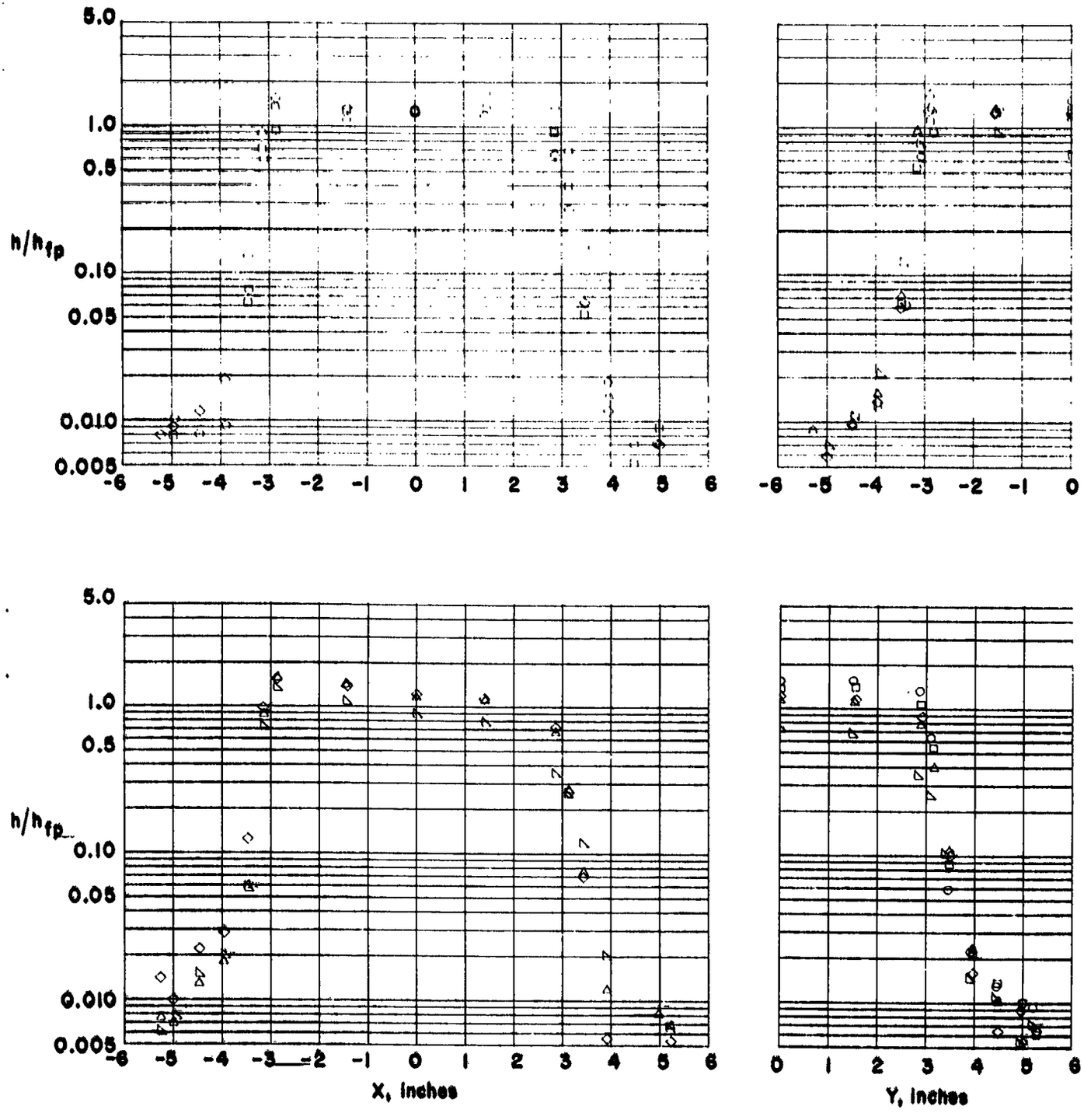

(d) θ = 30.0 degs.

Figure 15. - Continued.

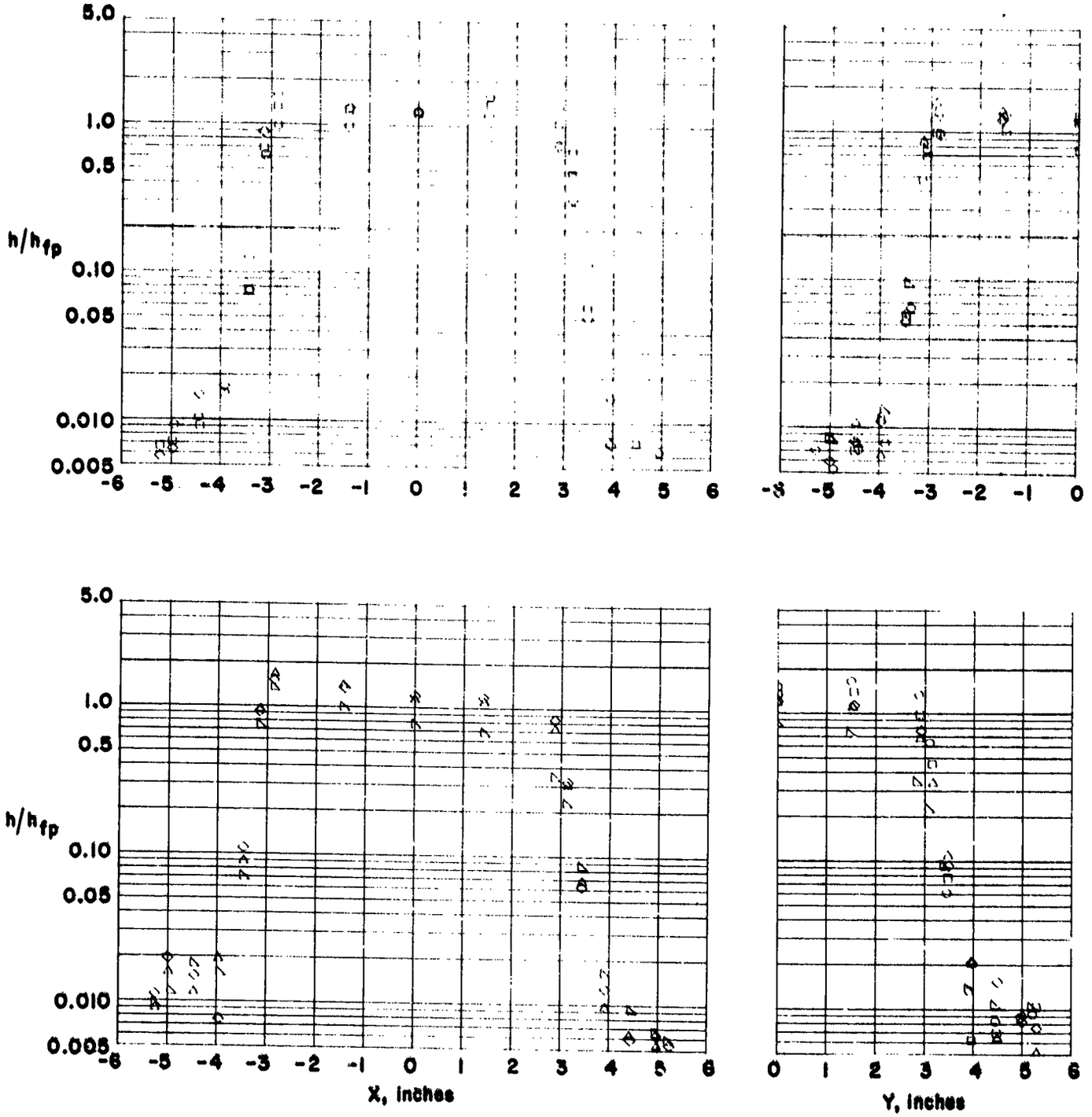

(e) θ = 45.0 degs.

Figure 15. - Concluded.

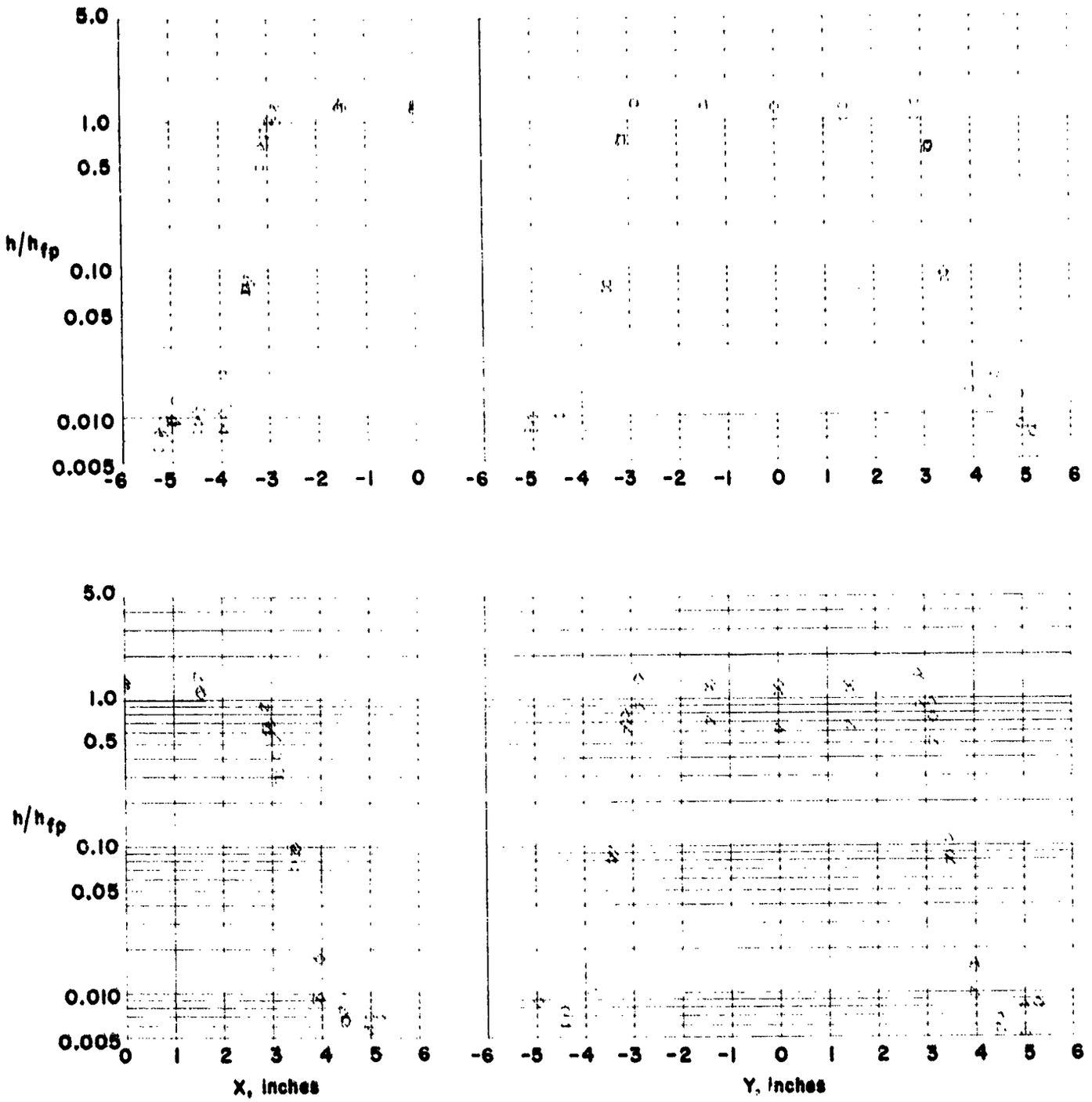

(a) θ = 0.0 degs.

Figure 16. - Heating to a flush mounted tile in an in-line array. w = 0.18 in.

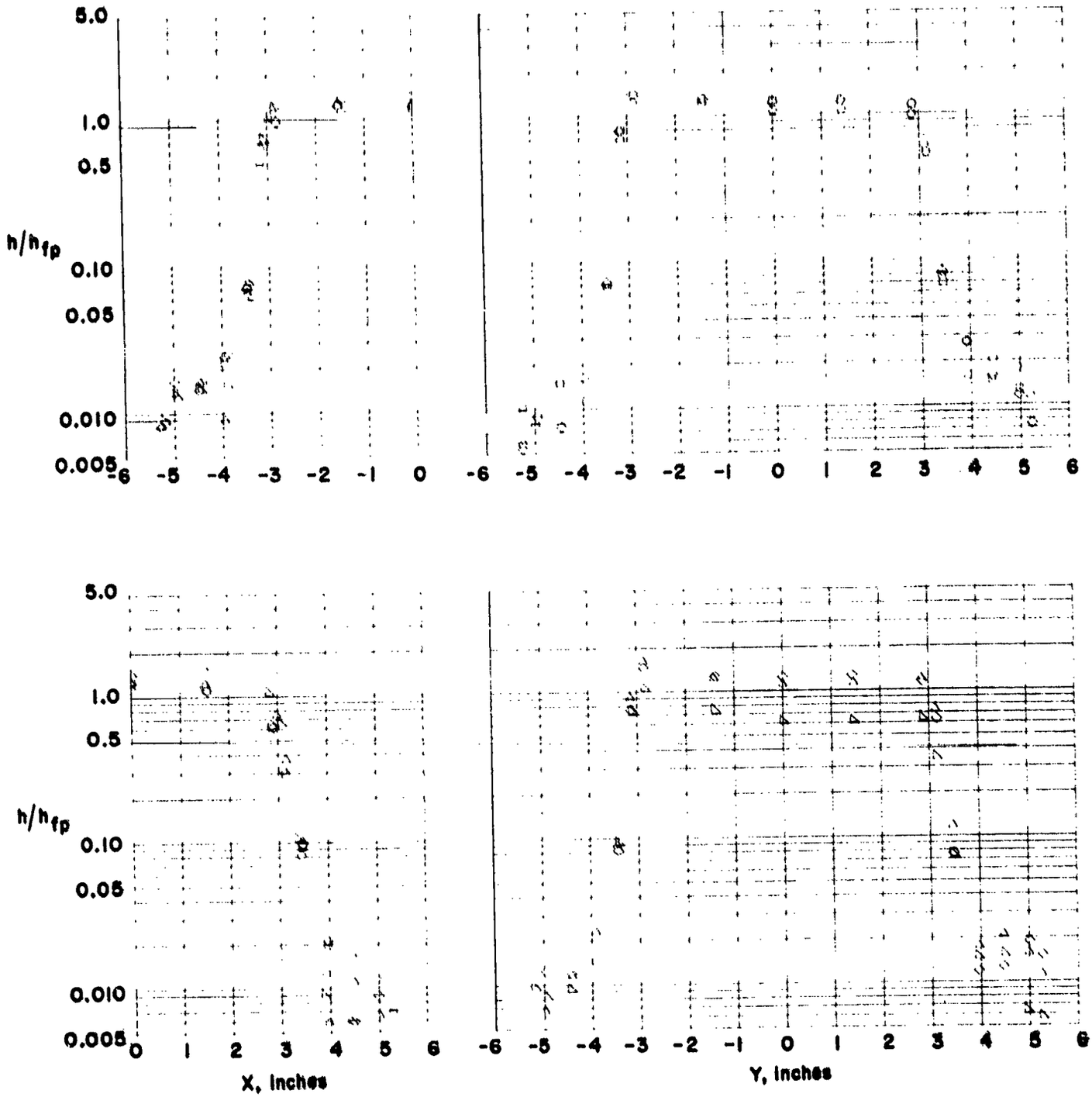

(b) θ = 7.5 degs.

Figure 16. - Continued.

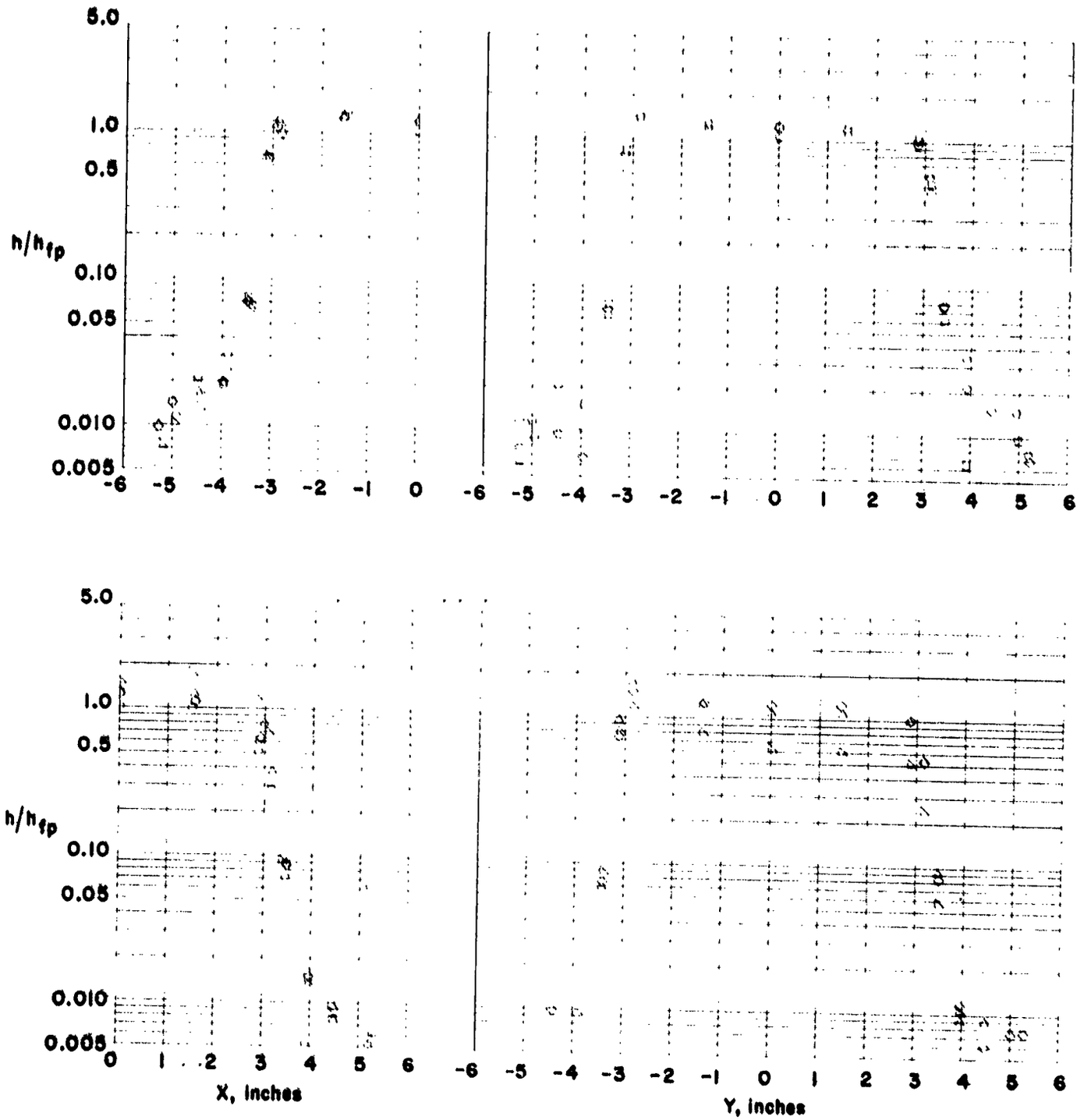

(c) θ = 15.0 degs.

Figure 16. - Continued.

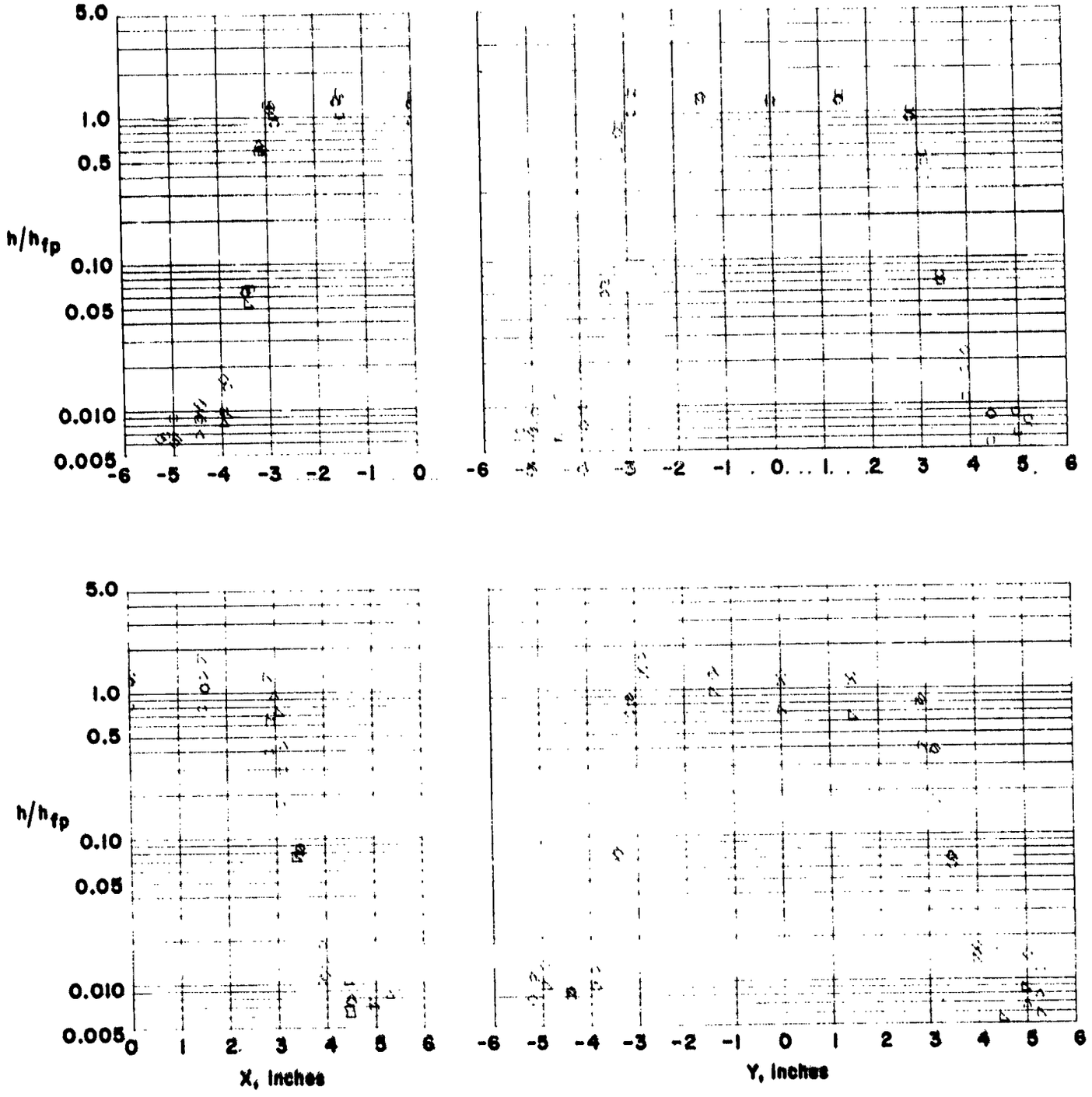

(d) θ = 30.0 degs.

Figure 16. - Concluded.

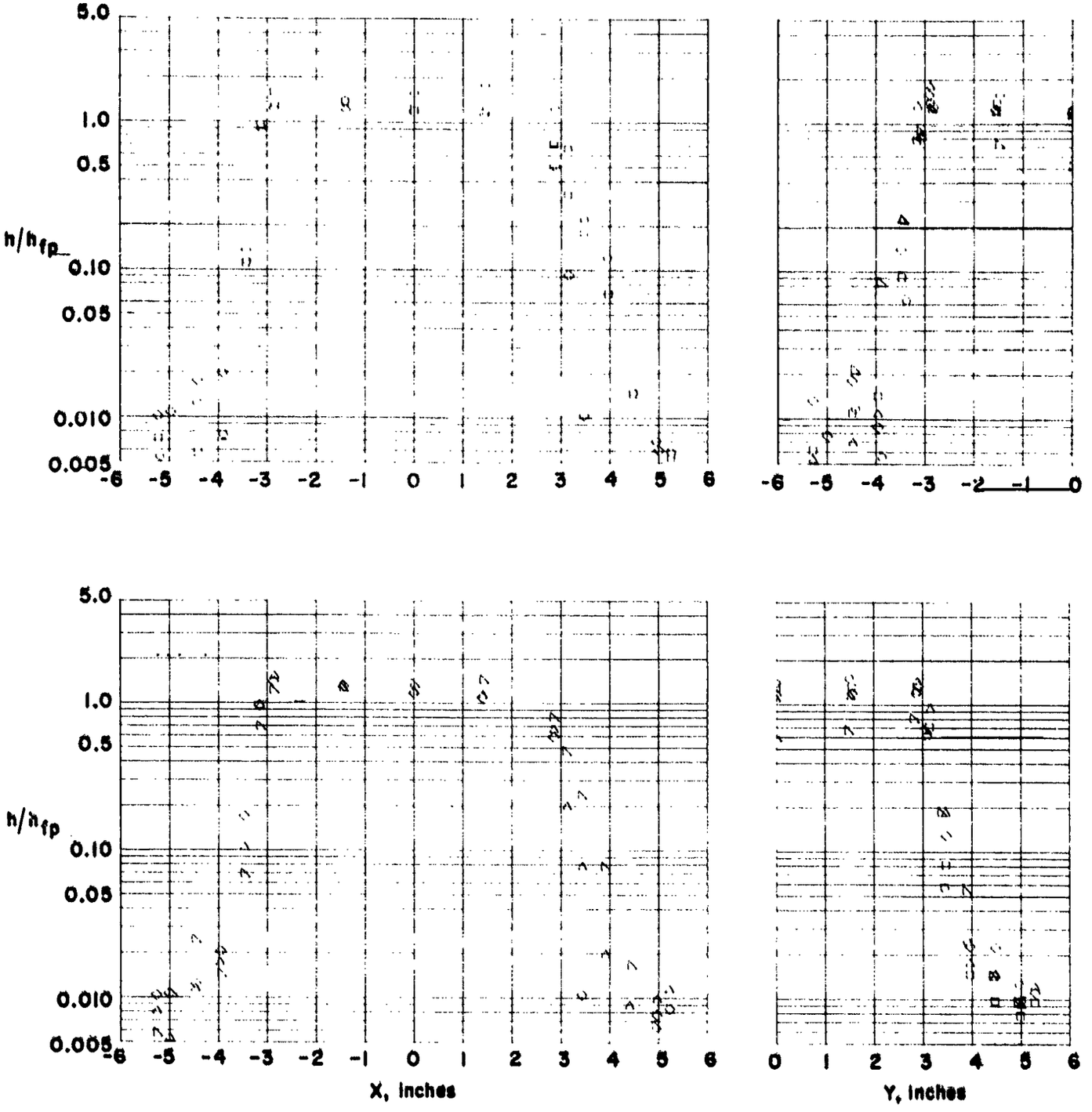

(a) θ = 0.0 degs.

Figure 17. - Heating to a flush mounted tile in a staggered array. w = 0.28 in.

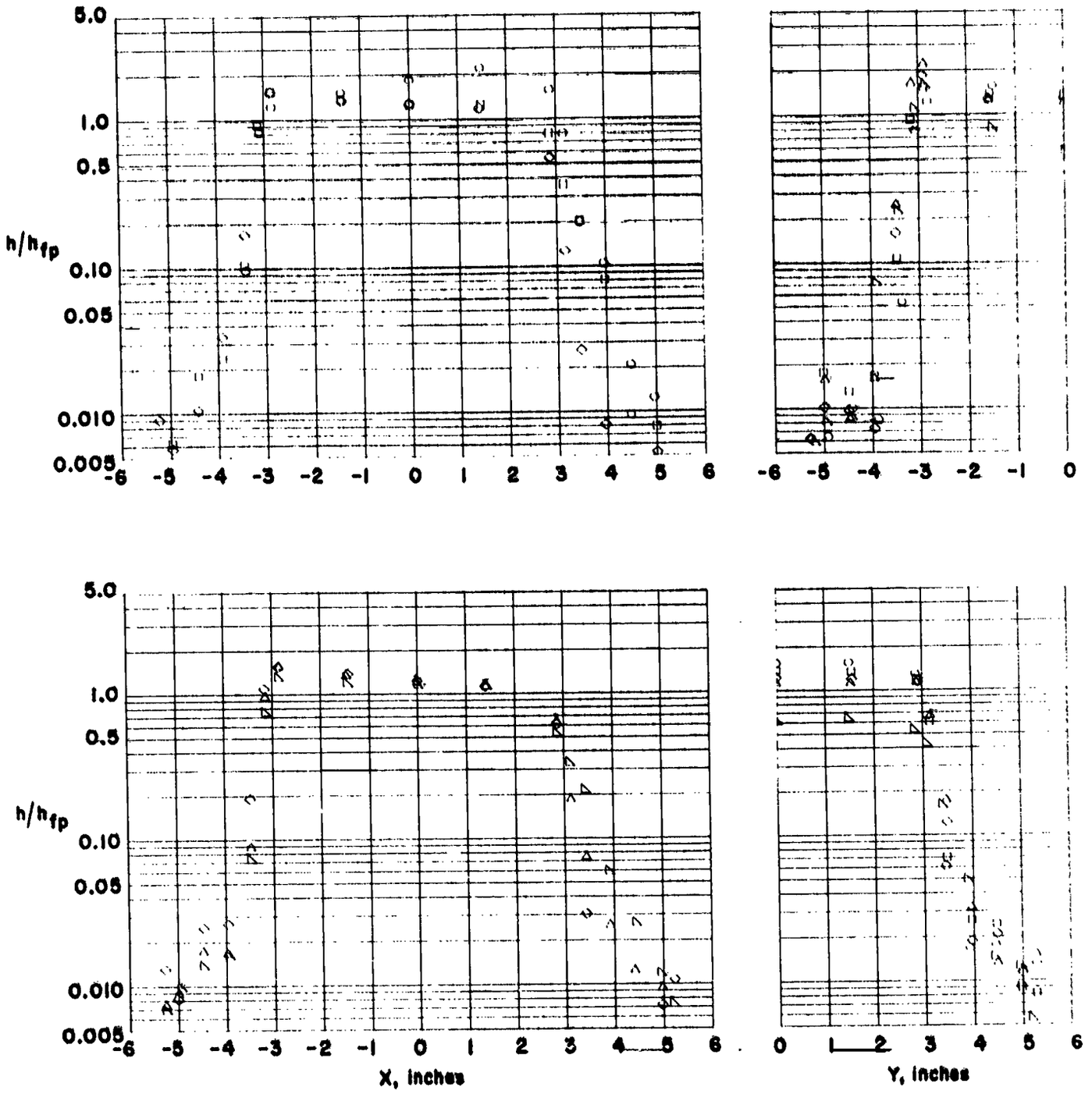

(b) θ = 7.5 degs.

Figure 17. - Continued.

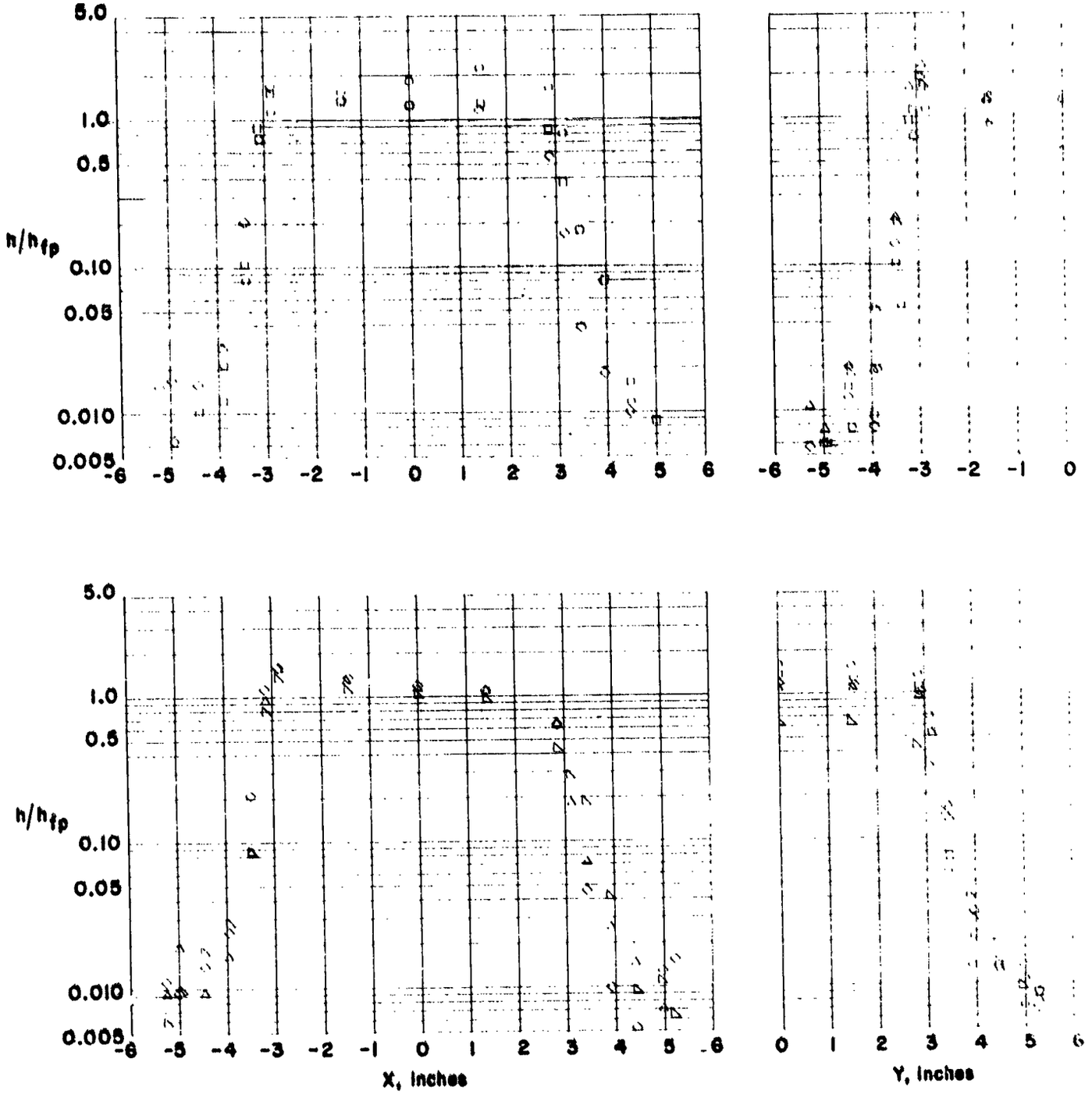

(c) θ = 15.0 degs.

Figure 17. - Continued.

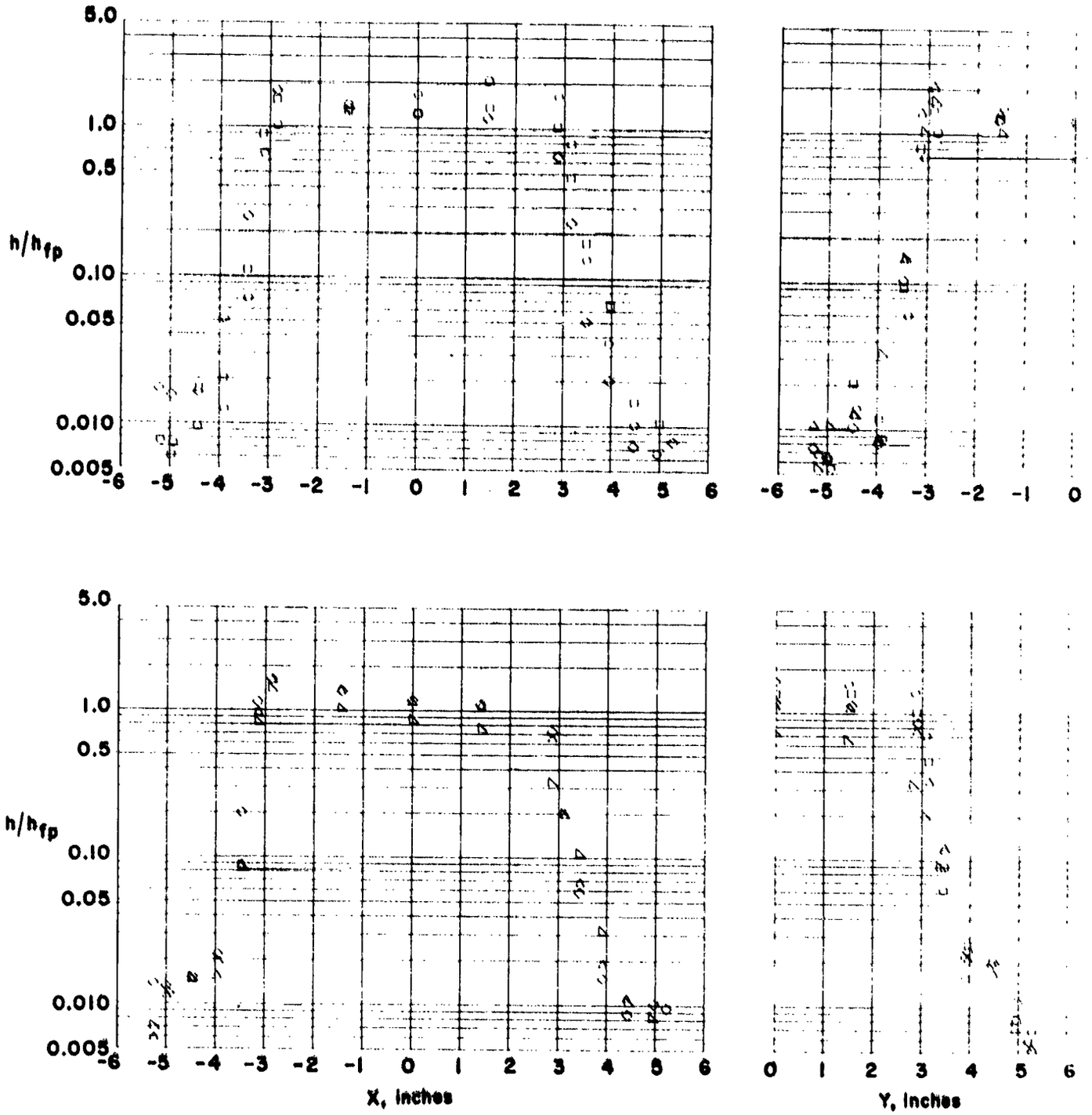

(d) θ = 30.0 degs.

Figure 17. - Continued.

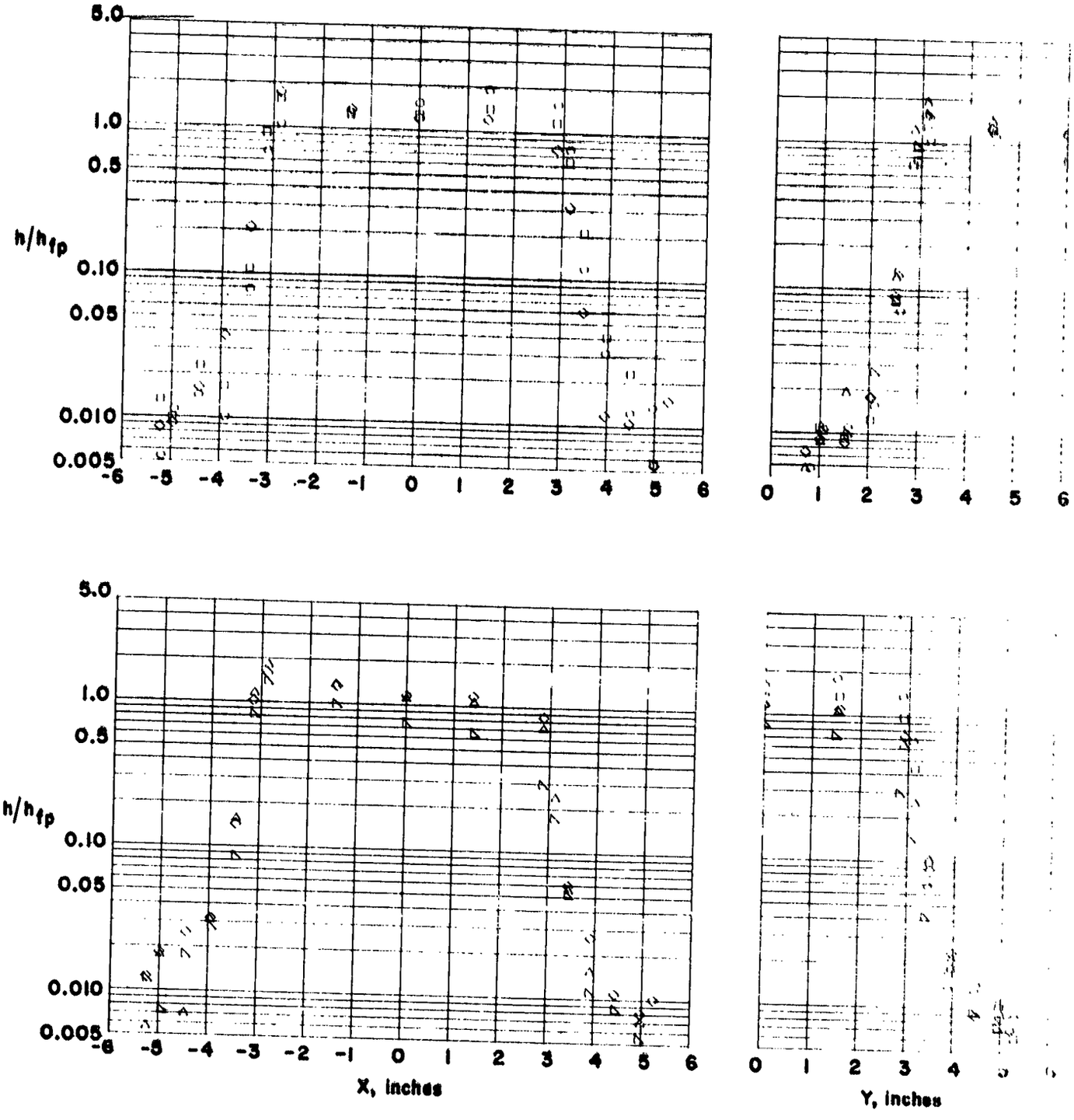

(e) θ = 45.0 degs.

Figure 17. - Concluded.

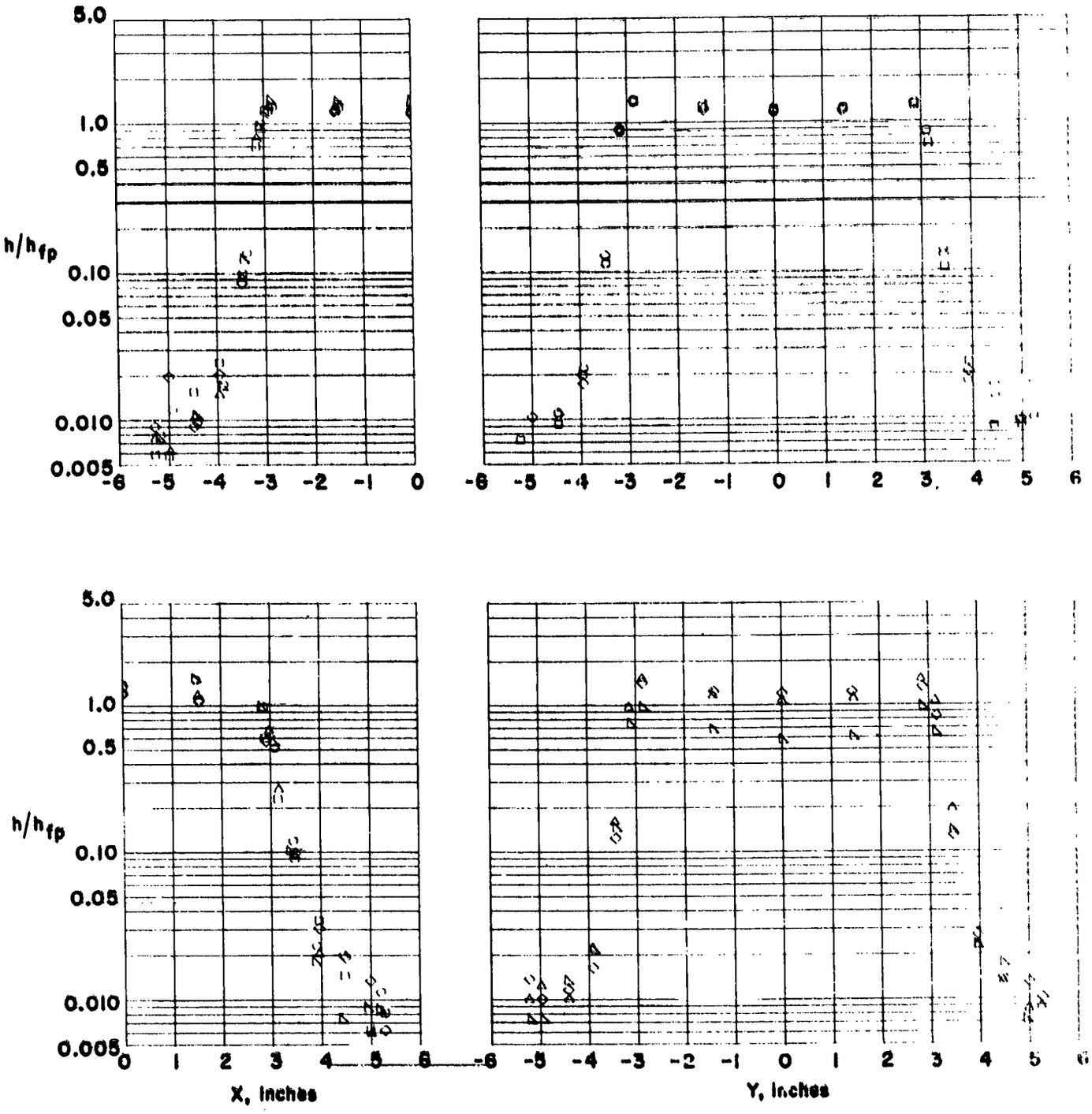

(a) θ = 0.0 degs.

Figure 18. - Heating to a flush mounted tile in an in-line array. w = 0.28 in.

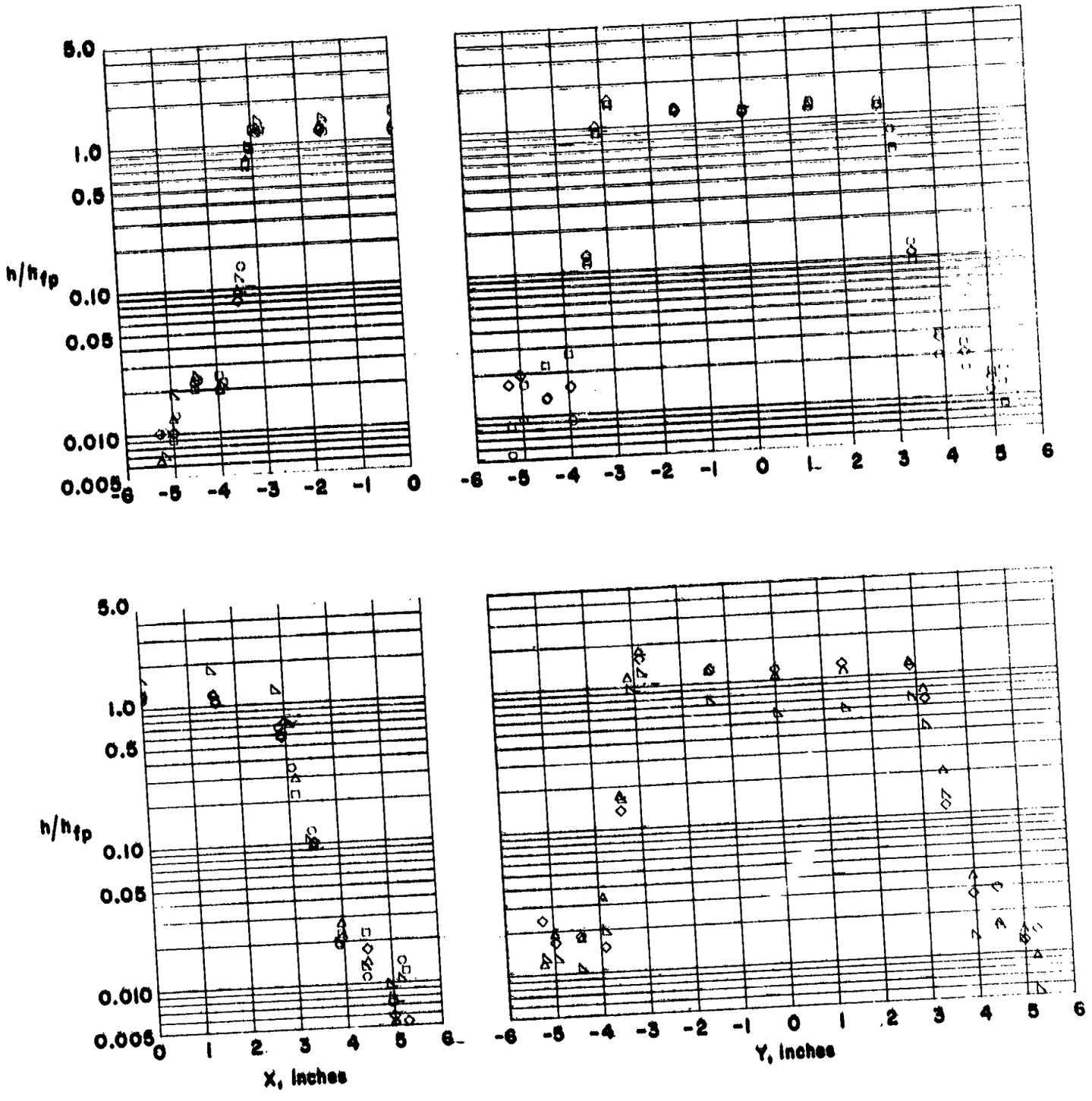

(b) θ = 7.5 degs.

Figure 18 - Continued.

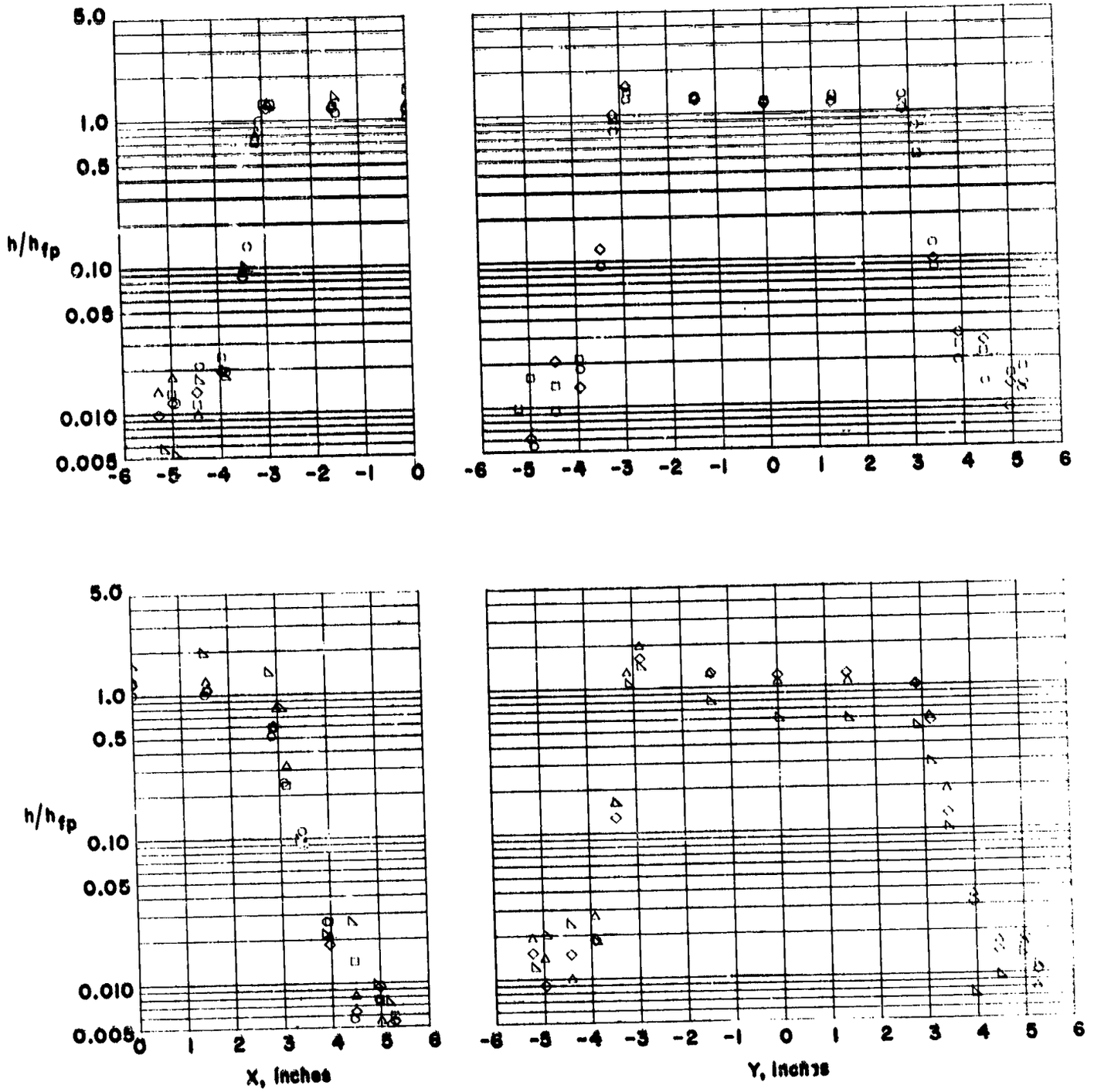

(c) θ = 15.0 degs.

Figure 18. - Continued.

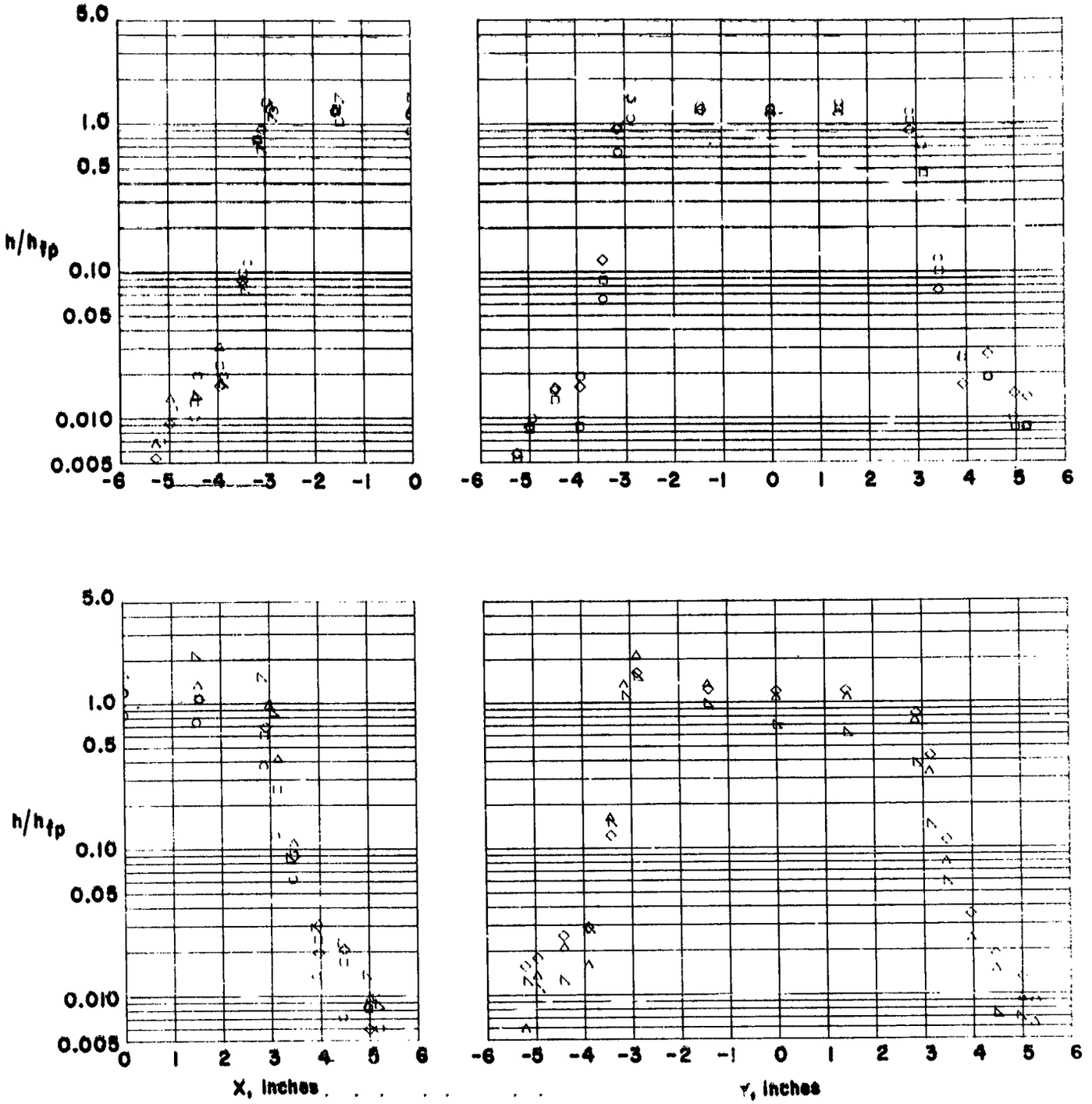

(d) θ = 30.0 degs.

Figure 18. - Concluded.

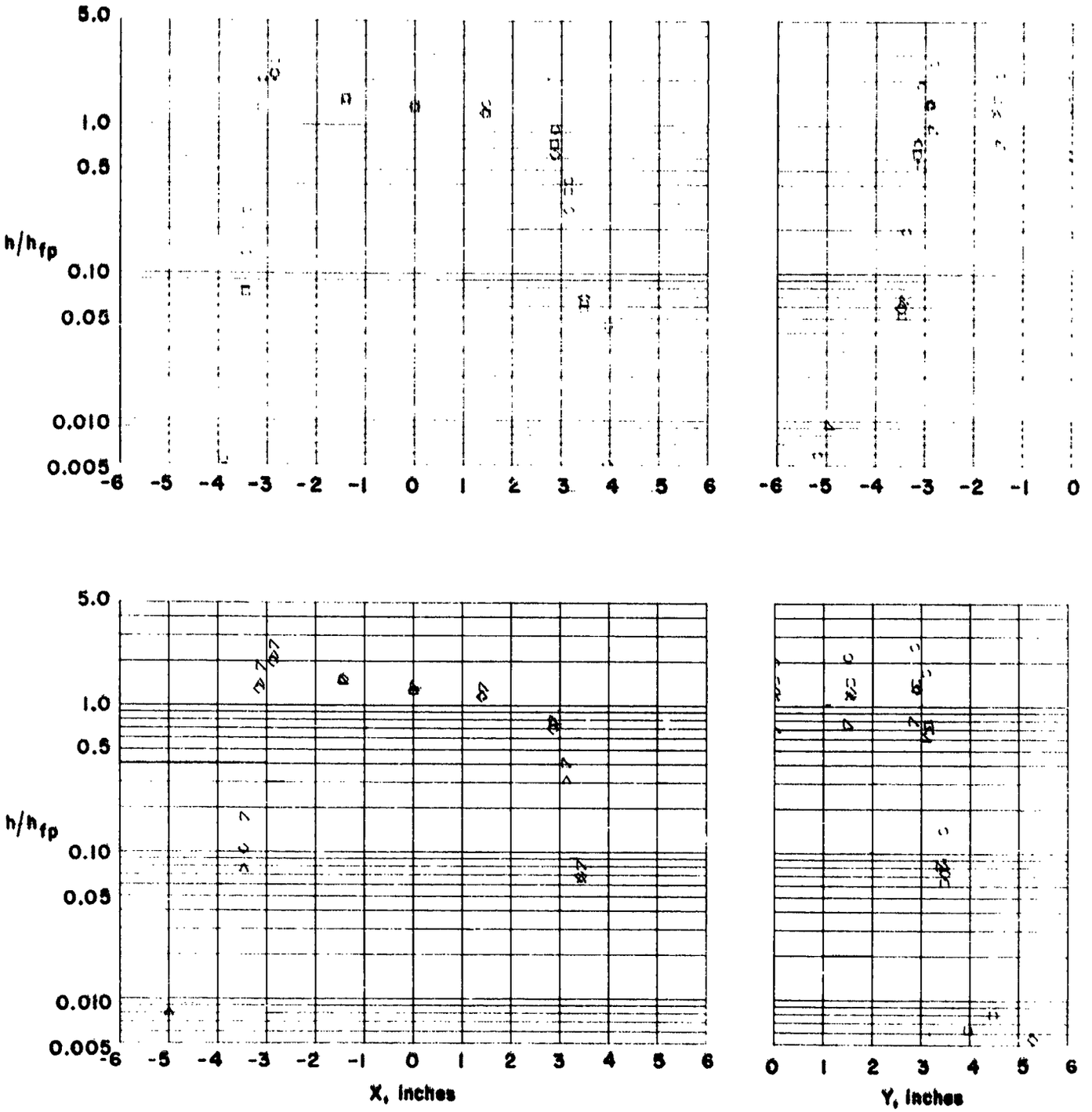

(a) θ = 0.0 degs.

Figure 19. - Heating to a protruding tile in a staggered array. w = 0.05 in., s = 0.10 in.

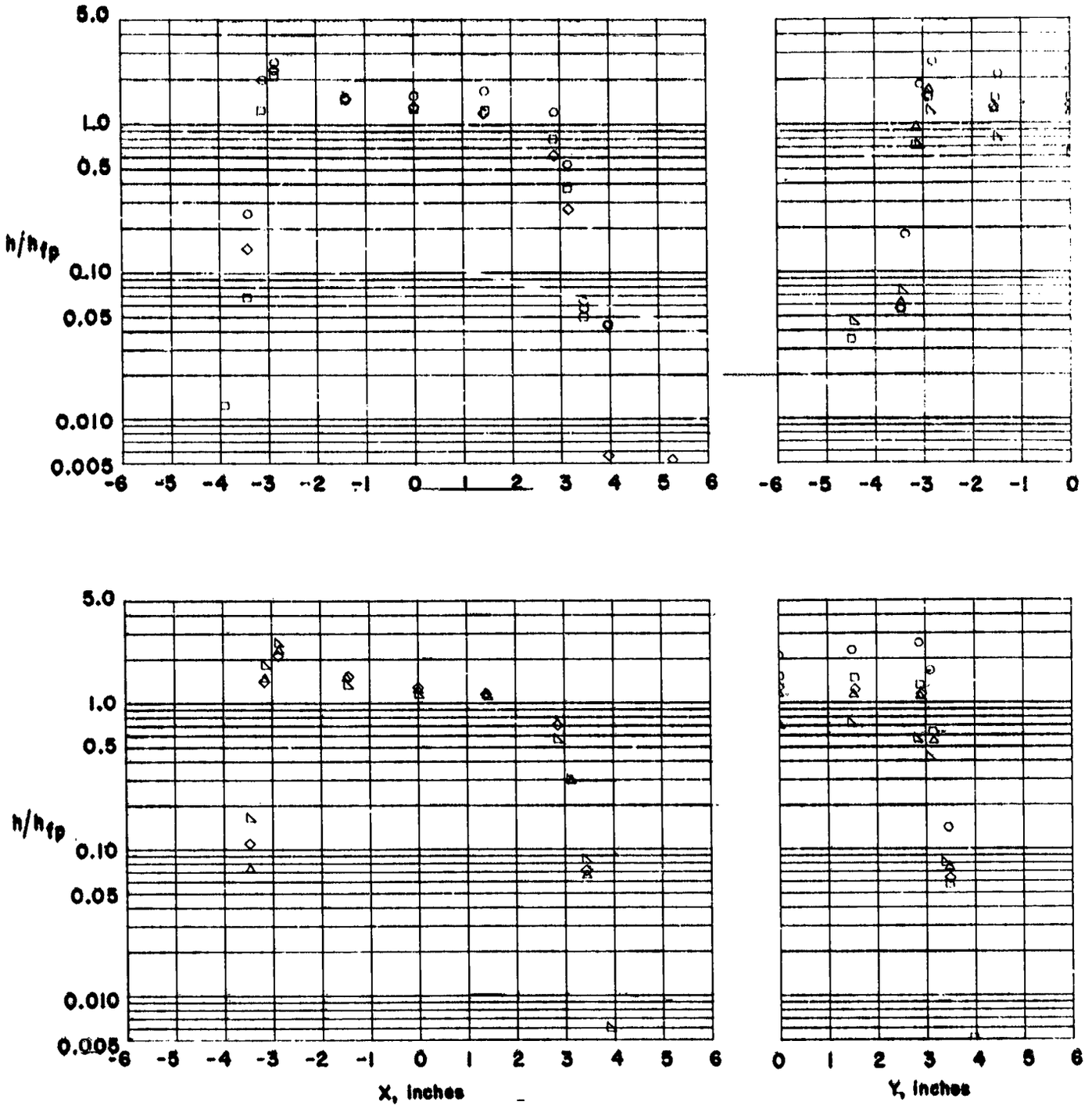

(b) θ = 7.5 degs.

Figure 19. - Continued.

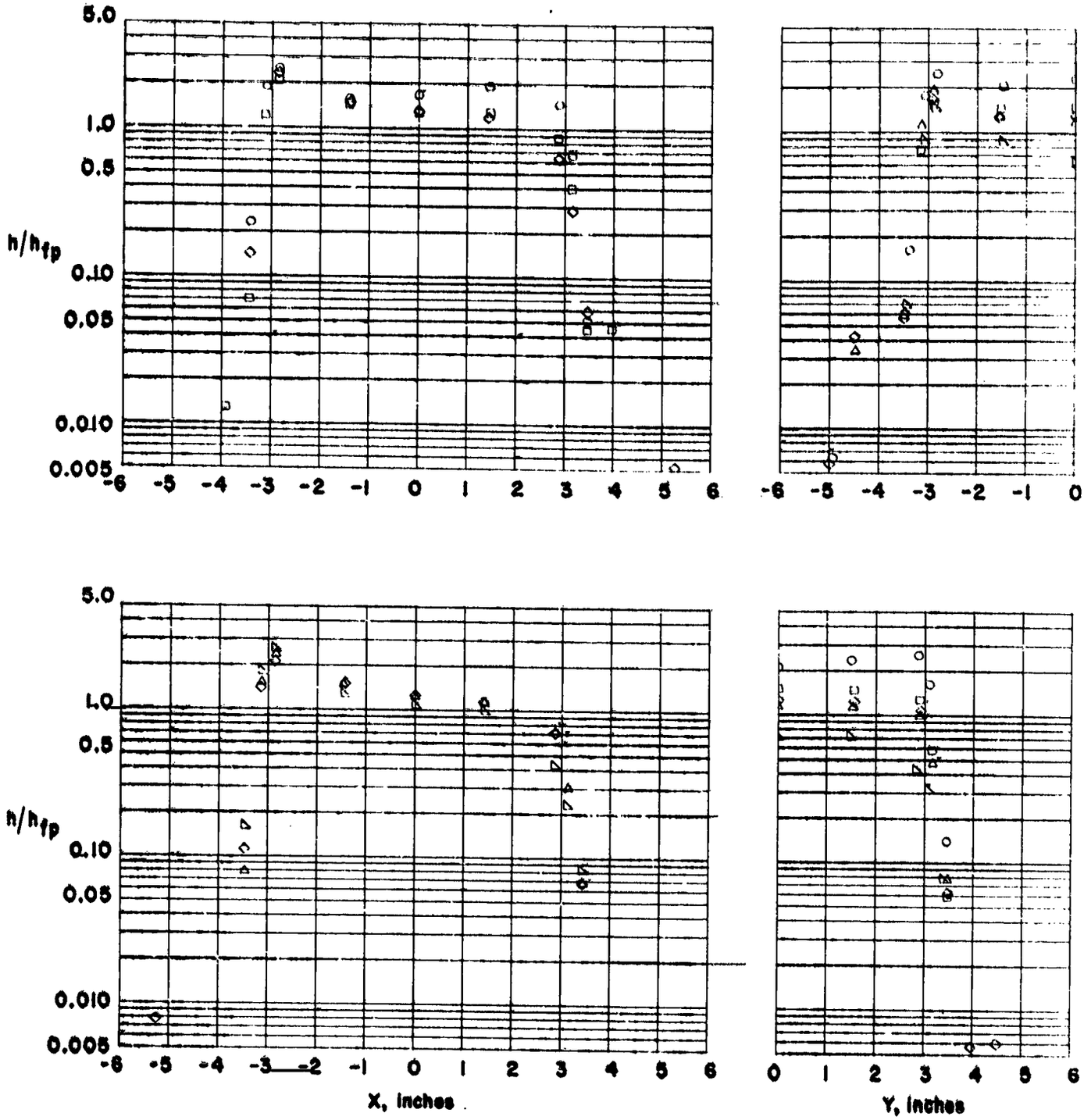

(c) θ = 15.0 degs.

Figure 19. - Continued.

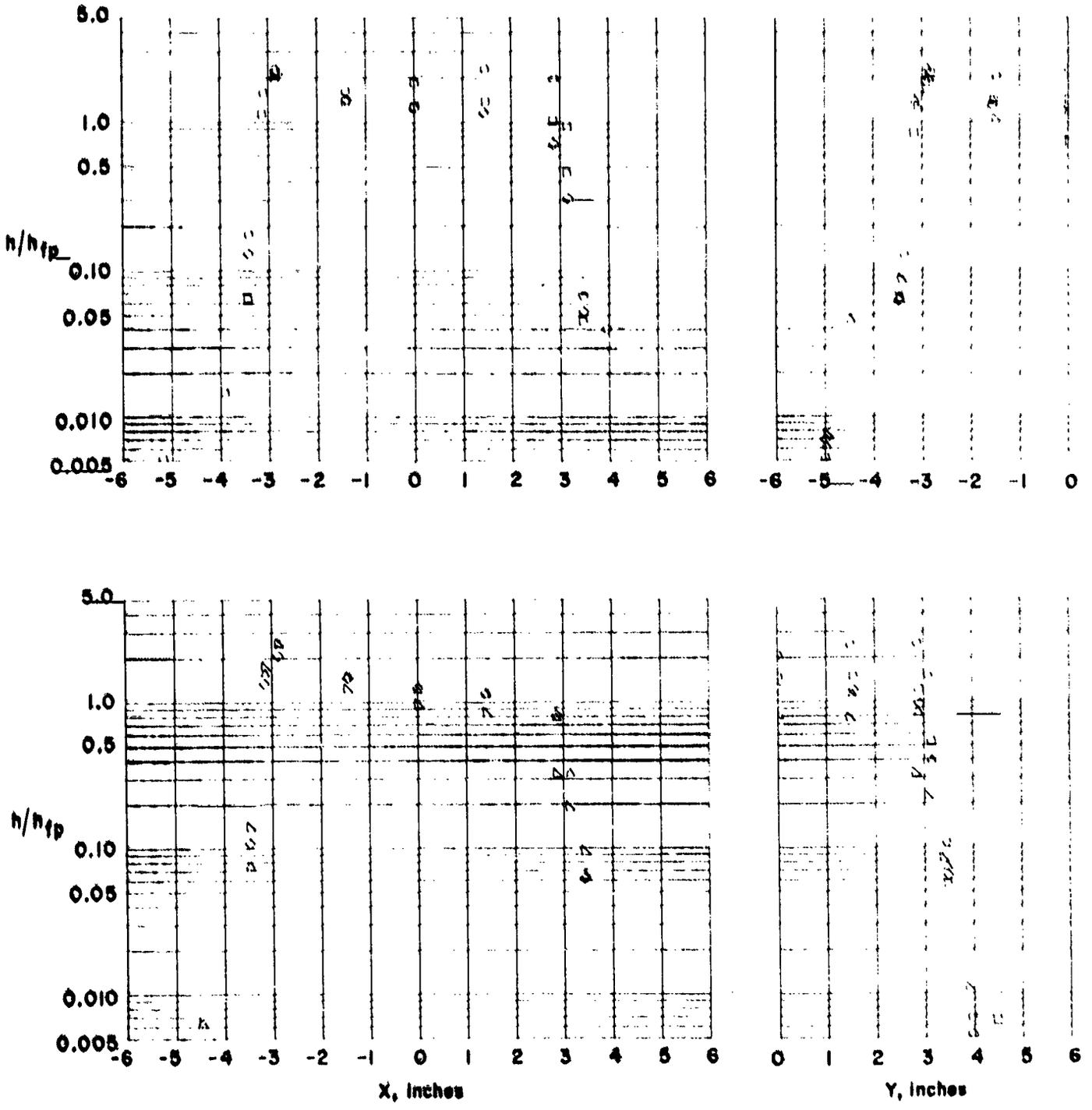

(d) θ = 30.0 degs.

Figure 19. Continued.

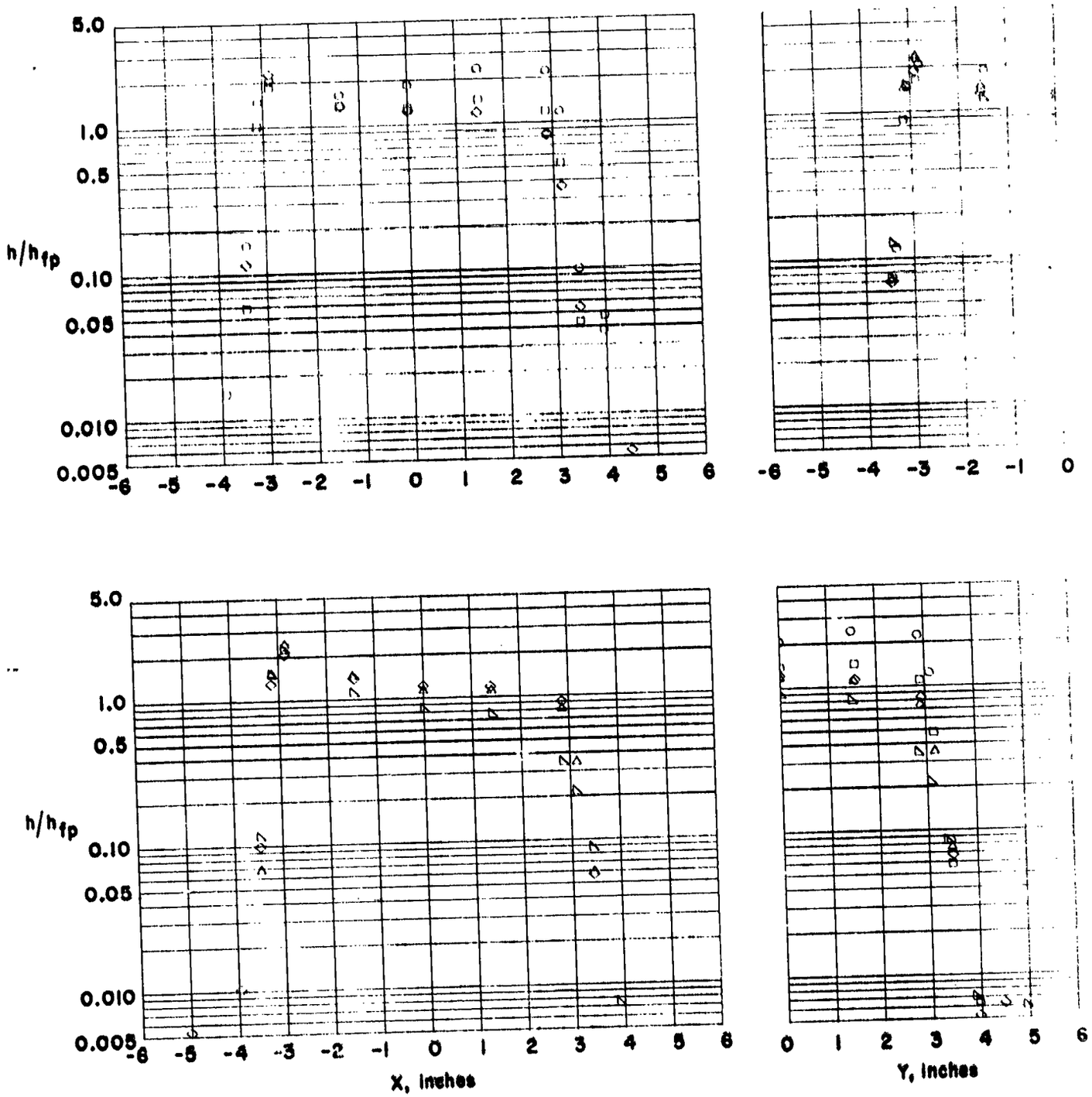

(e) θ = 45.0 degs.

Figure 19. - Concluded.

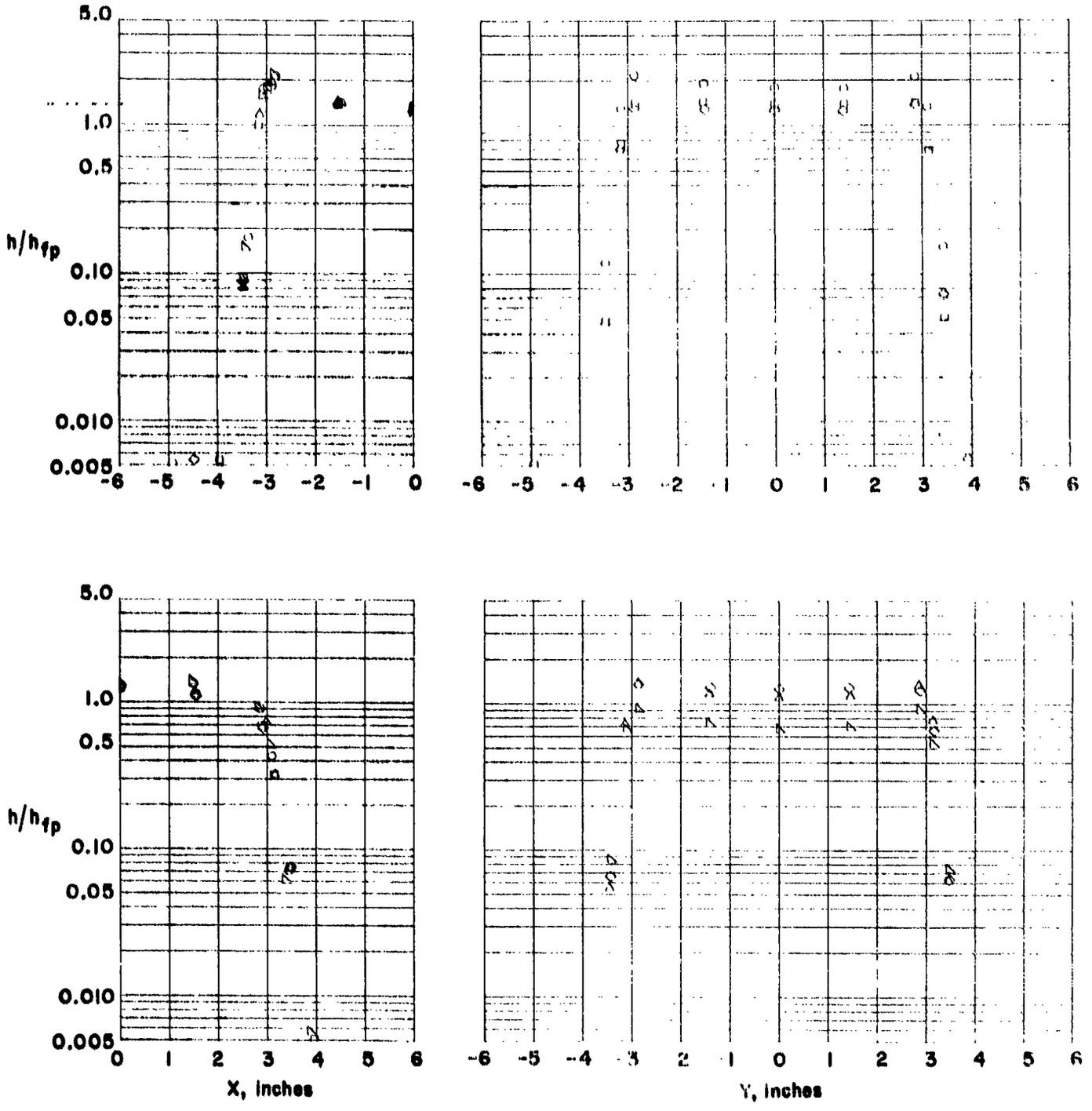

(a) θ = 0.0 degs.

Figure 20. - Heating to a protruding tile in an in-line array. w = 0.05 in., s = 0.10 in.

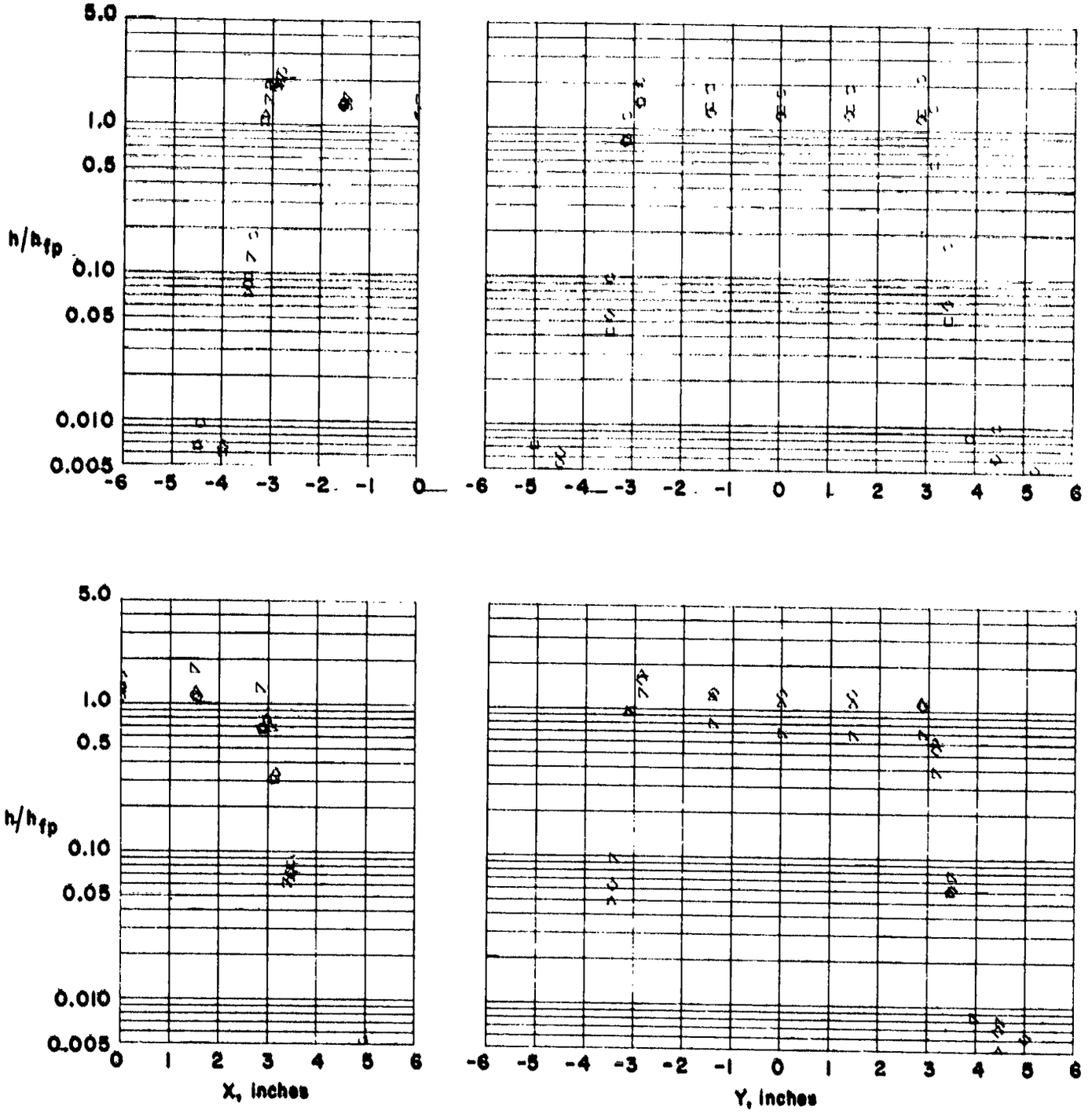

(b) θ = 7.5 degs.

Figure 20. - Continued.

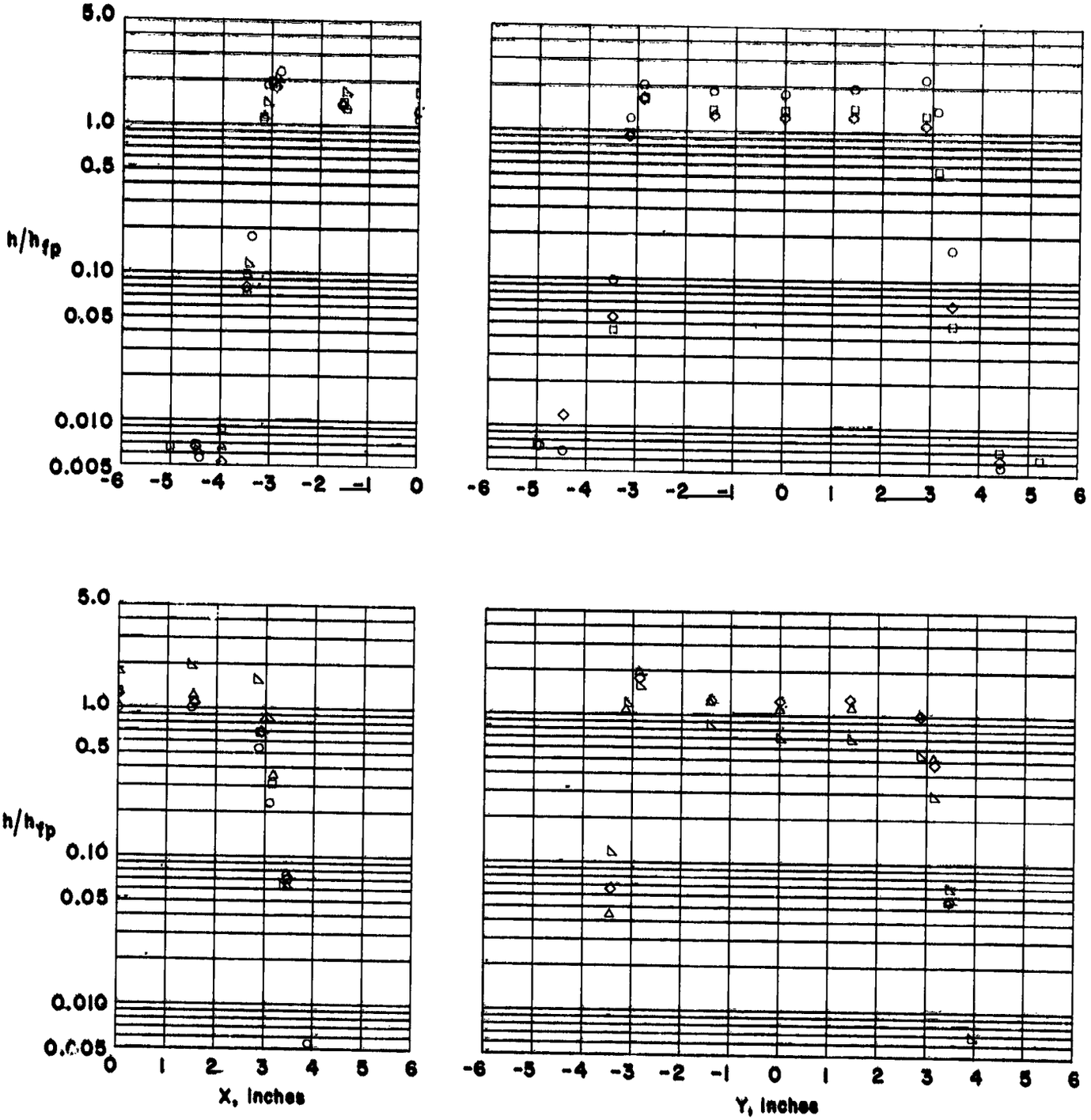

(c) θ = 15.0 degs.

Figure 20. - Continued.

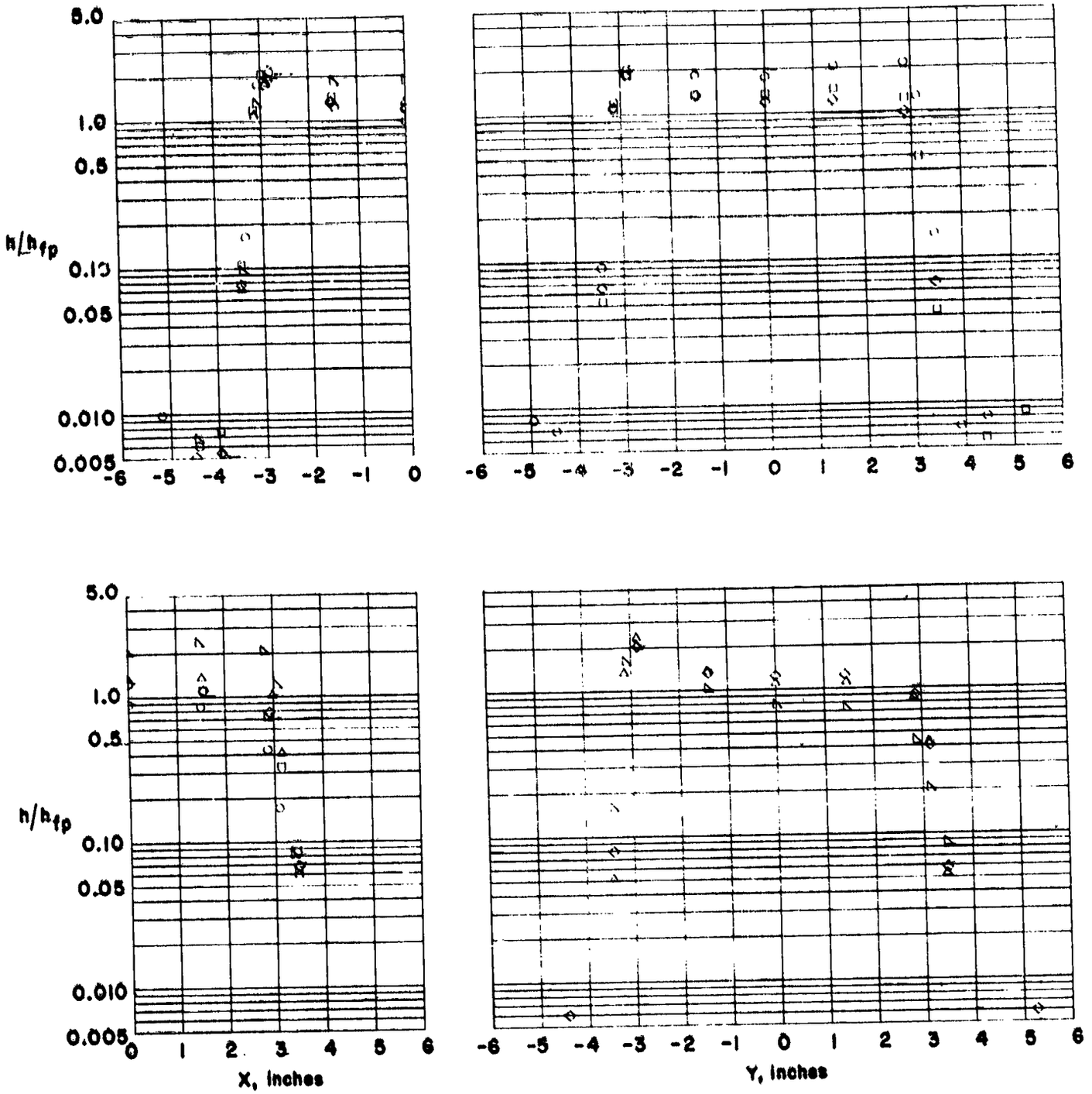

(d) θ = 30.0 degs.

Figure 20. - Concluded.

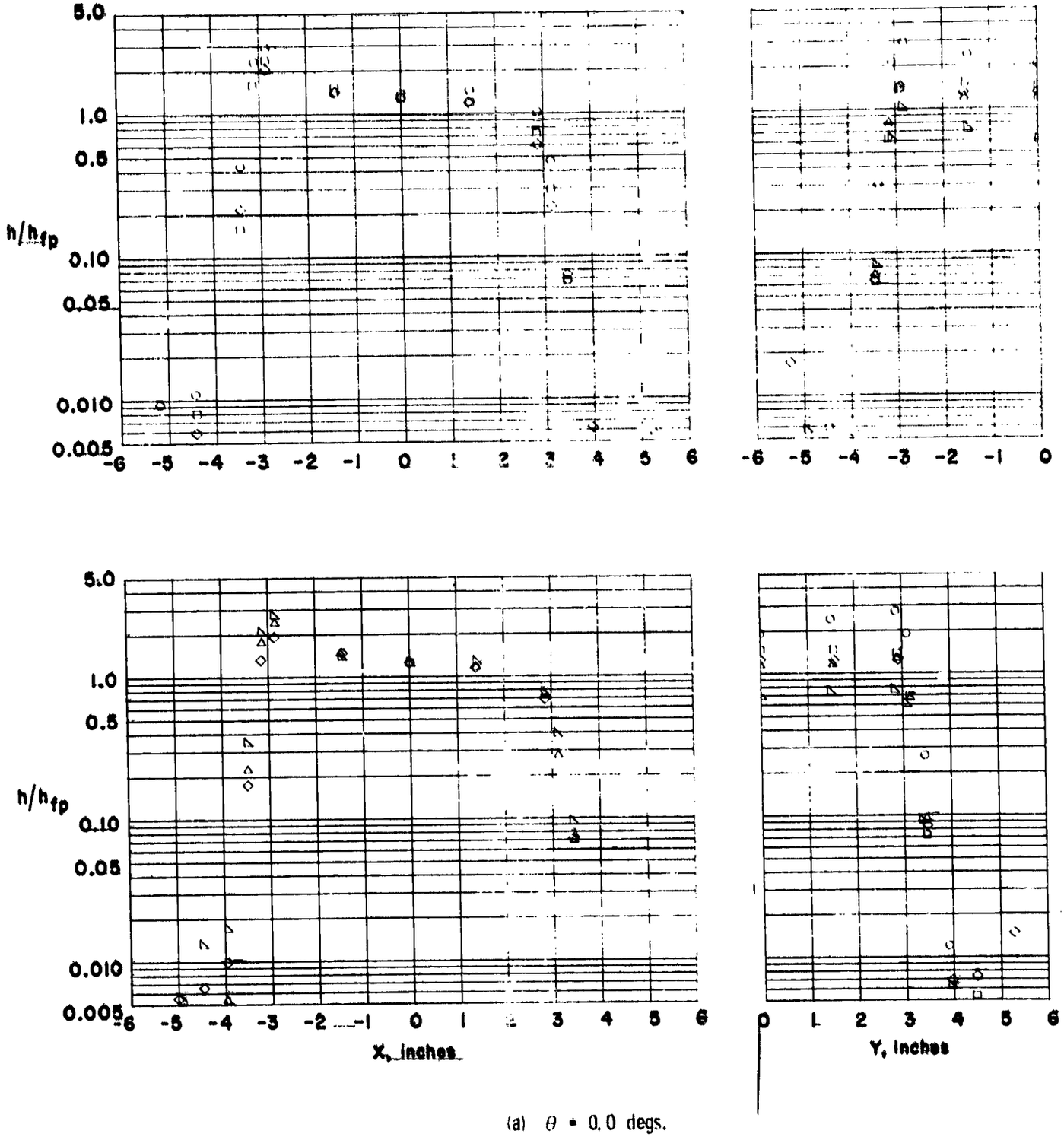

(a) θ = 0.0 degs.

Figure 21. - Heating to a protruding tile in a staggered array w = 0.09 in. s = 0.10 in.

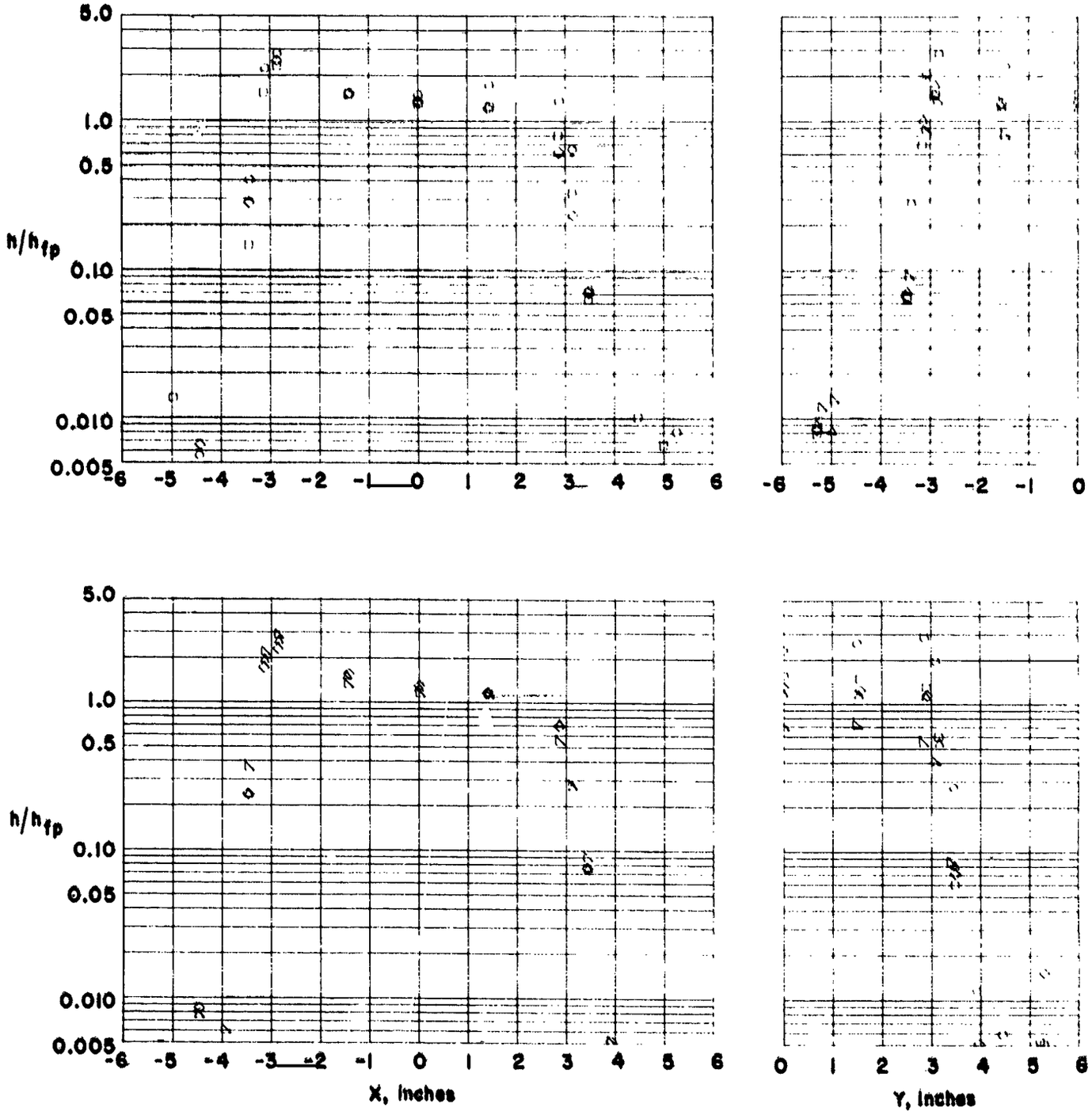

(b) θ = 7.5 degs.

Figure 21. - Continued.

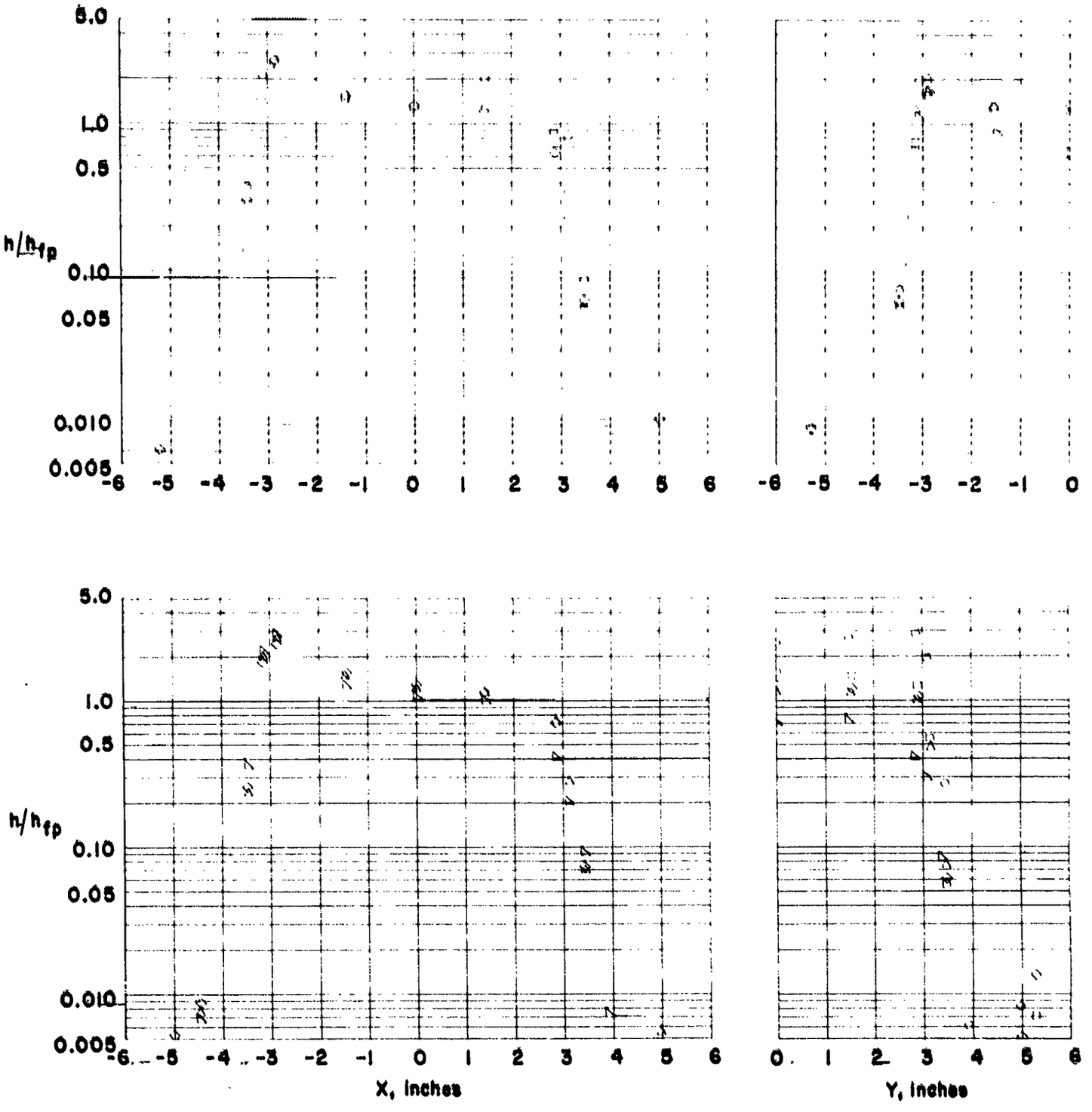

(c) θ = 15.0 degs.

Figure 21. - Continued.

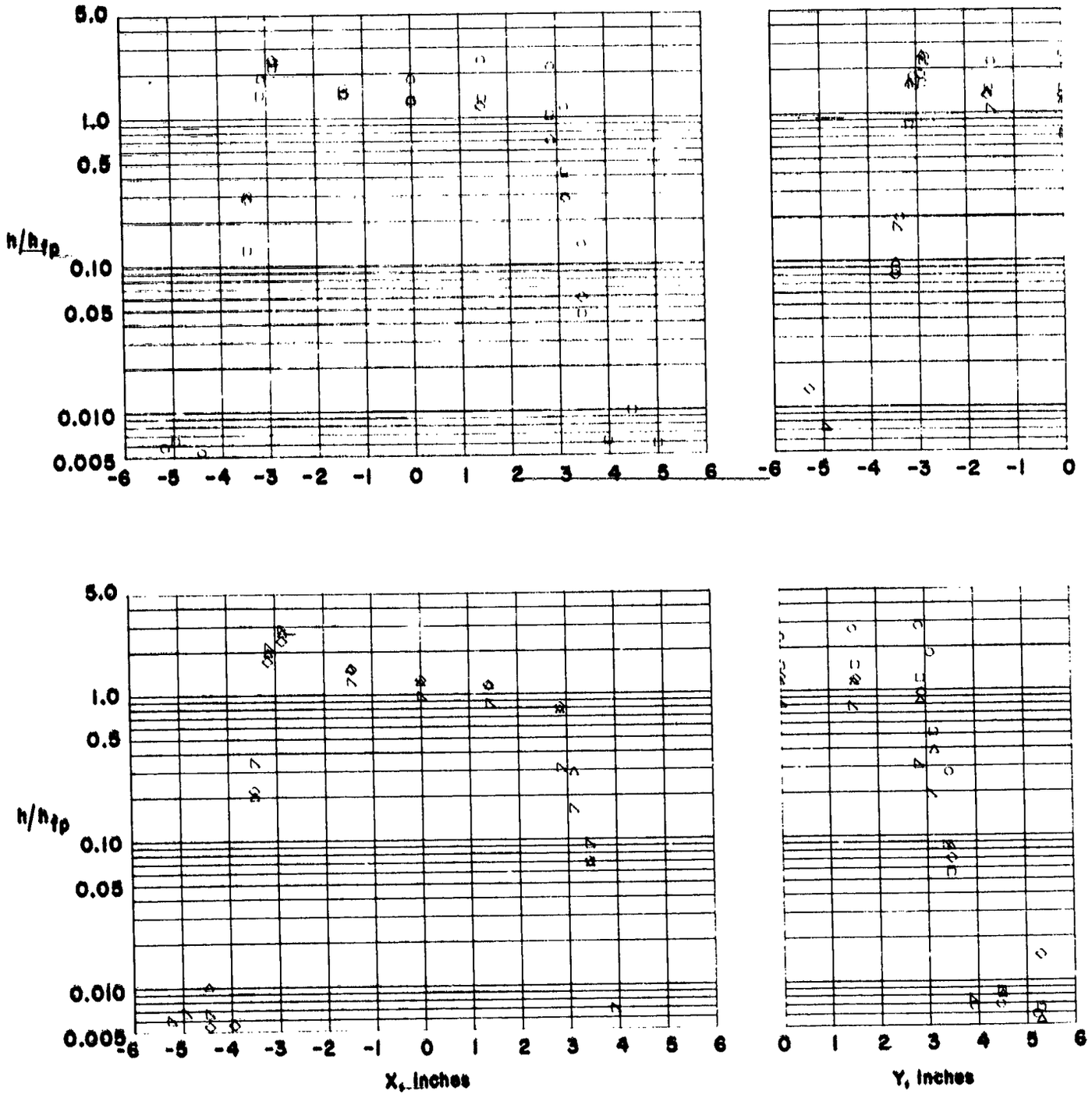

(d) θ = 30.0 degs.

Figure 21. - Continued.

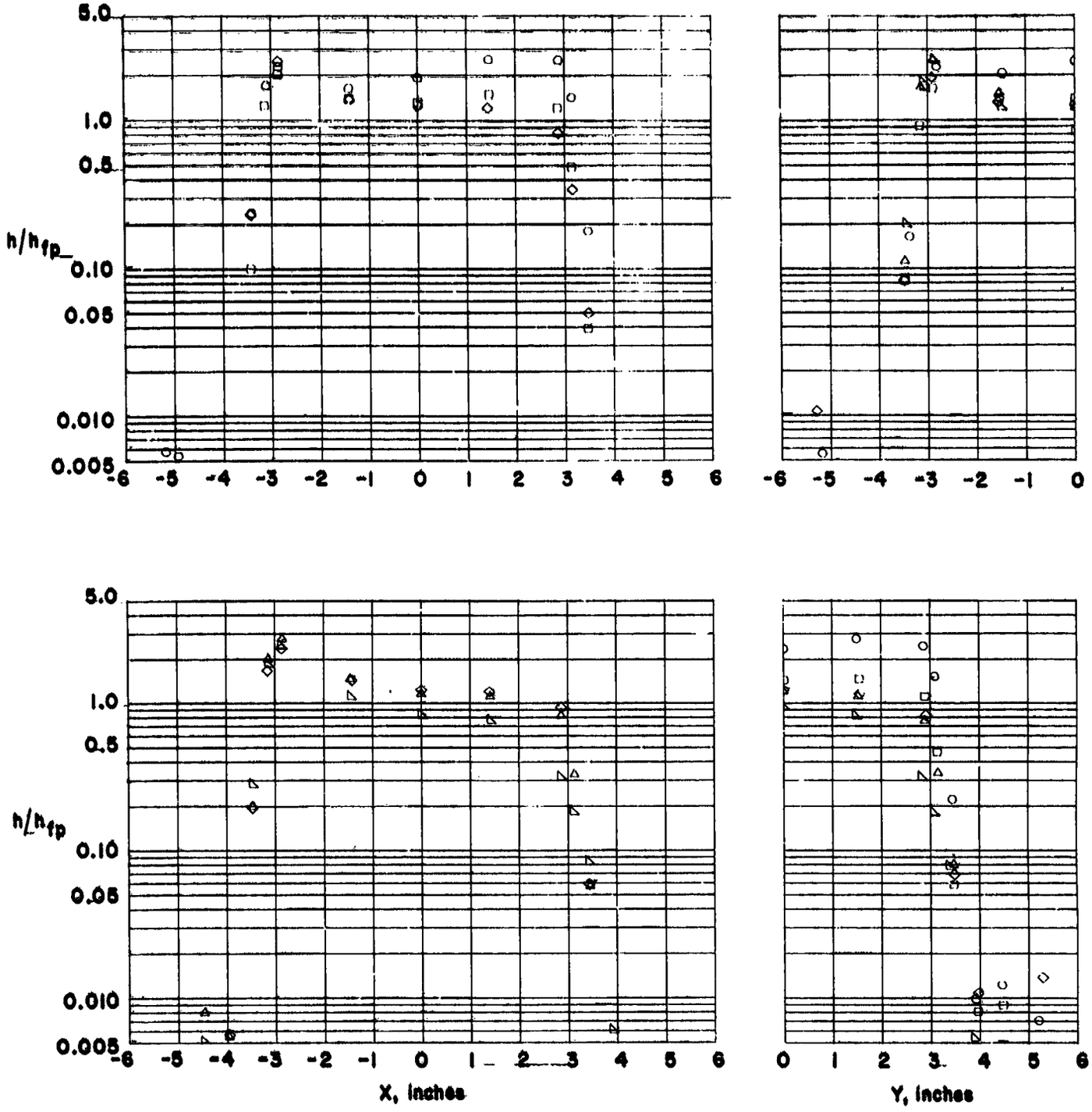

(e) θ = 45.0 degs.

Figure 21. - Concluded.

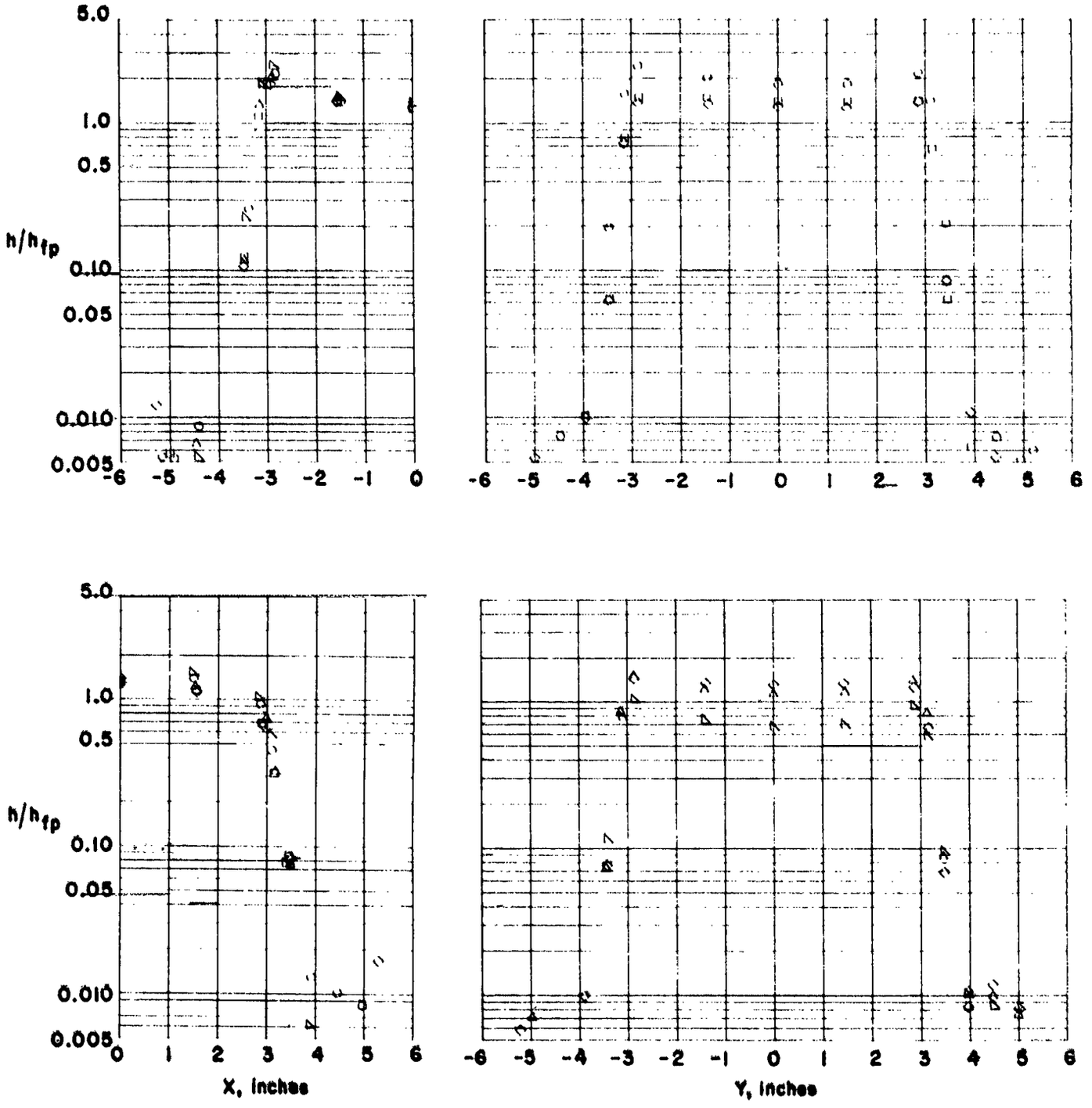

(a) θ = 0.0 degs.

Figure 22.- Heating to a protruding tile in an in-line array. w = 0.09 in., s = 0.10 in.

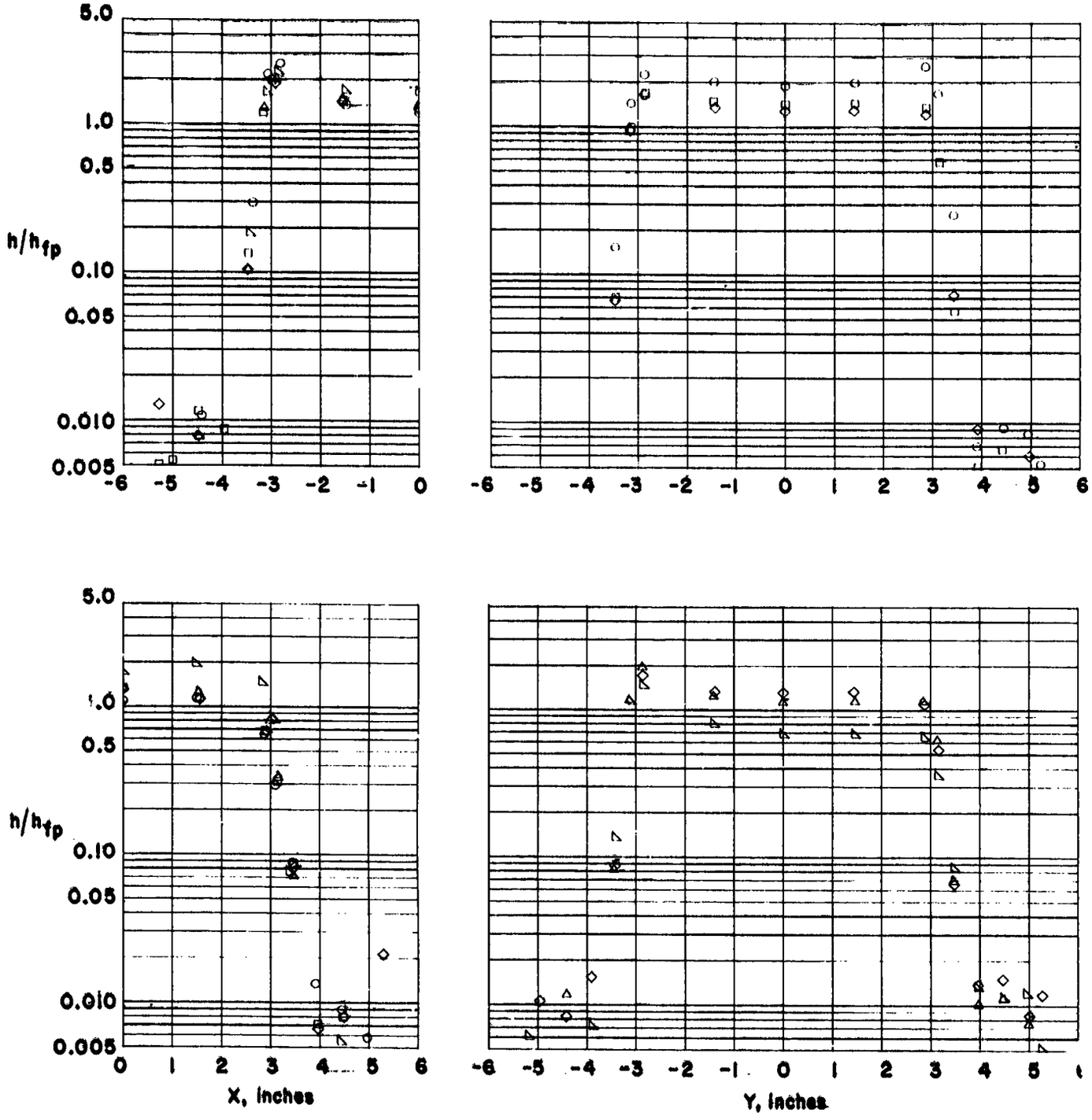

(b) θ = 7.5 degs.

Figure 22 - Continued.

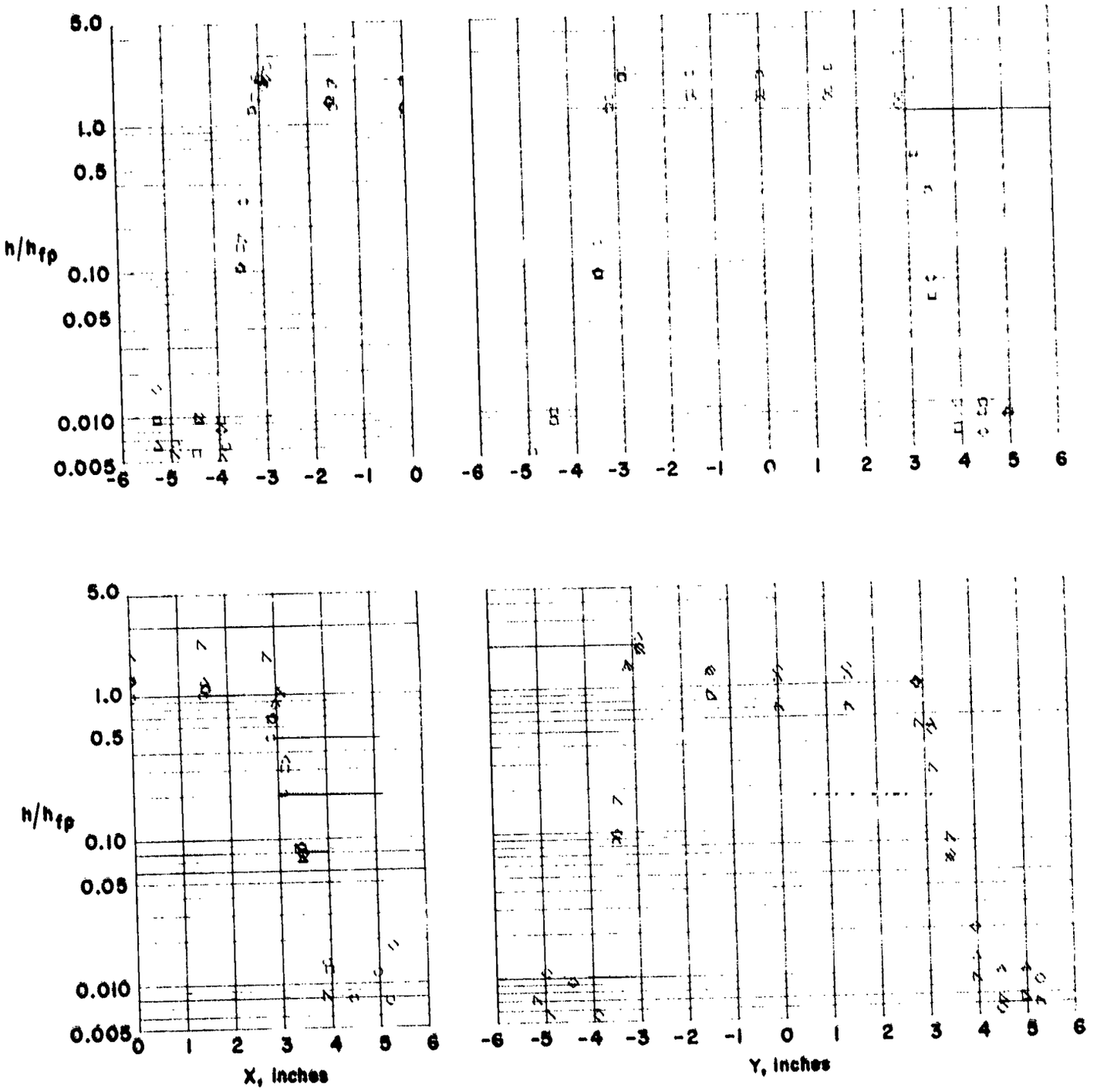

(c) θ = 15.0 degs.

Figure 22 - Continued.

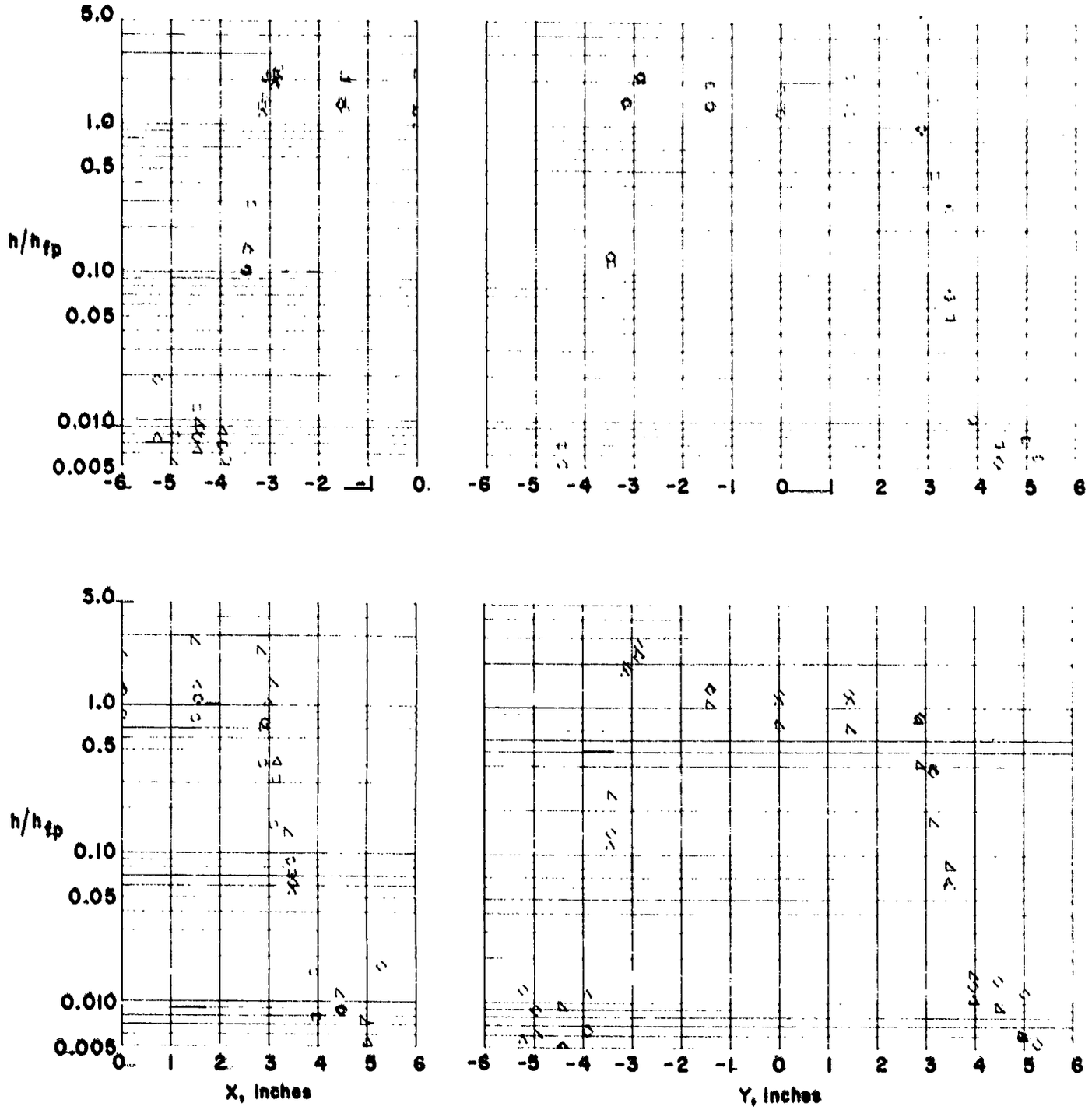

(d) θ = 30.0 degs.

Figure 22 - Concluded.

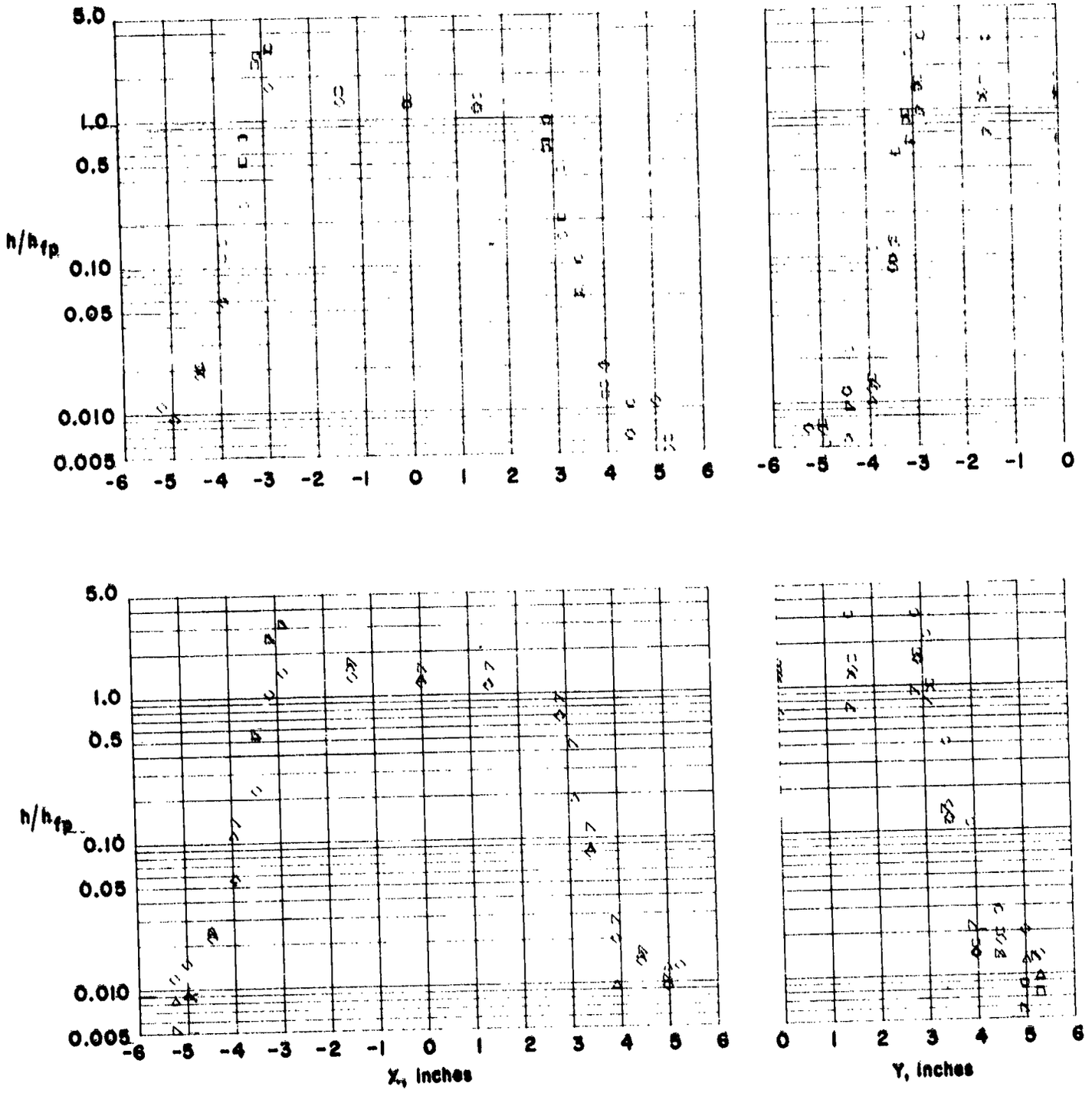

(a) θ = 0.0 degs.

Figure 23.- Heating to a protruding tile in a staggered array. w = 0.18 in., s = 0.10 in.

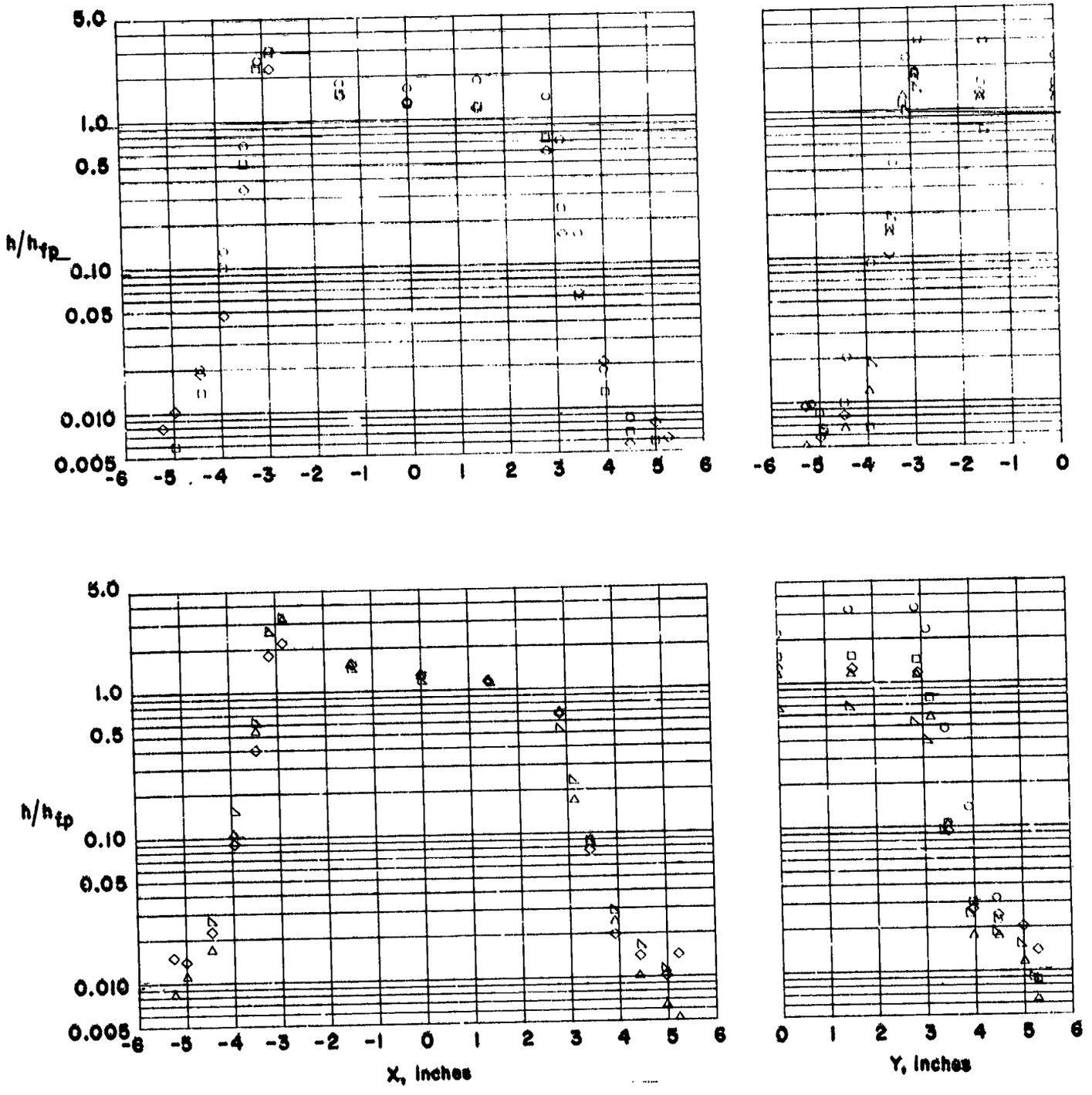

(b) θ = 7.5 degs.

Figure 23. - Continued.

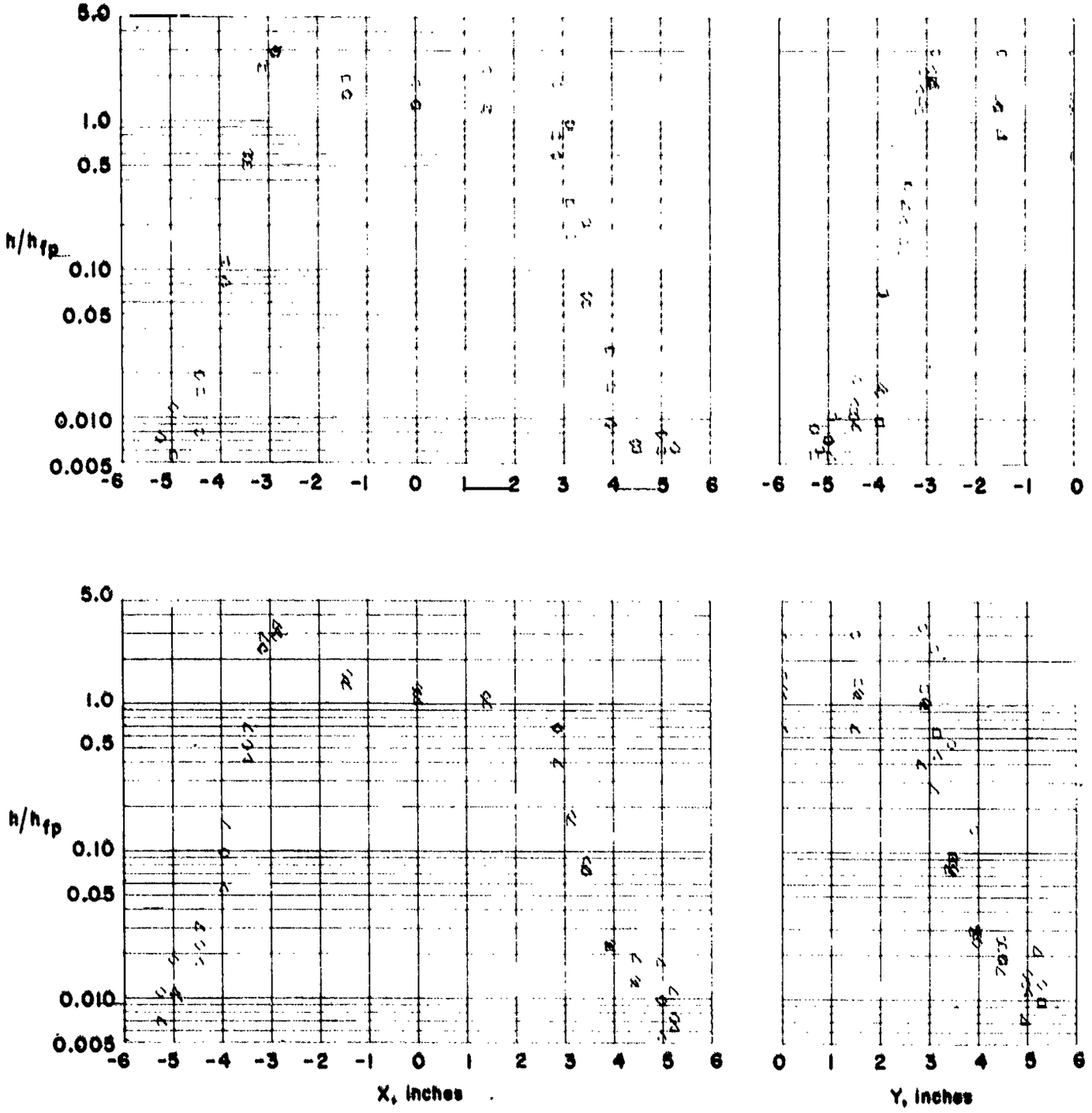

(c) θ = 15.0 degs.

Figure 23. - Continued.

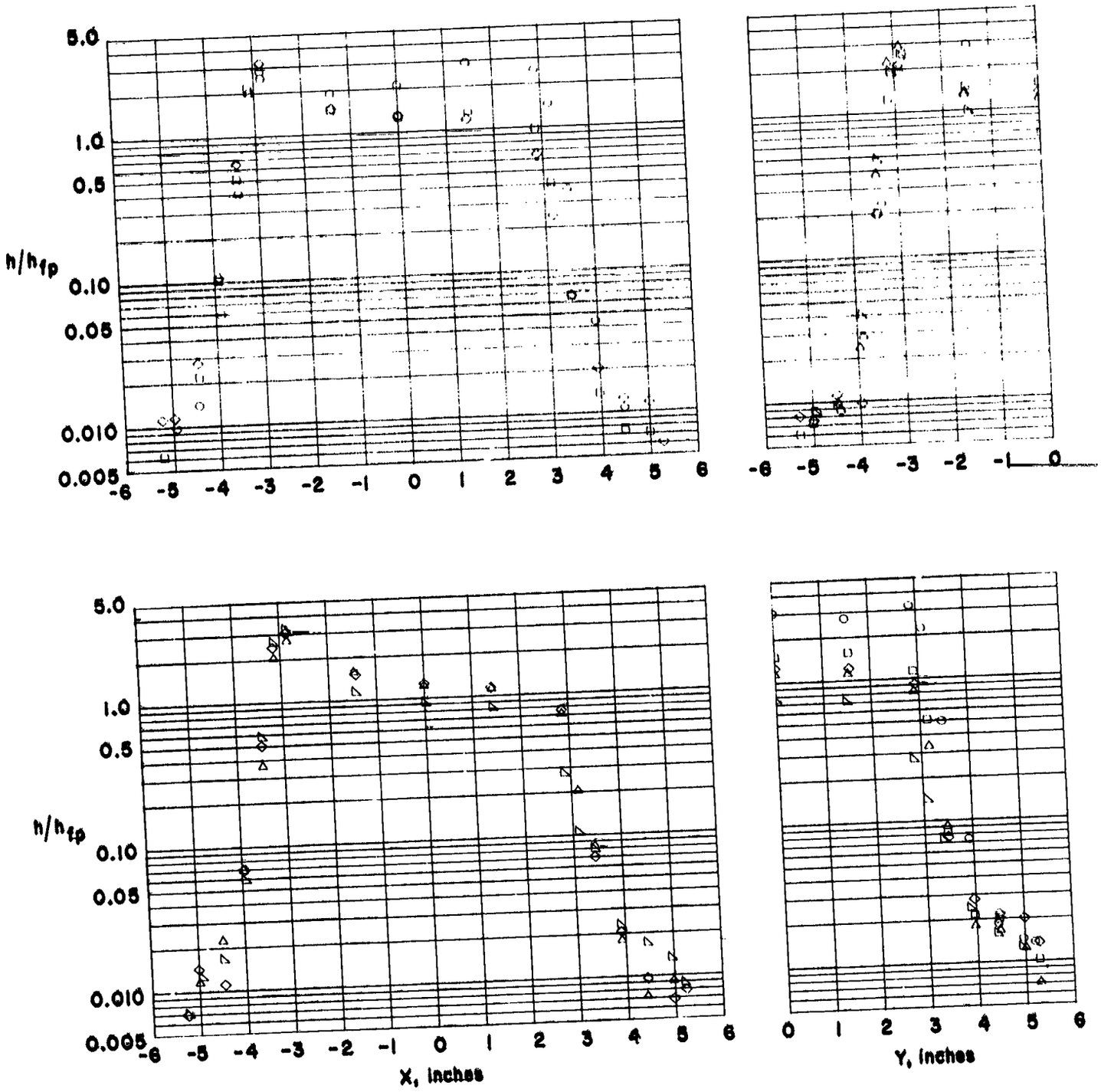

(d) θ = 30.0 degs.

Figure 23. - Continued.

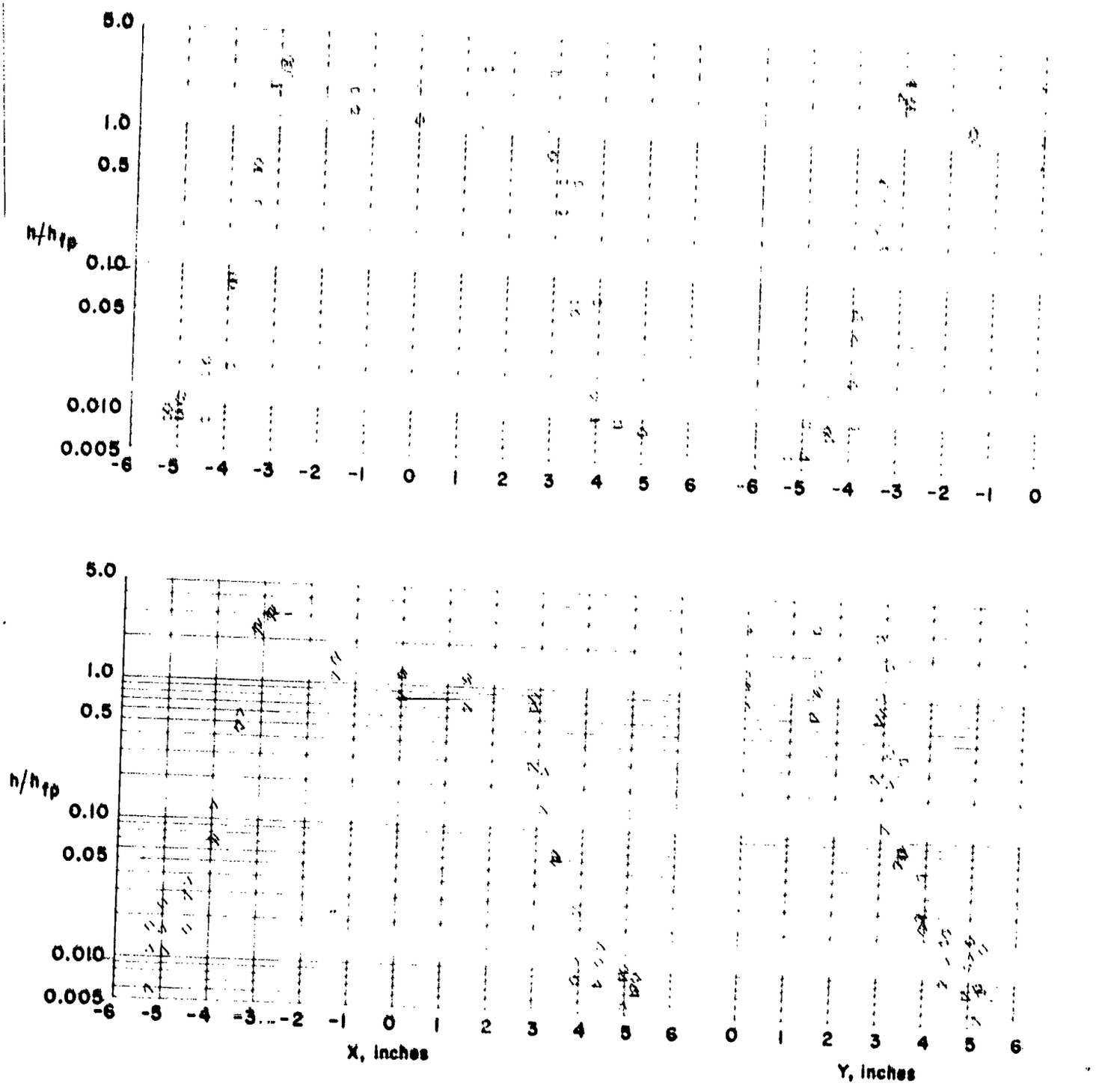

(e) θ = 45.0 degs.

Figure 23. - Concluded.

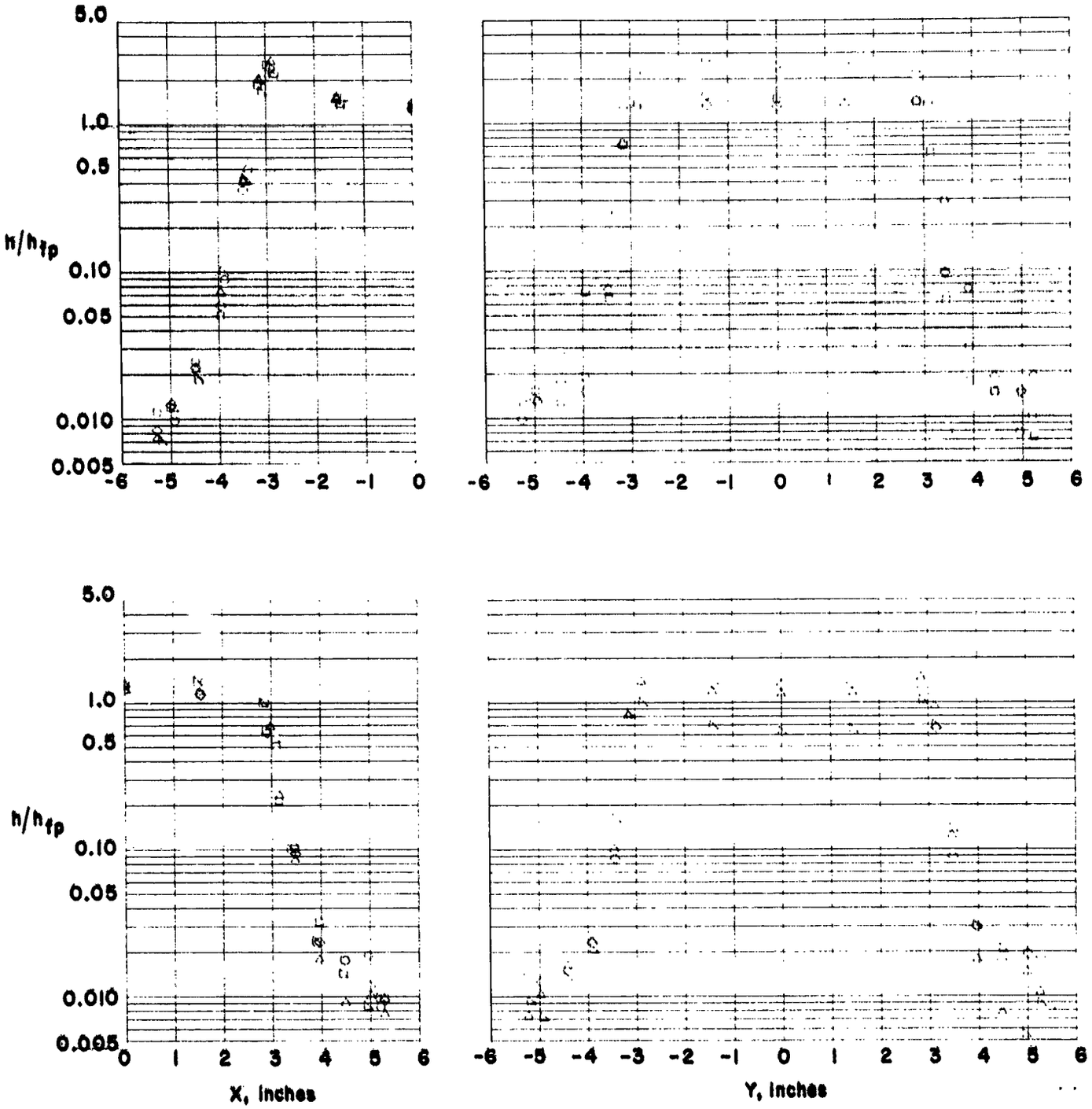

(a) θ = 0.0 degs.

Figure 24. - Heating to a protruding tile in an in-line array. w = 0.18 in., s = 0.10 in.

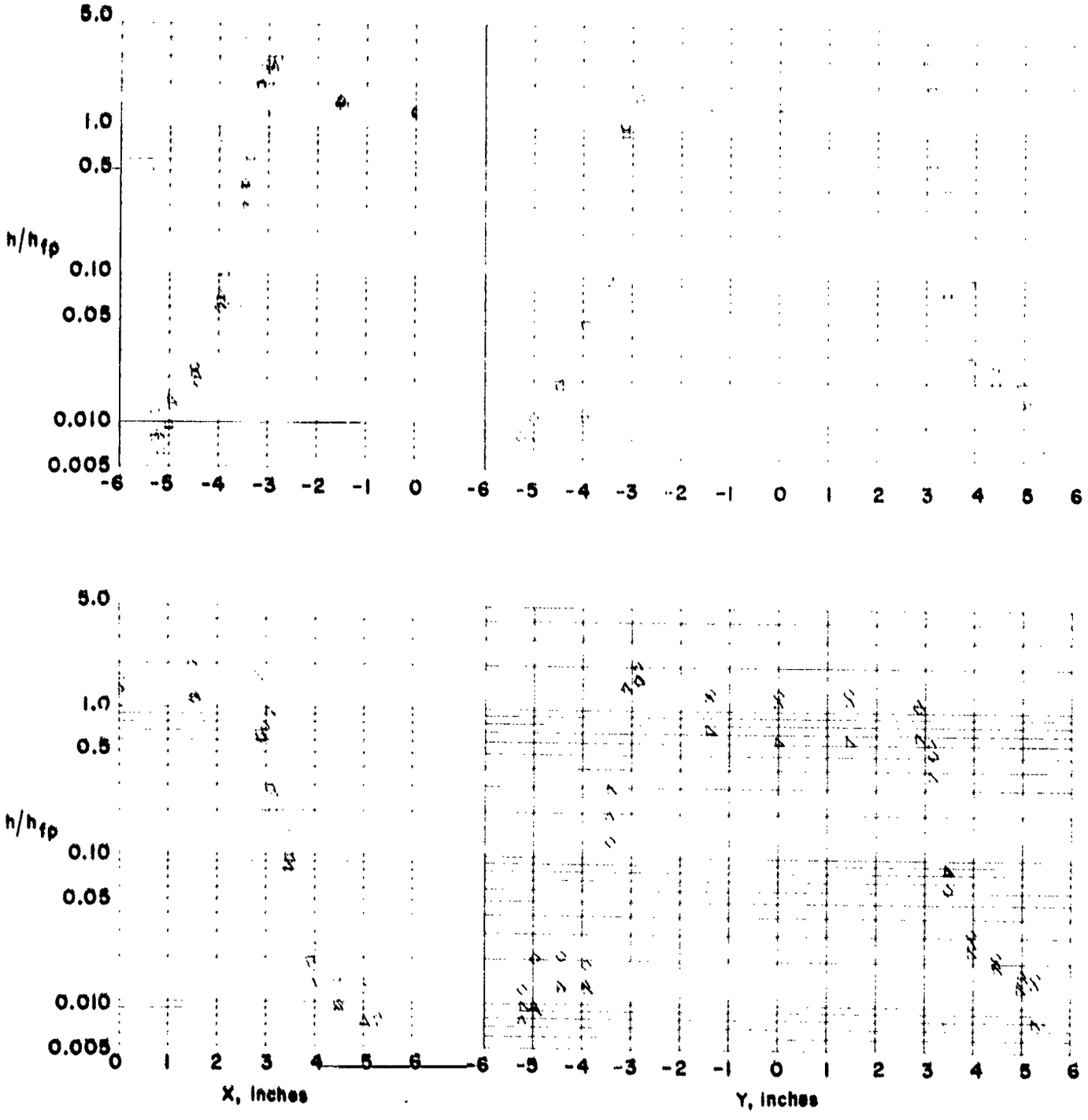

(b) θ = 7.5 degs.

Figure 24. - Continued.

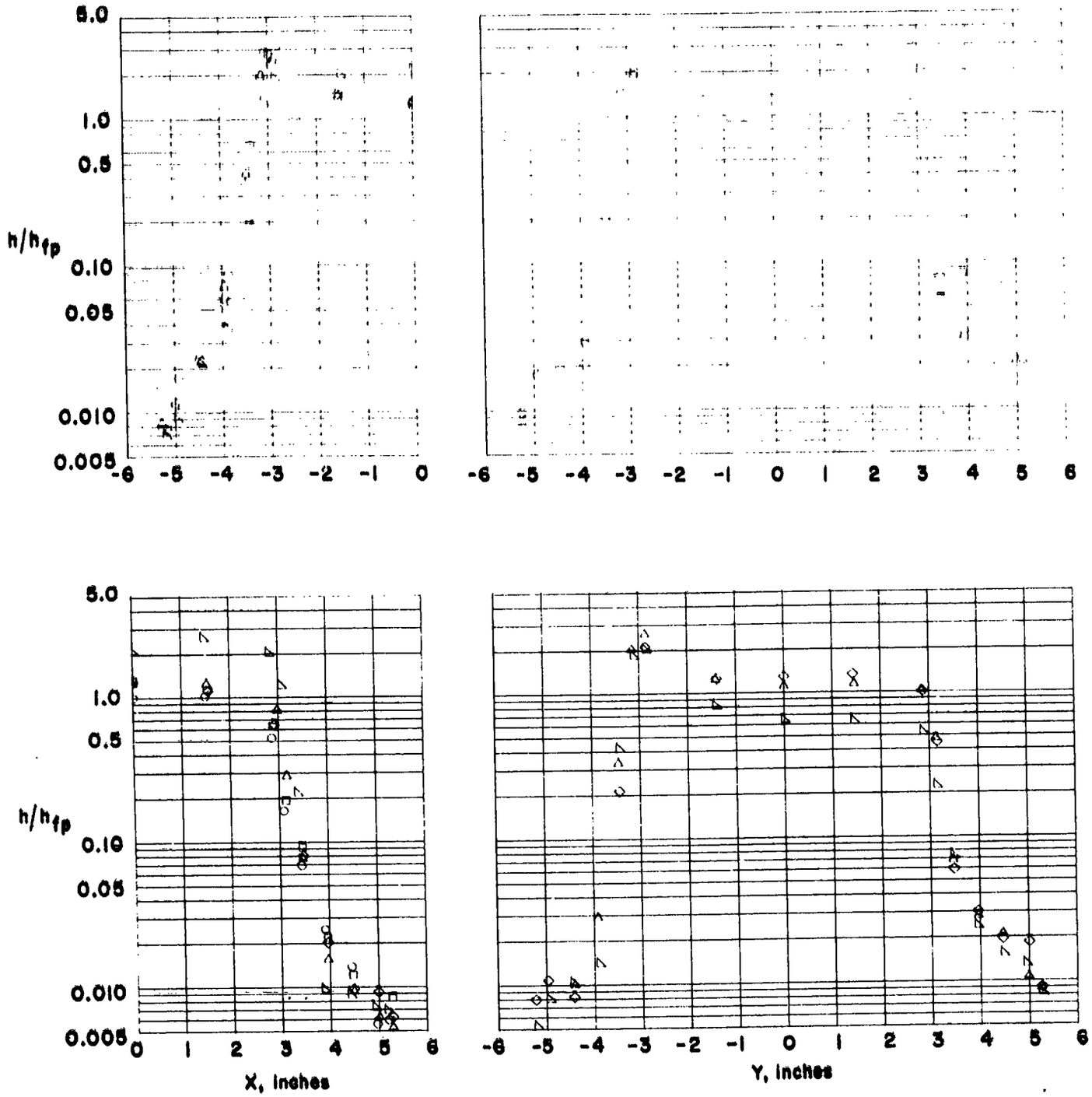

(c) θ = 15.0 degs.

Figure 24. - Continued.

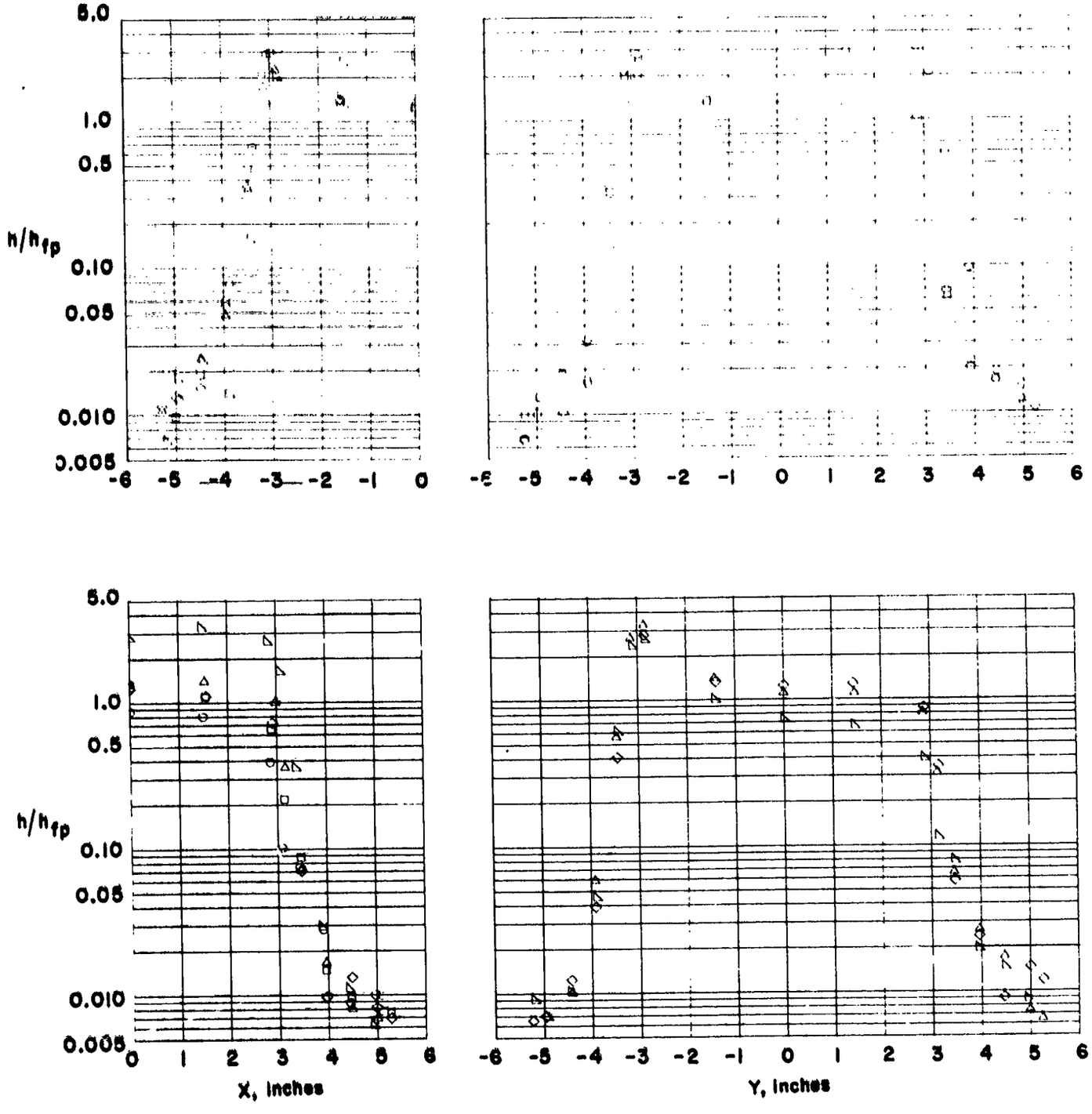

(d) θ = 30.0 degs.

Figure 24. - Concluded.

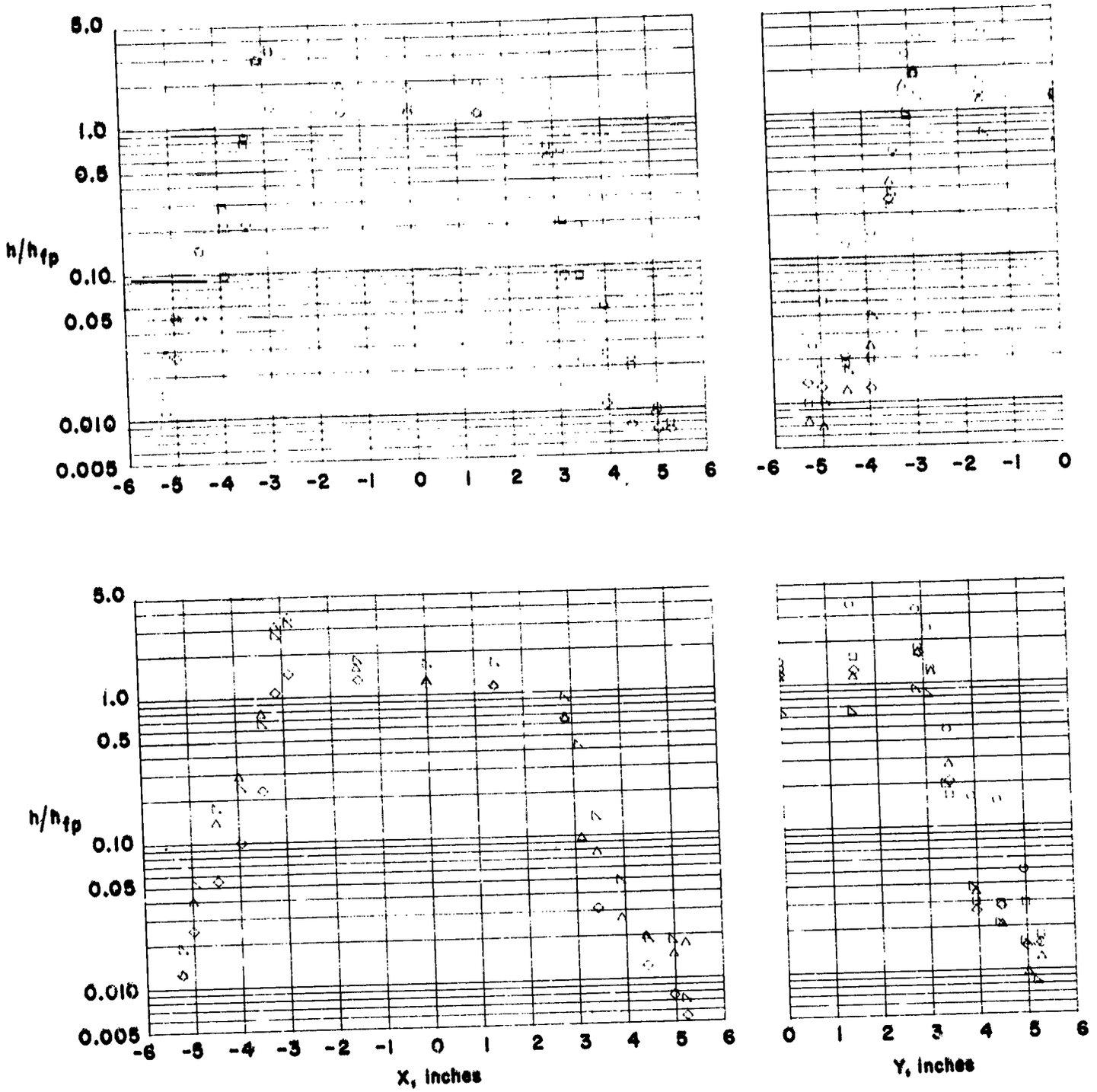

(a) θ = 0.0 degs.

Figure 25. - Heating to a protruding tile in a staggered array. w = 0.28 in., s = 0.10 in.

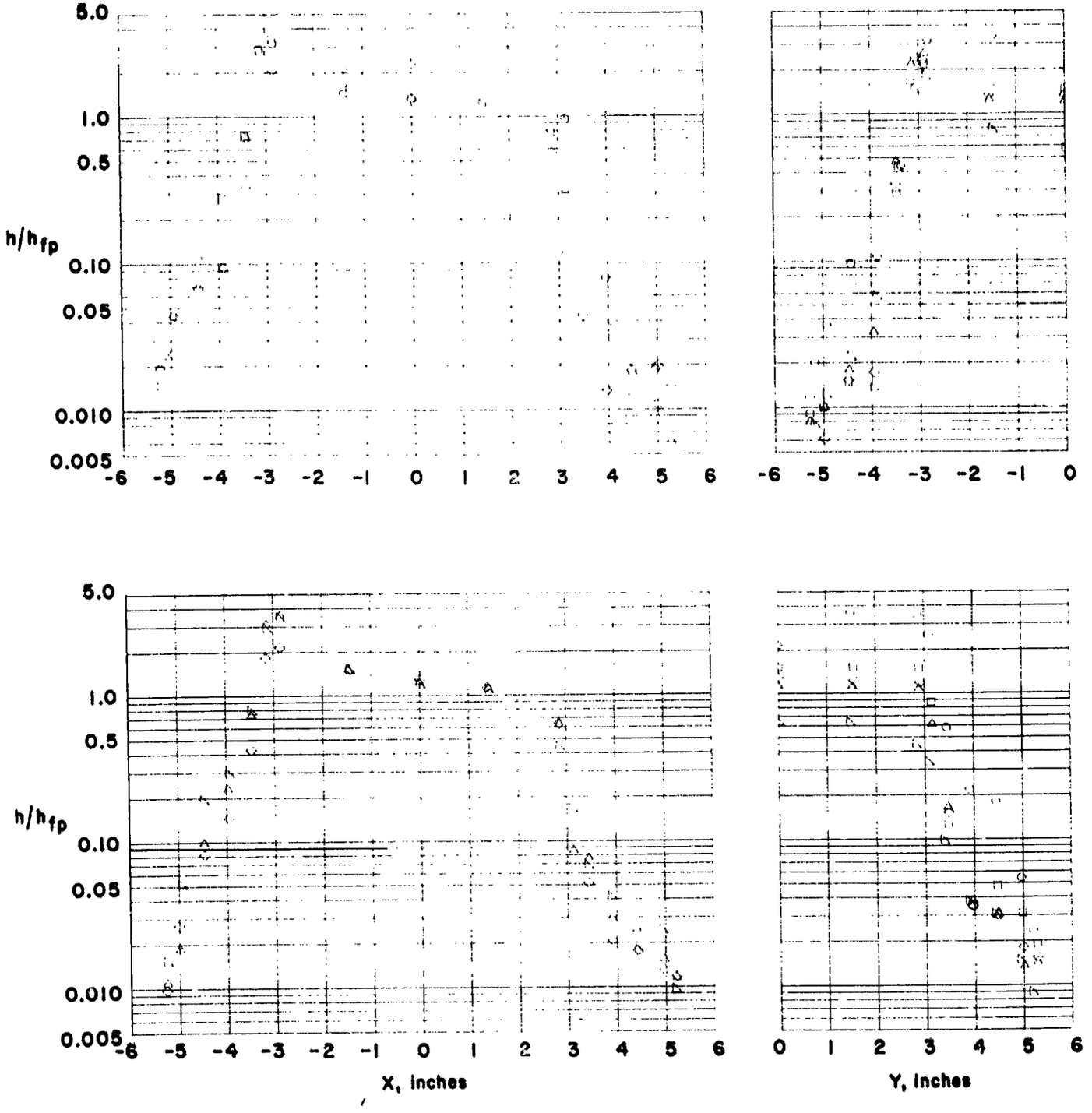

(b) θ = 7.5 degs.

Figure 25. - Continued.

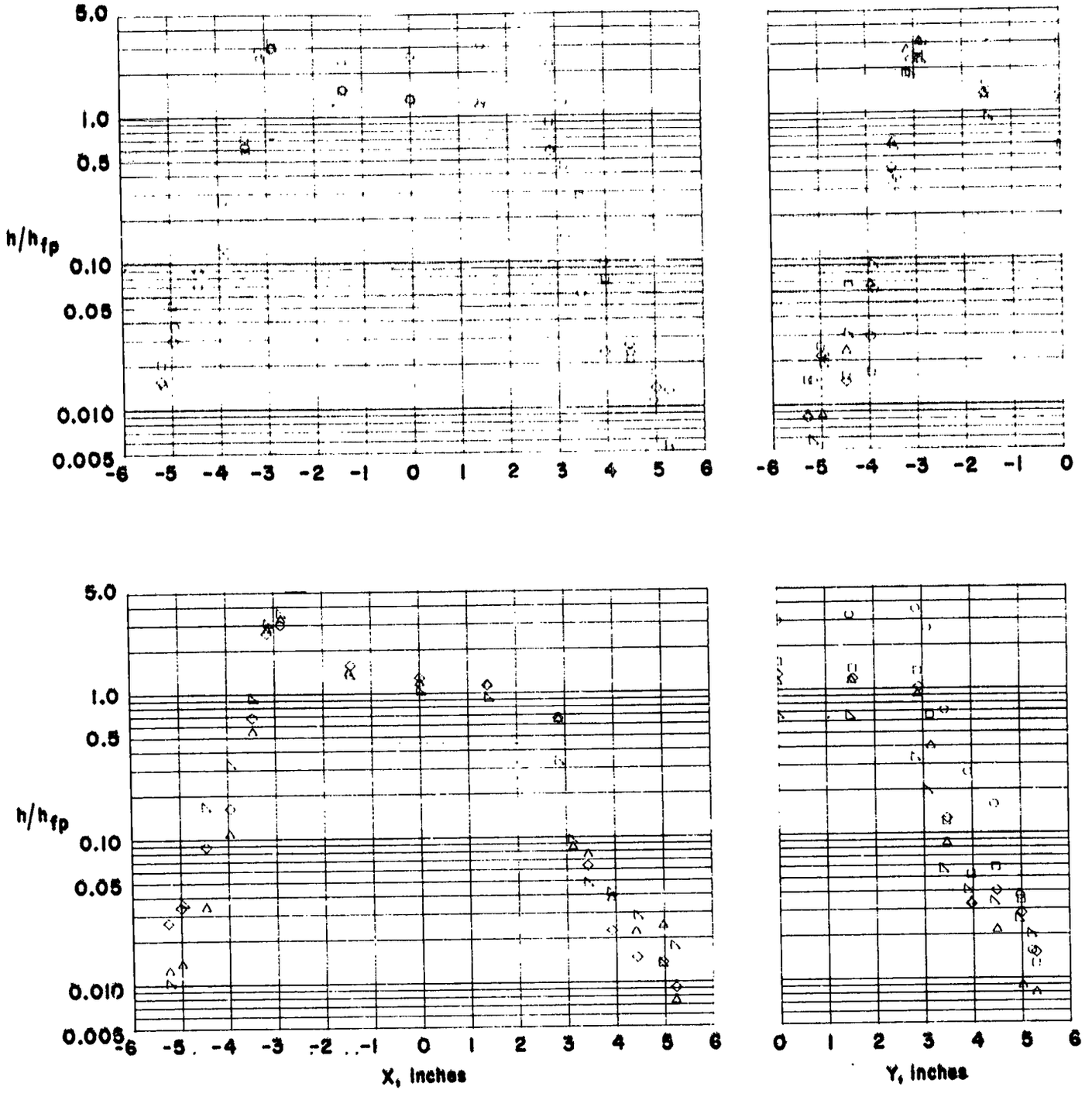

(c) θ = 15.0 degs.

Figure 25. - Continued.

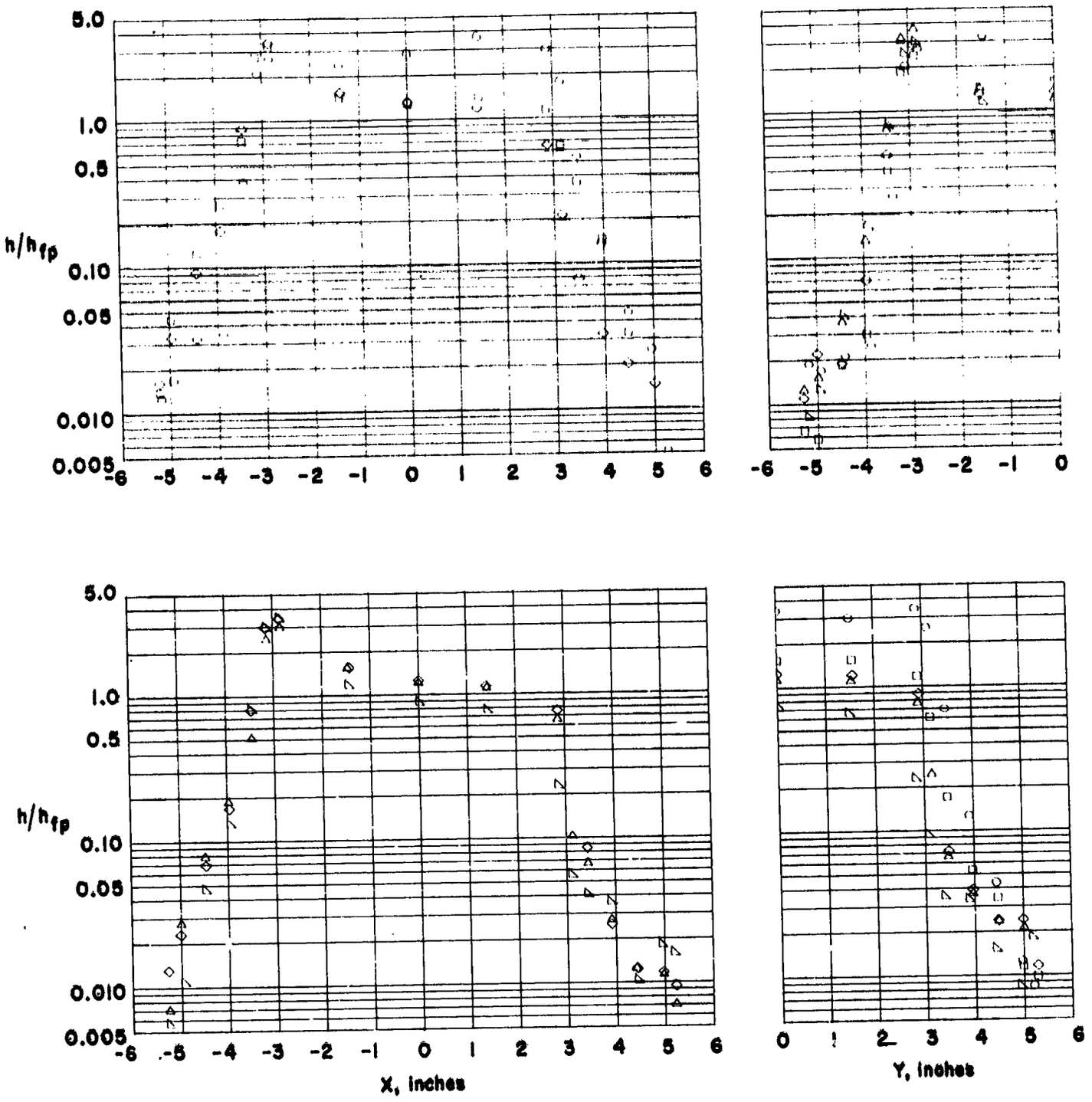

(d) θ = 30.0 degs.

Figure 25. - Continued.

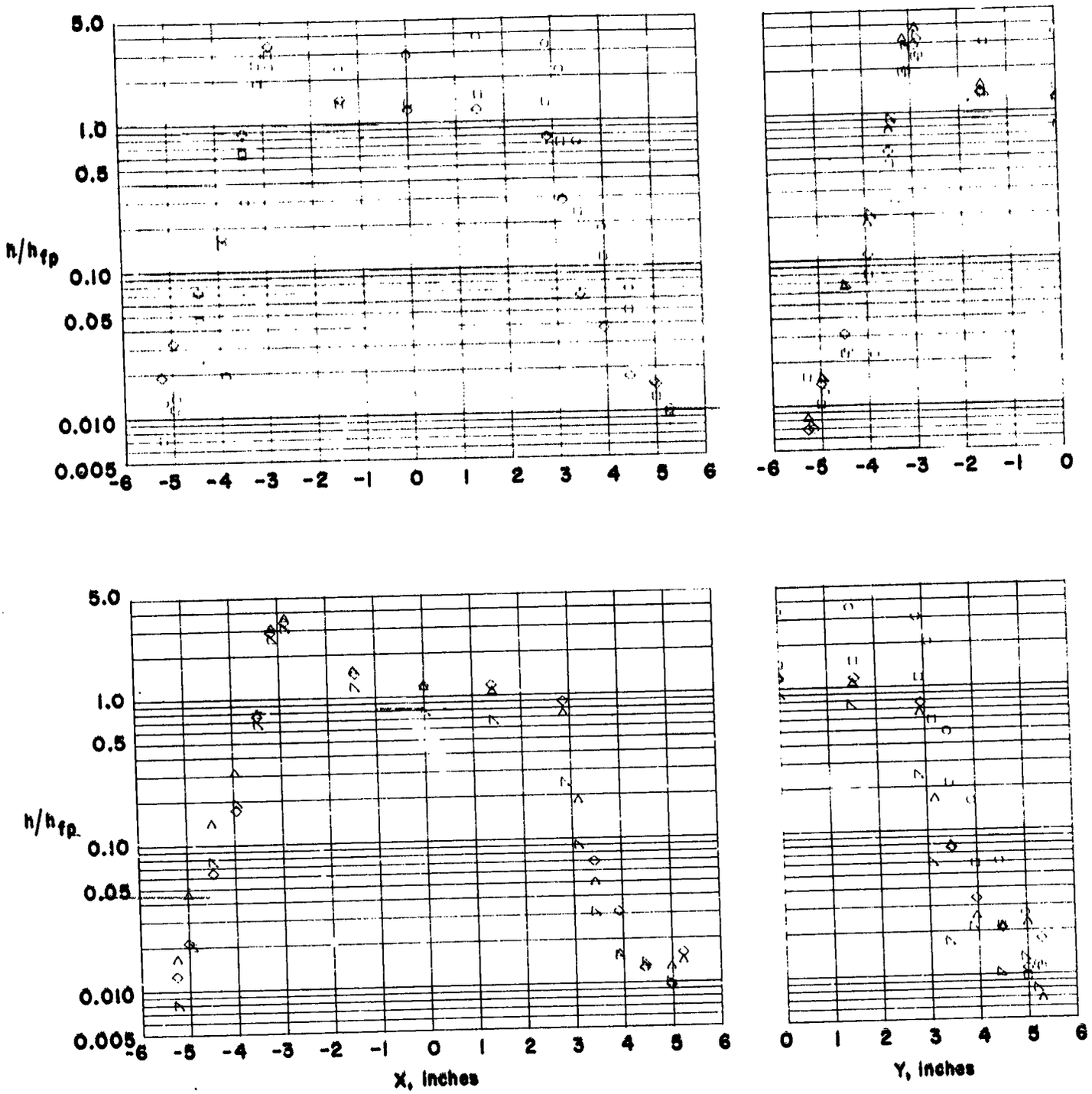

(e) θ = 45.0 degs.

Figure 25. - Concluded.

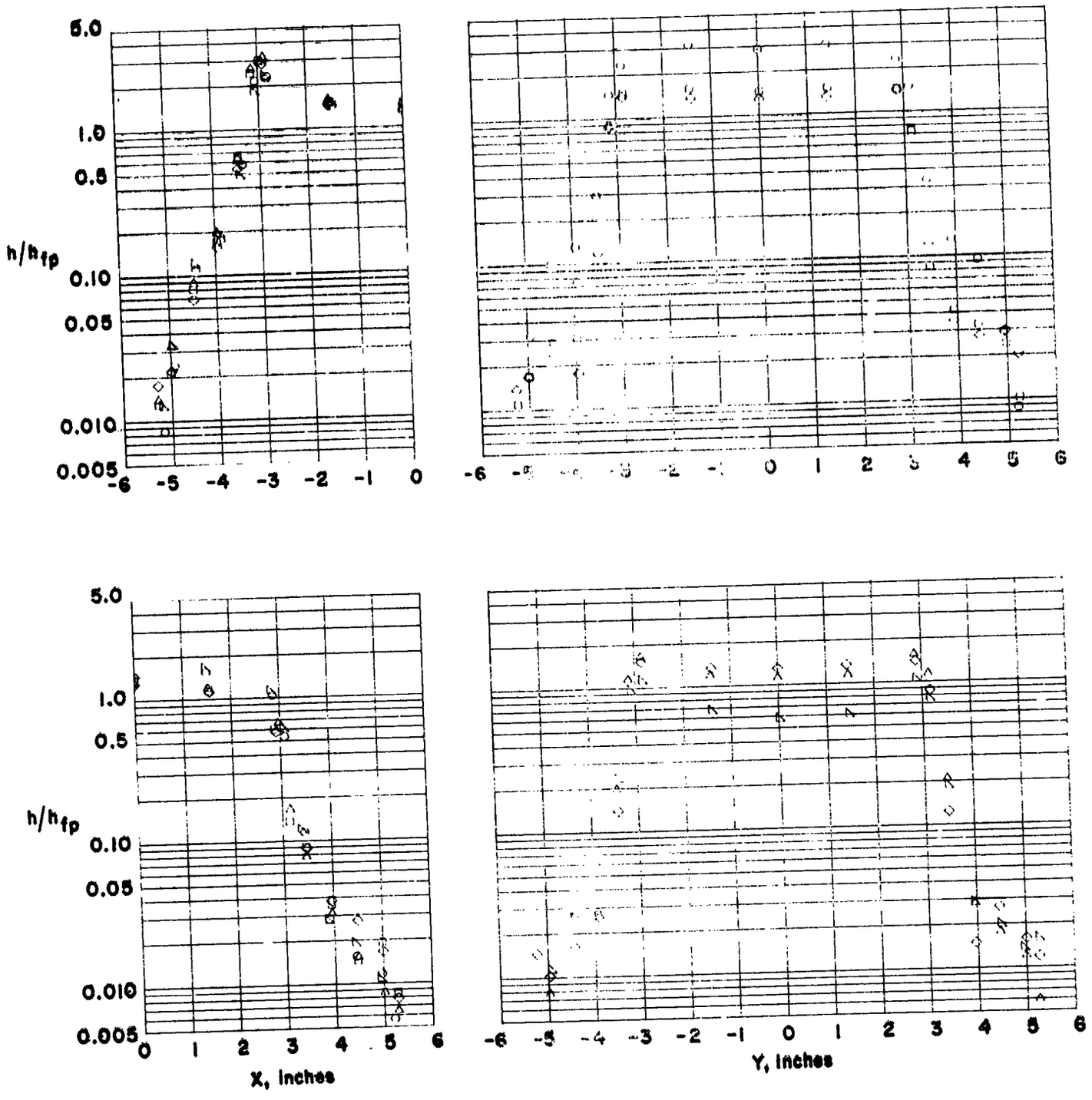

(a) θ = 0.0 degs.

Figure 26.- Heating to a protruding tile in an in-line array. w = 0.28 in., s = 0.10 in.

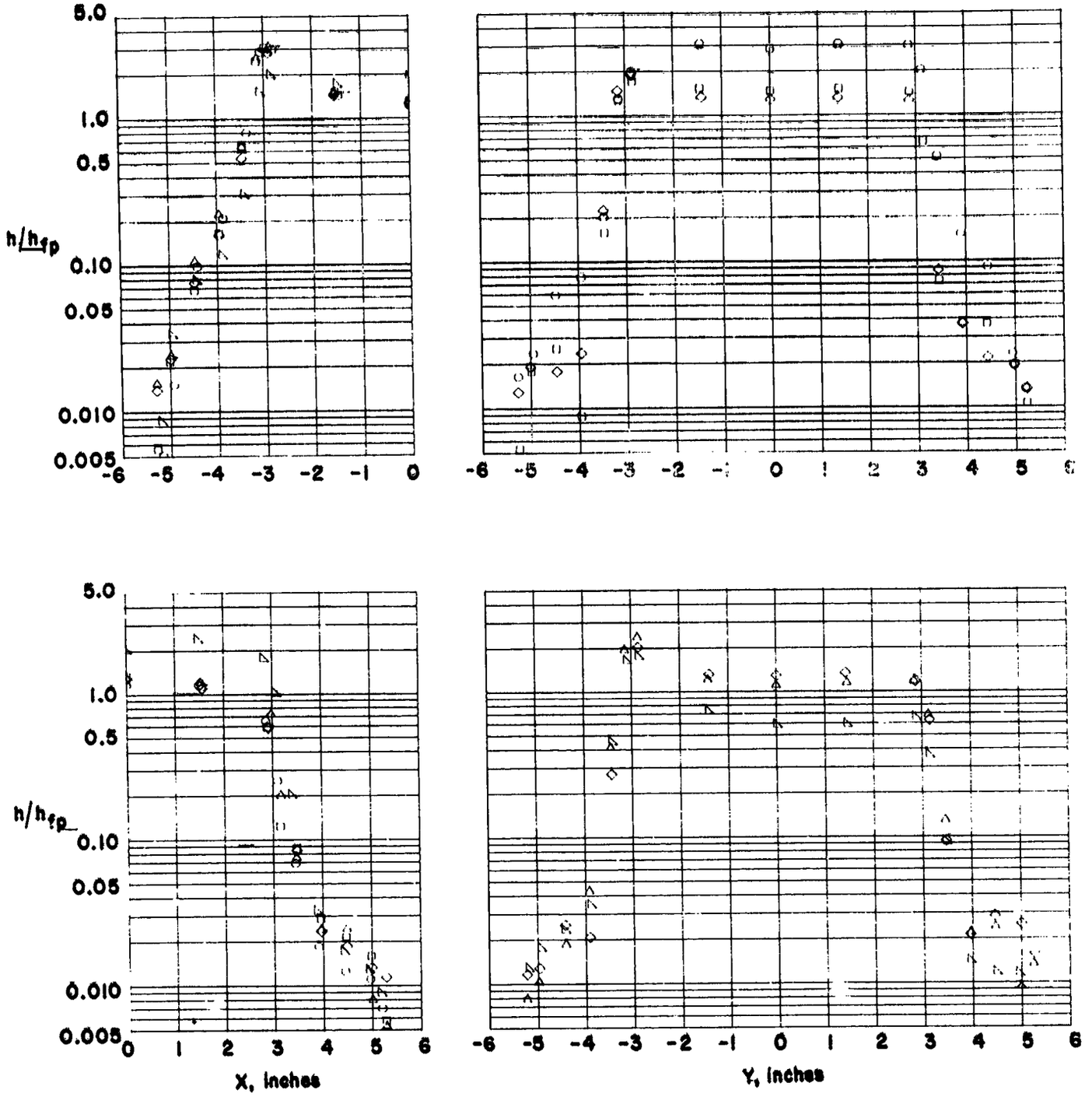

(b) θ = 7.5 degs.

Figure 26. - Continued.

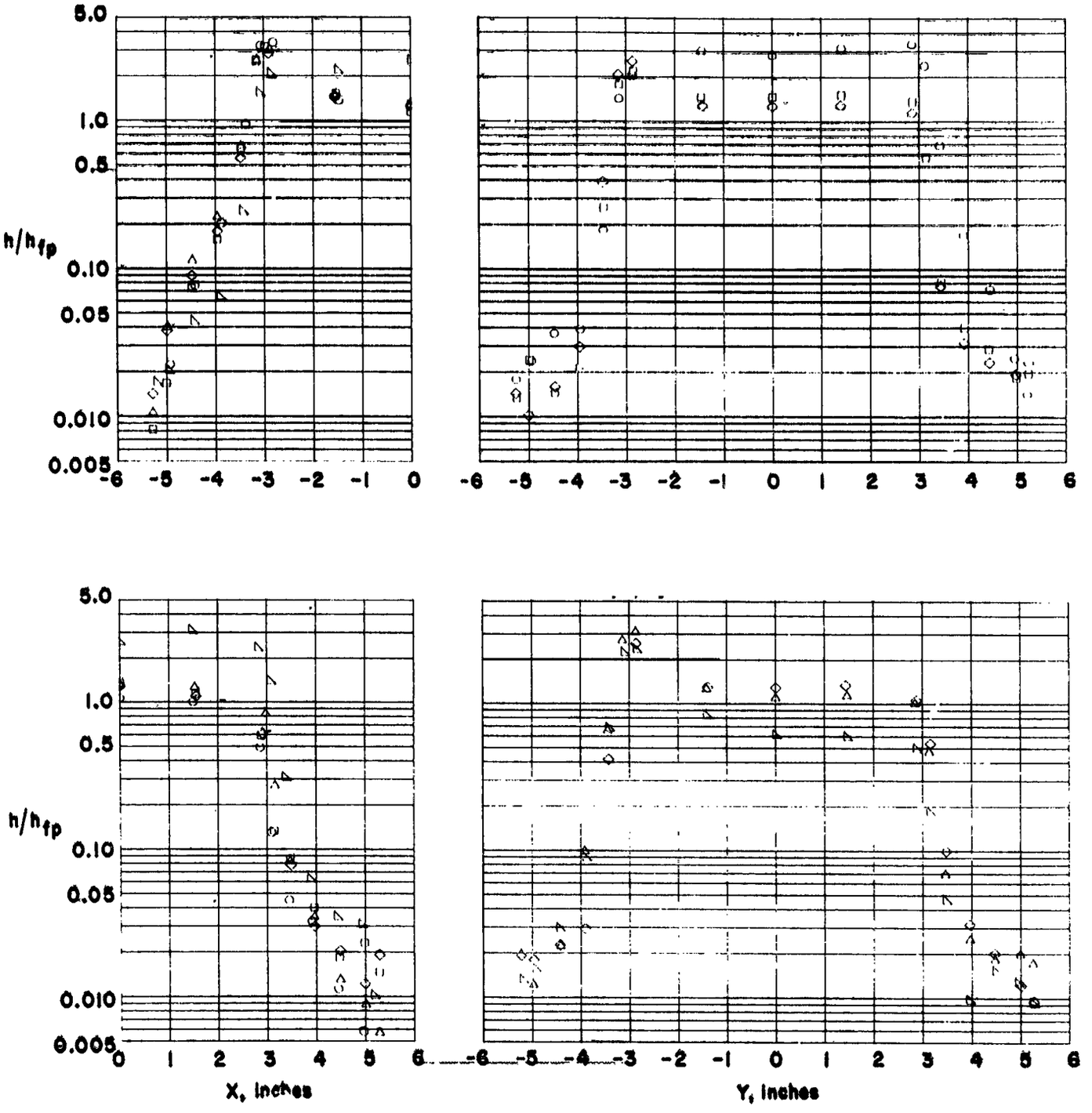

(c) θ = 15.0 degs.

Figure 26. - Continued.

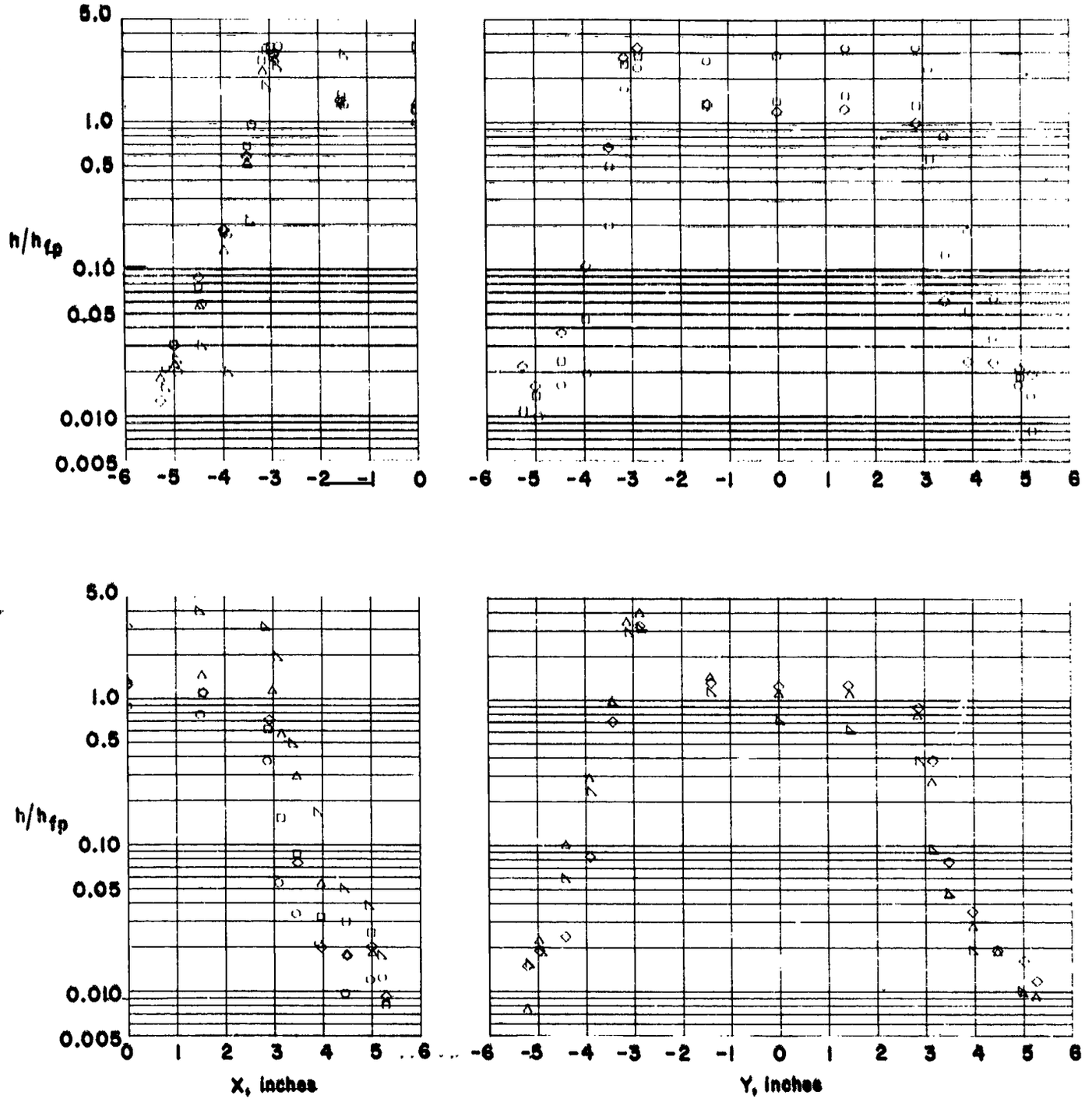

(d) θ = 30.0 degs.

Figure 26. - Concluded.

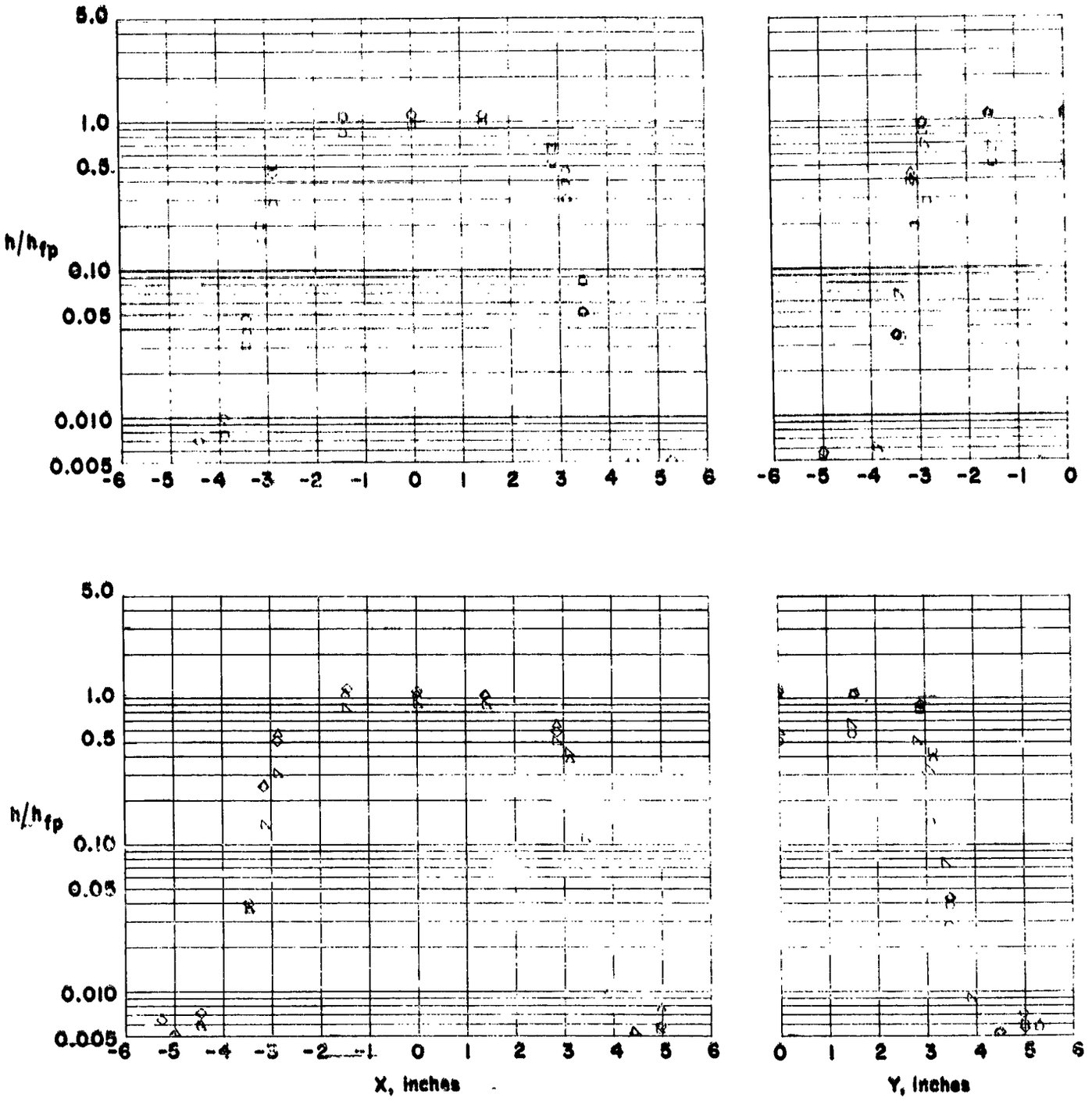

(a) θ = 0.0 degs.

Figure 27.- Heating to a recessed tile in a staggered array. w = 0.09 in., s = -0.066 in.

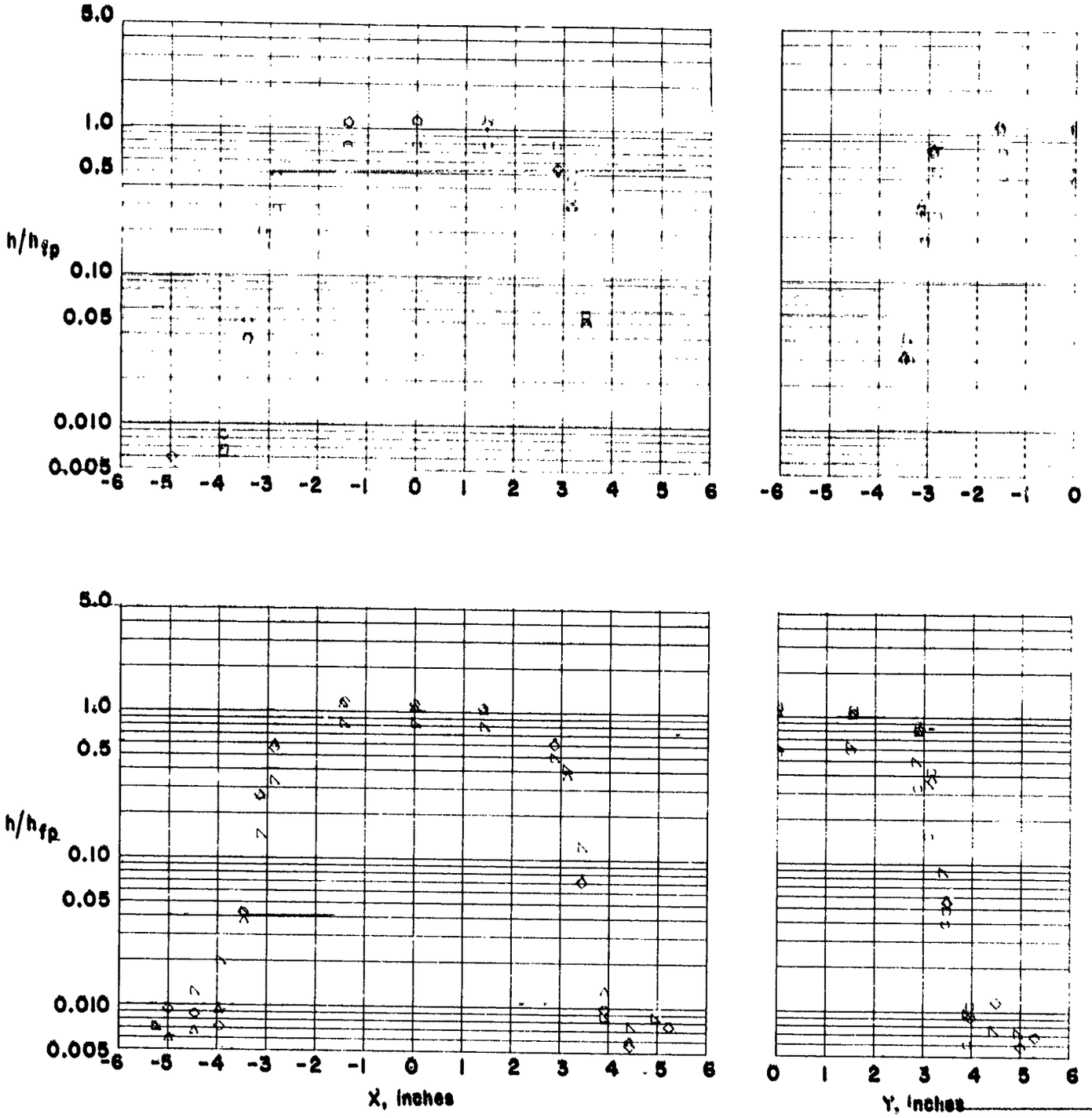

(b) θ = 15.0 degs.

Figure 27. - Continued.

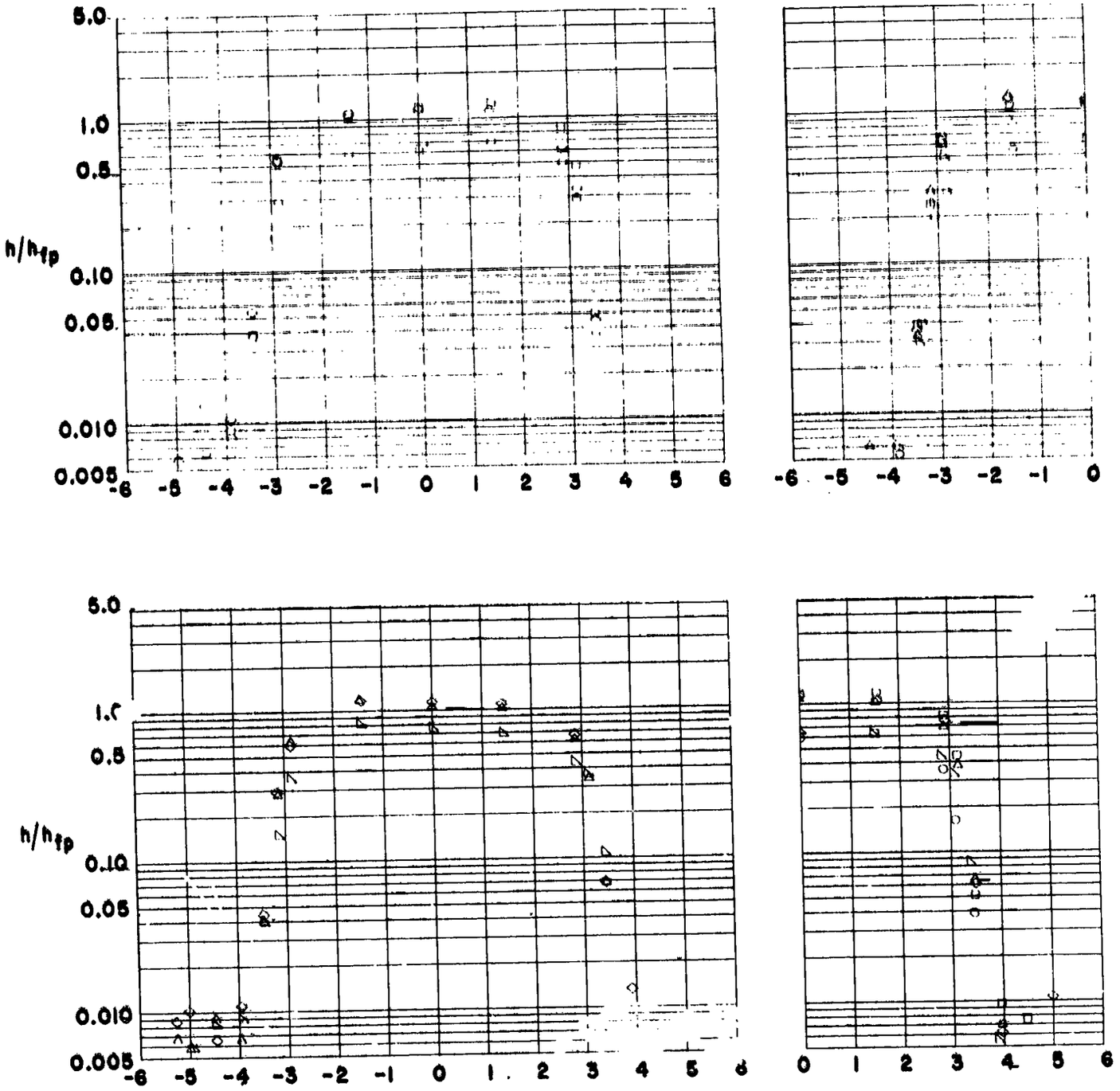

(c) θ = 30.0 degs.

Figure 27. - Continued.

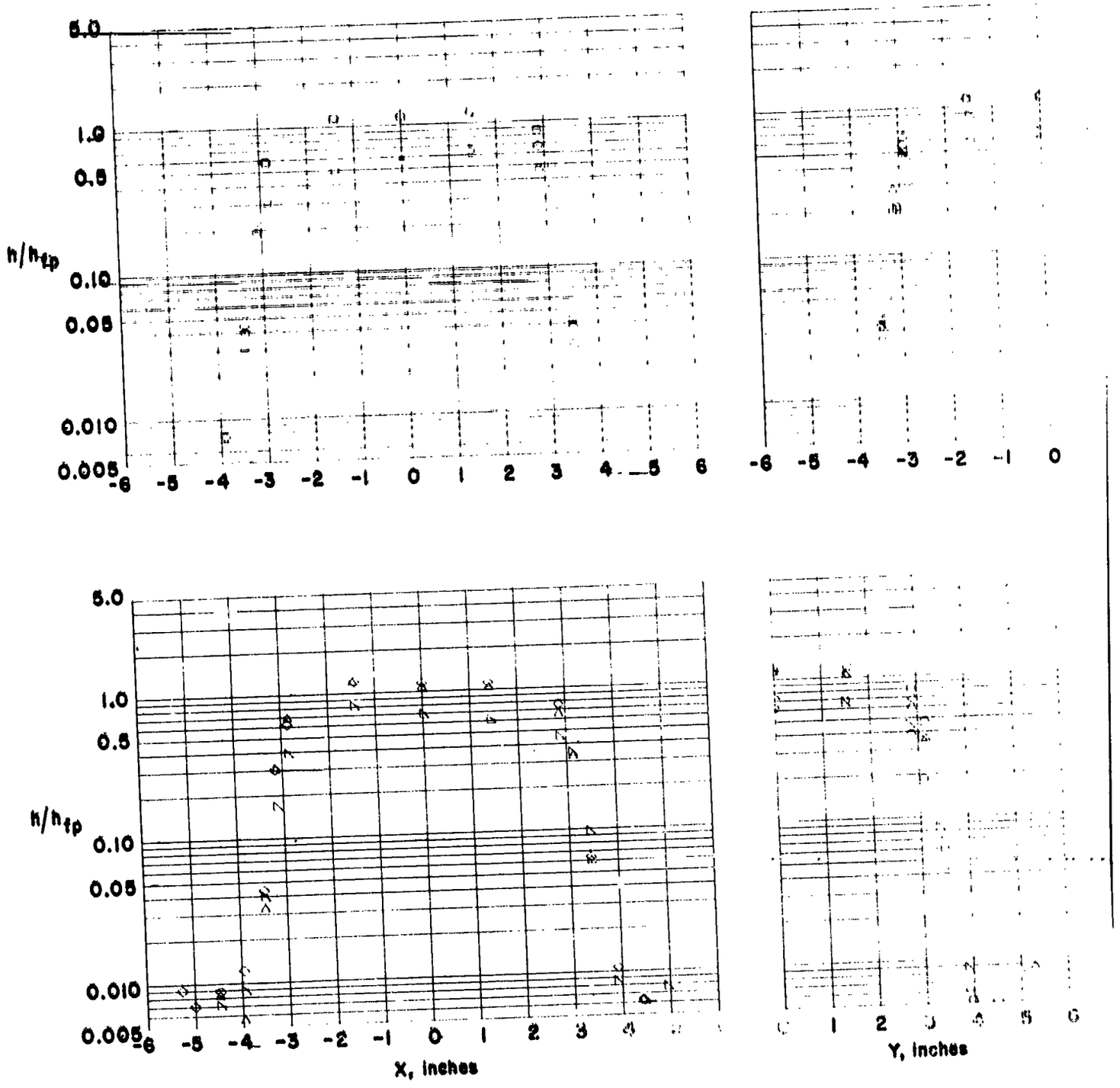

(d) θ = 45.0 degs.

Figure 27. - Concluded.

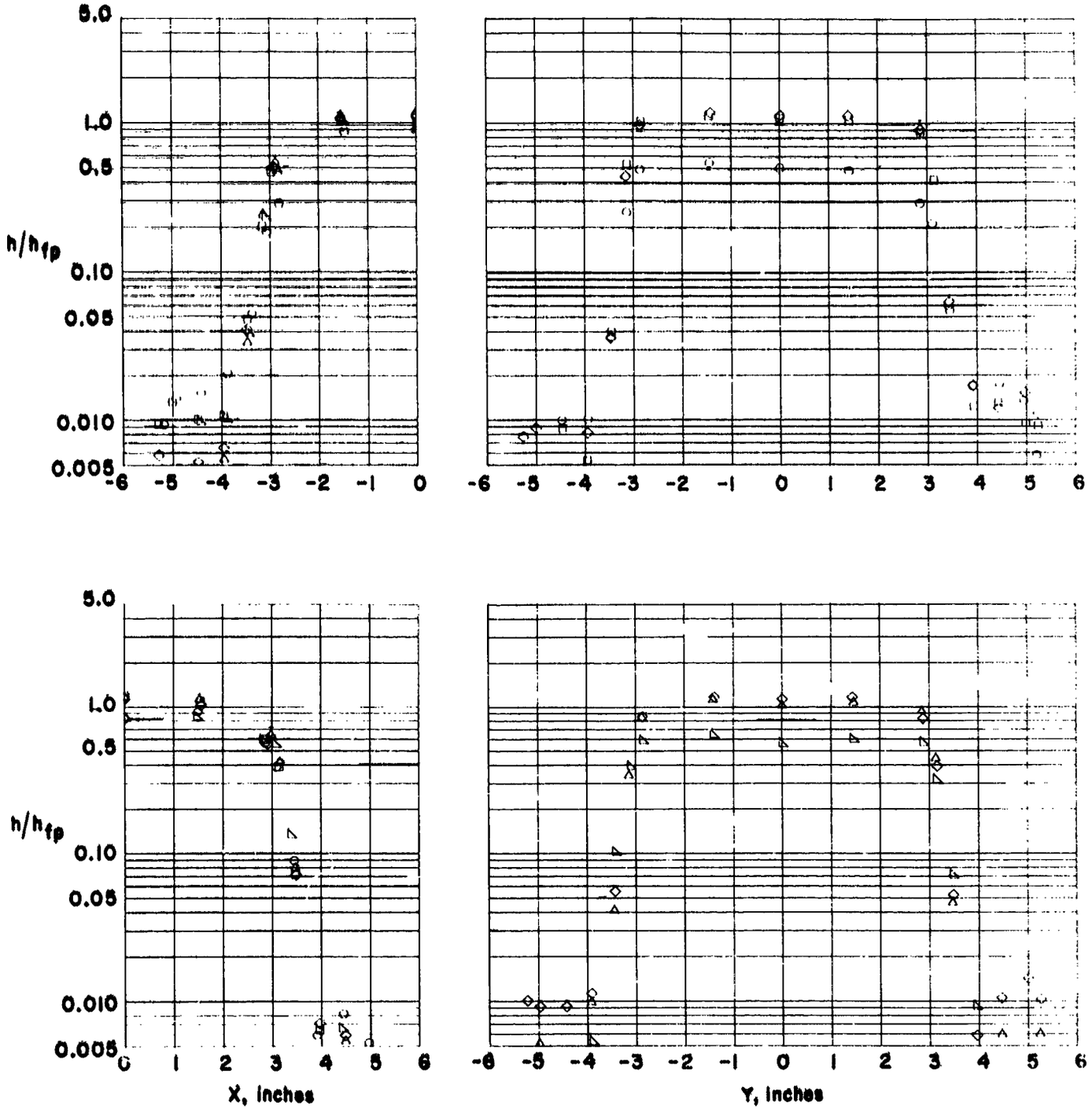

(a) θ = 0.0 degs.

Figure 28.- Heating to a recessed tile in an in-line array. w = 0.09 in., s = -0.066 in.

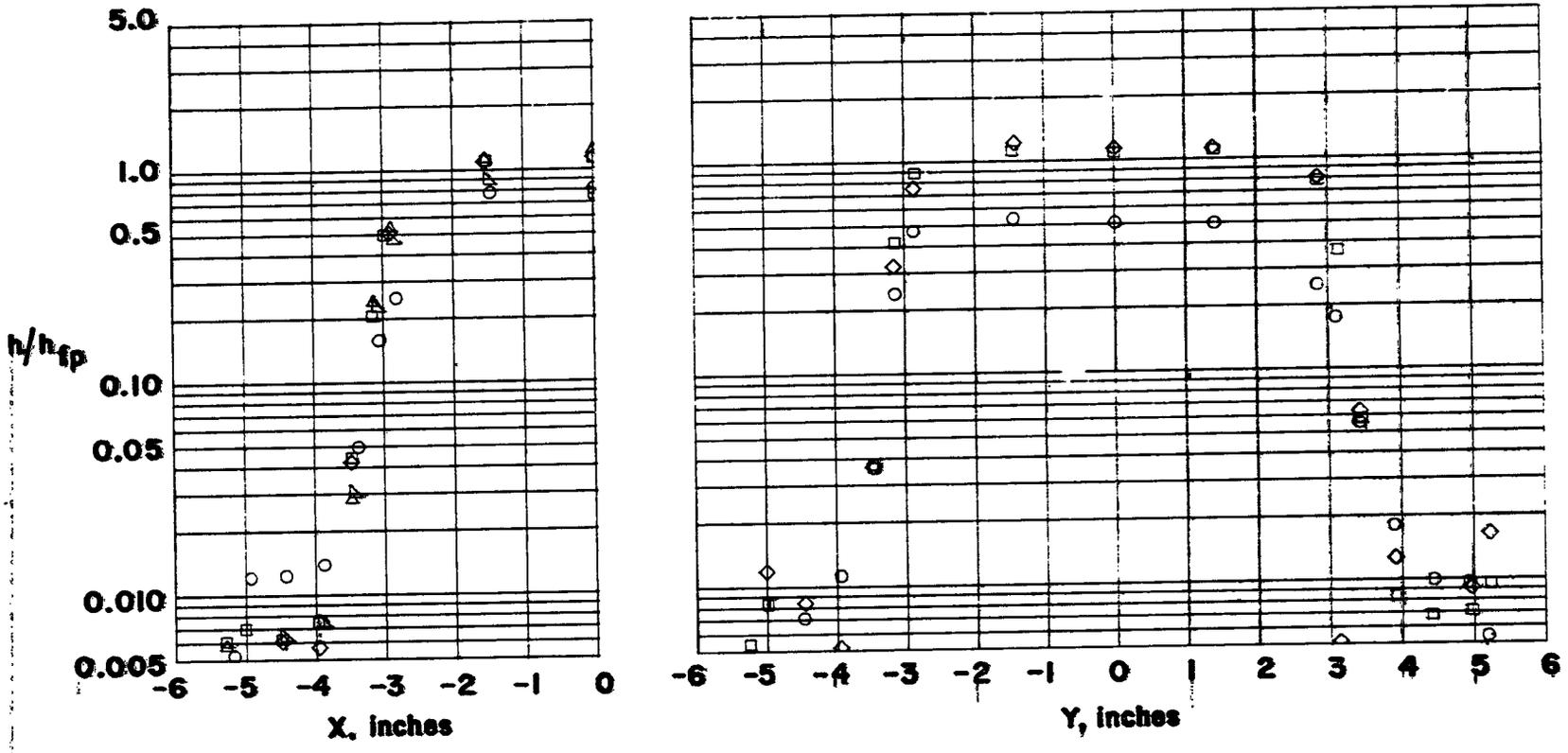

(b) θ = 15.0 degs.

Figure 28 - Continued.

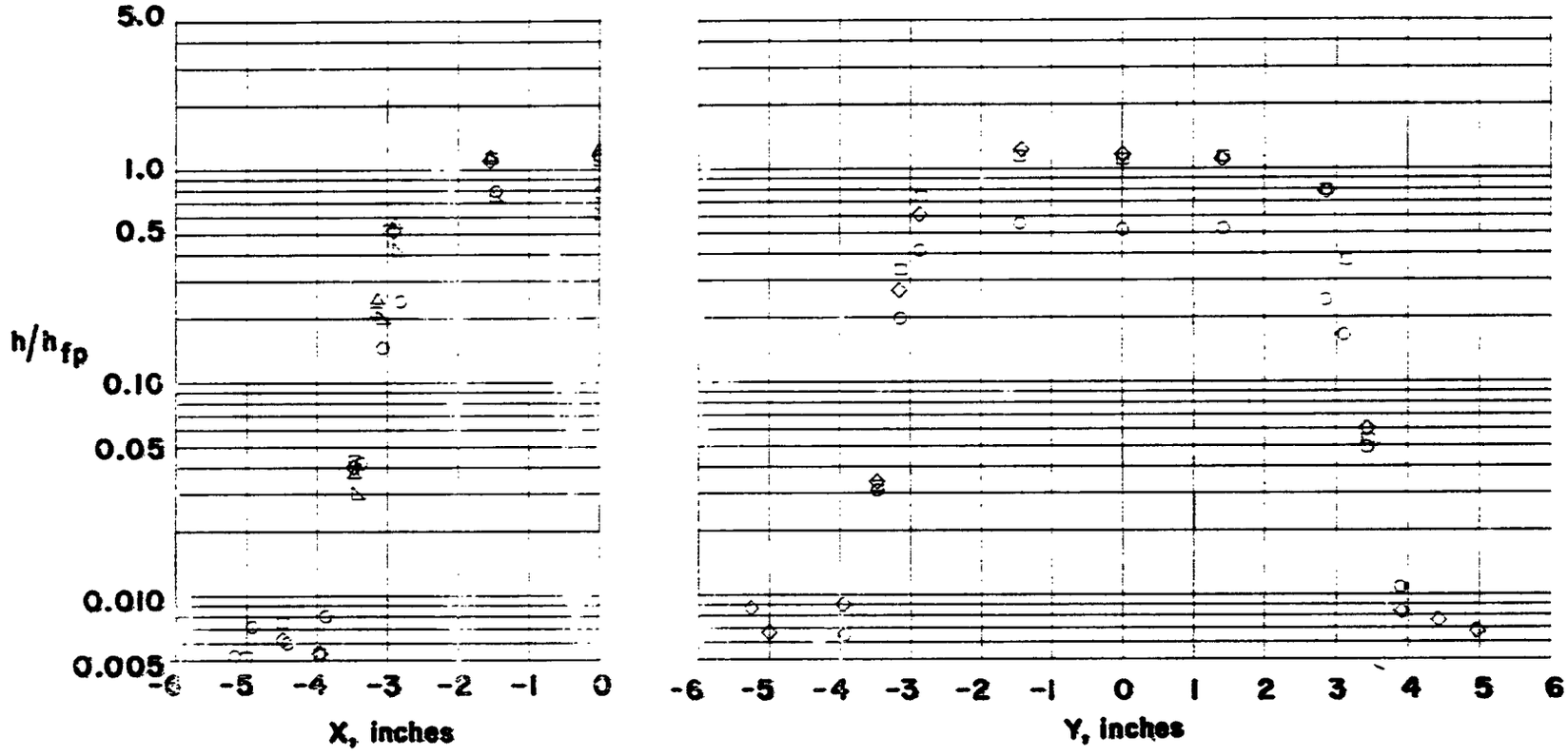

(c) θ = 30.0 degs.

Figure 28. - Concluded.